DEVELOPMENT OF A COMPOSITE GUIDE FOR
PERIPHERAL NERVE REGENERATION

A THESIS SUBMITTED TO
THE GRADUATE SCHOOL OF NATURAL AND APPLIED SCIENCES
OF
MIDDLE EAST TECHNICAL UNIVERSITY

BY

DAMLA ARSLANTUNALI ŞAHİN

IN PARTIAL FULFILLMENT OF THE REQUIREMENTS
FOR
THE DEGREE OF DOCTOR OF PHILOSOPHY
IN
BIOTECHNOLOGY

FEBRUARY 2022

Approval of the thesis:

**DEVELOPMENT OF A COMPOSITE GUIDE FOR
PERIPHERAL NERVE REGENERATION**

submitted by **DAMLA ARSLANTUNALI ŞAHİN** in partial fulfillment of the requirements for the degree of **Doctor of Philosophy** in **Biotechnology, Middle East Technical University** by,

Prof. Dr. Halil Kalıpçılar
Dean, Graduate School of **Natural and Applied Sciences**   _____

Prof. Dr. Candan Gürakan Gültekin
Head of the Department, **Biotechnology**   _____

Assoc. Prof. Dr. Çağdaş Devrim Son
Supervisor, **Biology, METU**   _____

Prof. Dr. Vasıf Hasırcı
Co-Supervisor, **Medical Engineering, ACU**   _____

Examining Committee Members:

Prof. Dr. Sreeparna Banerjee
Biological Sciences, METU   _____

Assoc. Prof. Dr. Çağdaş Devrim Son
Biological Sciences, METU   _____

Prof. Dr. Dilek Keskin
Engineering Sciences, METU   _____

Prof. Dr. Yıldırım Sara
Faculty of Medicine-Internal Medicine, Hacettepe Üniversitesi   _____

Prof. Dr. Deniz Yücel
Faculty of Medicine-Basic Medical Sciences, ACU   _____

Date: 01.02.2022

I hereby declare that all information in this document has been obtained and presented in accordance with academic rules and ethical conduct. I also declare that, as required by these rules and conduct, I have fully cited and referenced all material and results that are not original to this work.

Name Last name : Damla Arslantunalı Şahin

Signature :

ABSTRACT

**DEVELOPMENT OF A COMPOSITE GUIDE FOR
PERIPHERAL NERVE REGENERATION**

Arslantunalı Şahin, Damla
Doctor of Philosophy, Biotechnology
Supervisor : Assoc. Prof. Dr. Çağdaş Devrim Son
Co-Supervisor: Prof. Dr. Vasıf Hasırcı

February 2022, 122 pages

Any injury in peripheral nerves may result in a loss of neuronal communication along sensory and motor nerves, affecting patients' daily activities. Today, there are various FDA approved commercial conduit materials; hollow tubes preventing them from used in gaps bigger than 10 mm, because they may lead axonal sprouts to form. The presented study includes pHEMA wrapping structure filled with GelMA-HaMA gel matrix as a nerve guidance channel. Following the structural analysis of the nerve guide, *in vitro* studies were performed with Schwann cells seeded on pHEMA as support cells and it continued with SHSY5Y neuroblastoma cells seeded on the gel matrix. Tensile modulus and tensile strengths of pHEMA hydrogels were determined as 570.9 ± 92.13 and 501.8 ± 93.7 kPa, respectively. Although tensile strengths of the hydrogels were significantly smaller than the acellular nerve tissue, tensile modulus values were comparable to that of an acellular nerve tissue; showing that the conduits would be able to stay intact during nerve regeneration. In addition, 70% of SCs cells seeded were attached and increased their numbers 5 times in 4 weeks; showing the biocompatibility of the surfaces. GelMA-HaMA gel matrix, sacrificial inner part of the conduits, degraded completely in 5 weeks so that the

regenerating cells were become able to penetrate the structure. As a result of CSLM studies with SHSY5Y cells, it was shown that neuroblastoma cells were able to attach and grow through the gel matrix with the help of SCs secreting nerve growth factors and Netrin-1 as a guidance.

ÖZ

PERİFERİK SİNİR REJENERAYONU İÇİN KOMPOSİT SİNİR TÜPÜ GELİŞTİRİLMESİ

Arslantunalı Şahin, Damla
Doktora, Biyoteknoloji
Tez Yöneticisi: Assoc. Prof. Çağdaş Devrim Son
Ortak Tez Yöneticisi: Prof. Dr. Vasıf Hasırcı

Şubat 2022, 122 sayfa

Periferik sinirlerde meydana gelebilecek bir yaralanma, hastaların günlük aktivitelerini etkileyecek duyu ve motor sinirleri boyunca nöronal iletişim kaybına neden olabilir. Günümüzde, FDA onaylı ticari kanal malzemeleri bulunmaktadır. Bu kanalların, genellikle, içi boş tüp yapısındadır ve bu da akson filizlenmesine sebep olabileceği için 10 mm'den büyük boşluklarda kullanılmalarını önlemektedir. Bu çalışma sinir klavuzu olarak kullanılmak üzere içi GelMA-HaMA jel matrisi ile doldurumuş silindirik pHEMA önermektedir. Sinir klavuzunun yapısal özellikleri test edildikten sonra, *in vitro* çalışmalarda pHEMA üzerine destek olarak ekilmiş Schwann hücreleri ve gel matris üzerine ekilmiş SHSY5Y nöroblastom hücreleri kullanılmıştır. pHEMA hidrojellerinin çekme modulu ve çekme direnci sırası ile 570.9 ± 92.13 ve 501.8 ± 93.7 kPa olarak belirlenmiştir. Çekme direnci aselüler sinir dokusundan düşük olsa da, çekme modulu oldukça yakındır. Bu da kanalların sinir rejenerasyonu sırasında intakt kalmasını sağlamaktadır. Ek olarak, ekilen Schwann hücrelerinin %70'inin yüzeye yapışması ve 4 hafta içinde sayılarının 5 katına çıkması yüzeyin biyouyumluluğunu göstermektedir. Kanalın bozunacak olan iç kısı olan GelMA-HaMA jel matris 5 hafta içinde tamamen yok olmaktadır; bu da

yenilenmekte olan hücrelerin yapının içine gimesini kolaylaştırmaktadır. Sonuç olarak, nöroblastom hücreleri yönlendirici olarak büyüme faktörü salgılayan Schwann hücrelerinin ve Netrin-1 molekülünün varlığında gel matris boyunca akson gelişimi göstermişlerdir.

Anahtar Kelimeler: Periferik Sinir Yaralanması, Sinir Doku Mühendisliği, Sinir Tüpü, Hidrojel

Dedicated to my beloved daughter Asya Şahin

ACKNOWLEDGMENTS

> *"Insanity is doing the same thing, over and over again,*
> *but expecting different results."*
> *Albert Einstein*

TABLE OF CONTENTS

LIST OF TABLES

LIST OF FIGURES

FIGURES

xvii

xviii

LIST OF ABBREVIATIONS

ABBREVIATIONS

μm	micrometer
2D	Two Dimensional
3D	Three Dimensional
ANAs	Acellular Nerve Allograft
APS	Ammonium Persulfate
BDNF	Brain-derived Stem Cells
b-FGF	Basic Fibroblast Growth Factor
BMSC	Bone Marrow Stem Cell
BSA	Bovine Serum Albumin
Ca	Calcium
CLSM	Confocal Laser Scanning Microscopy
cm	Centimeter
CNS	Central Nervous System
CO_2	Carbon Dioxide
Da	Dalton
DAPI	4', 6-Diamidino-2-Phenylindole
DM	Degree of Methacrylation
DMEM	Dulbecco's Modified Eagle Medium
DMSO	Dimethyl Sulfoxide
ECM	Extracellular Matrix
FBS	Fetal Bovine Serum
FITC	Fluorescein Isothiocyanate
FTIR	Fourier-transform Infrared Spectroscopy
g	Gram
GelMA	Methacrylated Gelatin

h	Hour
HA	Hyaluronic Acid
kDa	Kilo Dalton
L	Liter
M	Molarity
mA	Milliampere
MA	Methacrylic Acid
MBP	Myelin Basic Protein
mg	Milligram
min	Minute
mL	Milliliter
mm	Millimeter
mM	Millimolar
MW	Molecular Weight
Na	Sodium
NaCl	Sodium Chloride
ng	Nanogram
NG	Nerve Guide
NGC	Nerve Guide Channel
NGF	Nerve Growth Factor
nm	Nanometer
NMR	Nuclear Magnetic Resonance
NSC	Neural Stem Cell
NT	Neurothrophin
PBS	Phosphate Buffer Saline
PCL	Poly(ϵ-caprolactone)
PDMS	Poly(dimethylsiloxane)
PE	Polyethylene
PEG	Polyethylene Glycole
Pen/Strep	Penicillin/Streptomycin
PGA	Poly(glycolic acid)

PHB	Poly(3-hydroxybutyrate)
pHEMA	Poly(2-hydroxyethyl methacrylate)
PLA	Poly(lactic acid)
PLGA	Poly(Lactic acid-co-Glycolic Acid)
PLLA	Poly(L-Lactic Acid)
PMMA	Poly(methyl methacrylate)
PNI	Peripheral Nerve Injury
PNS	Peripheral Nervous System
RP	Rapid Prototyping
rpm	Rotation per minute
RT	Room Temperature
s.d.m.	Standard Deviation of the Mean
SC	Schwann Cell
SEM	Scanning Electron Microscopy
SLA	Stereolithography
SLS	Selective Laser Sintering
UV	Ultraviolet
UV-vis	UV-Visible
v/v	Volume/Volume
w/v	Weight/Volume
WC	Water Content

CHAPTER 1

INTRODUCTION

1.1 An Overview of the Nervous System

The nervous system is the most complex system in the body. The cells conducting the impulse that is coming from the sensory organs or the nervous system are the neurons, and the neurons are the basic elements of the nervous system. These basic elements are supported by several type of cells collectively called neuroglia. There are two parts of the nervous system: peripheral nervous system (PNS) consisting of nerves and ganglia of peripheral tissues and central nervous system (CNS) consisting of the brain and the spinal cord (Figure 1.1). The function of PNS is to carry information between CNS and peripheral tissues (Hasirci and Hasirci, 2018).
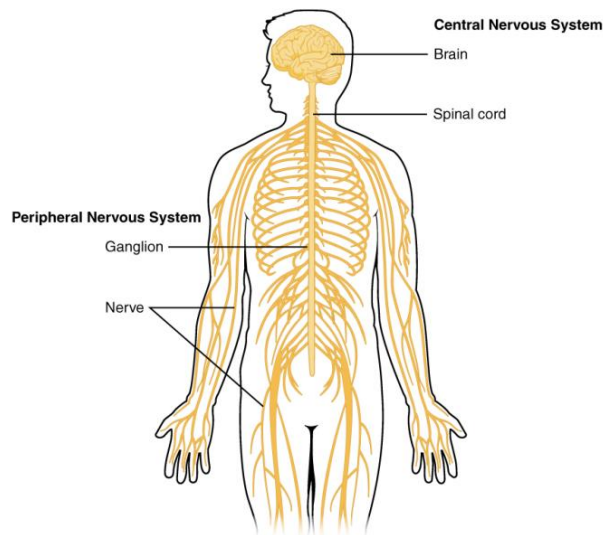
Figure 1.1 Central and Peripheral Nervous System (Heyden, 2016).

1.1.1 Peripheral Nervous System

Nerves of the peripheral nervous system have role in the communication between the central nervous system and various organs. There are two parts of PNS; somatic and autonomic nervous systems. The body movements are controlled by the somatic nervous system and the external stimuli is received by this system. Autonomic nervous system is responsible for unconscious movements like blood pressure, heartbeat, constriction of pupils; collectively autonomous internal functions. Divisions of the autonomous nervous system is defined as parasympathetic responsible of calming the body and sympathetic arousing the energy of the body (Figure 1.2) (Hasirci and Hasirci, 2018).
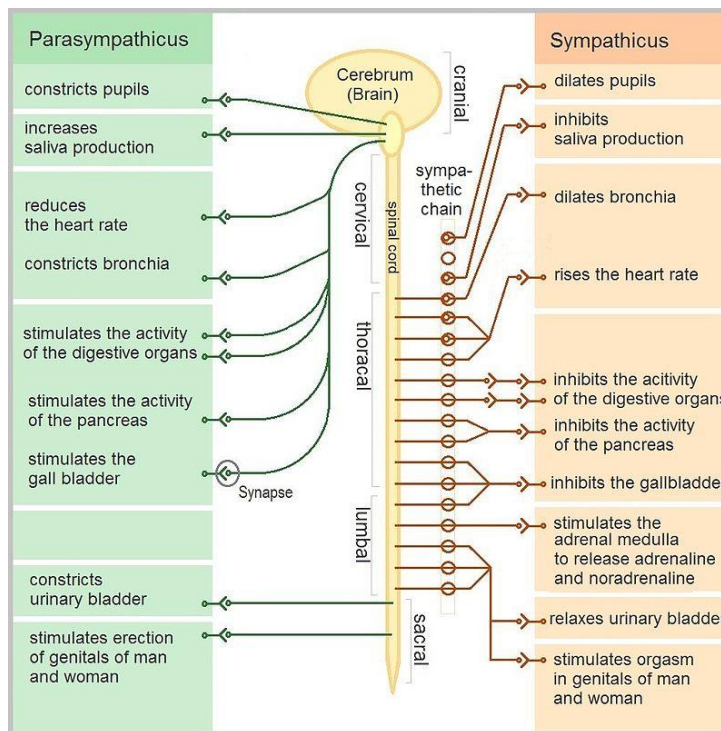
Figure 1.2 Autonomic nervous system functions (Neit et al., 2003).

1.1.2 Central Nervous System

The brain and the spinal cord are the parts of the central nervous system (CNS). The system has a protective covering having 3 layers. These coverings are called meninges and showed in Figure 1.3. The outermost layer is dura matter and its role is to carry blood between the brain and the heart. The middle layer has a web like arachnoid mater. The last layer is pia mater. This inner layer contacts and covers the brain and the spinal cord. Cerebrospinal fluid is found between the arachnoid and pia maters and works as a shock absorber (Myers and DeWall, 2017).
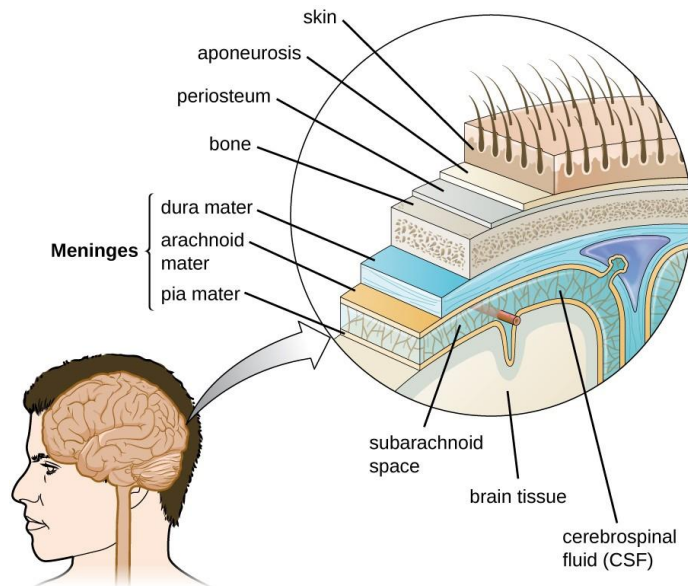
Figure 1.3 The structure of the layers surrounding the brain (Myers and DeWall, 2017).

1.1.3 Cells of the Nervous System

Nervous system has neurons and glial cells. The primary cell type of the system is a neuron which is responsible for receiving and carrying information. Thus, neurons which are electrically active and able to produce chemical signals, have major role in communication between nervous system and the other organs. (Heyden, 2016).

1.1.3.1 Neurons

Neurons, a basic building blocks of the nervous system, are specialized cells that transmit chemical and electrical signals in the body (Martini et al., 2018). Typical neuron has primary components; the cell body, the axon and dendrites (Figure 1.4). the axon has role in conducting electrical impulses away from the cell body. The tree like dendrites are responsible for receiving messages from other neurons. There are specialized junctions between neurons called synapses and the gap between two neurons at a synapse is called a synaptic cleft. For a neuron to receive and transmit a message to another, electrical and chemical signaling are necessary. When a chemical signal binds to a neuron, electrical events start. After the stimulus is received, intrinsic message is generated, if it is high enough, it is integrated and an action potential is created, triggering encoding and output, the synaptic activity (Augistin et al., 2004).

Peripheral nerves are composed of bundles of nerve fibers and surrounding connective tissue sheaths including blood vessels (Figure 1.5) (Arslantunali et al., 2014a).
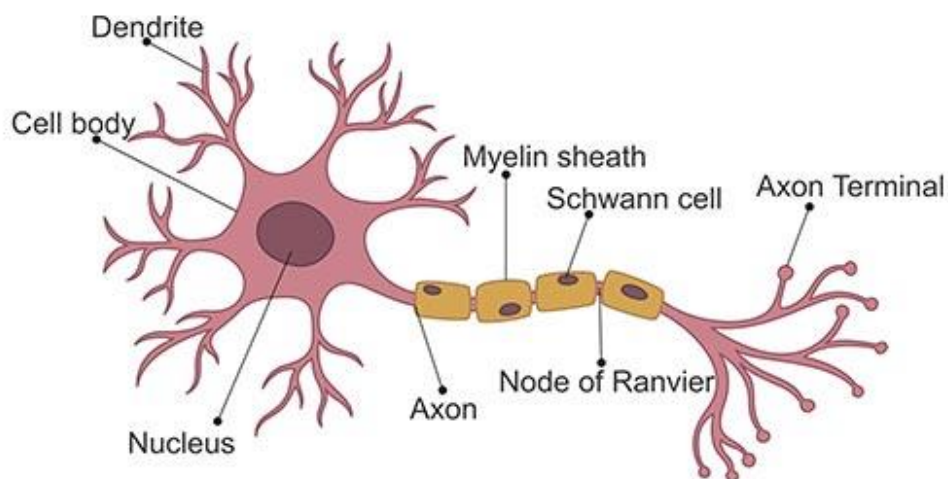
Figure 1.4 Structure of a nerve (Upadhyay et al., 2016).

4
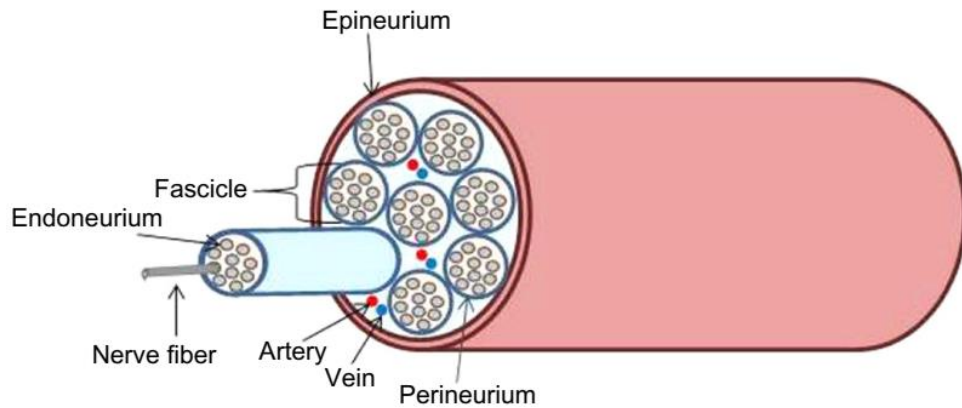
Figure 1.5 Structure of a peripheral nerve trunk (Arslantunalı et al., 2014a).

1.1.3.2   Support Cells of the Nervous System

The support cells of the nervous system are collectively called glial cells (Figure 1.6). They maintain homeostasis, form myelin, and provide support and protection for neurons. In the central nervous system, glial cells include oligodendrocytes (lay down myelin, the lipid rich wrapping), astrocytes (star like cells maintaining an appropriate chemical environment for signaling), ependymal cells (involved in the creation and secretion of cerebrospinal fluid), and microglia (removing cellular debris from the sites of injury). In the peripheral nervous system glial cells include Schwann cells (responsible for myelination) and satellite cells (regulating the external chemical environment). The major difference of the glial cells from the neurons is that they do not have a role in electrical signaling (Augistin et al., 2014).

Some axons are covered with myelin formed by Schwann cells, a fatty material that wraps around the axon. The function of the myelin sheath is to insulate the axon in order to minimize dissipation of the electrical signal. (Martini, 2018).

5
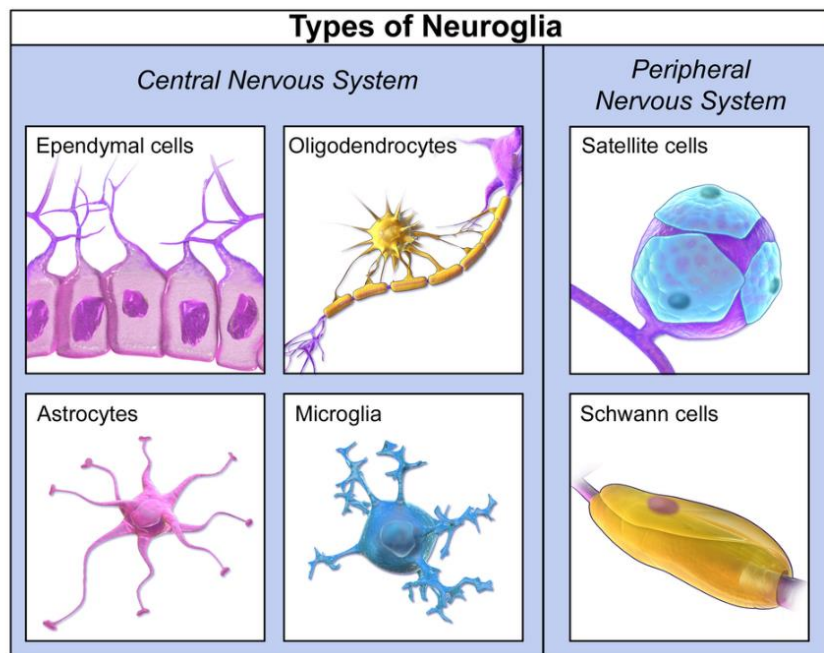
Figure 1.6 Types of the glial cells in the nervous system (Blausen.com staff (2014). "Medical gallery of Blausen Medical 2014").

1.2   Neuronal Injury

Injury in peripheral nerves seriously affects the patient's quality of life, this makes this a worldwide clinical problem. The injury may result in a loss of neuronal communication along sensory and motor nerves between the CNS and the peripheral organs. Peripheral nerve injuries often result in painful neuropathies via reduction in motor and sensory functions and can be catastrophic for patients, drastically affecting their daily activities (Arslantunali et al., 2014a).

Mechanical, thermal, chemical or ischemic damages may cause peripheral nerve injuries. These are mostly resulted from traumatic accidents or some degenerative disorders. The functional result depends on the level of the injury. The level is determined by the classifications reported by Seddon and Sunderland (Figure 1.7) (Seddon, 1943; Sunderland, 1951). In the classification of the Seddon, the categories are called as neurapraxia, axonotmesis and neurotmesis. However, Sunderland classifies the injury as 1-5-degree injuries. The first degree of Sunderland classification corresponds to neurapraxia. In this kind of injuries axons are anatomically intact and Wallerian degeneration is absent, but there is partial

demyelination and impulses cannot be transmitted. These injuries recover with a treatment within a few months. Axonotmesis, 2nd type of injury, includes intact endoneurium and Schwann cells but severely injured axons. By the help of the endoneurium, the axons can be healed. Axonotmesis also includes 3rd type of injury. In this type of injury, perineurium and fascicular structures are intact but endoneurium is injured. Fibrosis may take place and recovery time is so long. In the 4th type of injury, axons, endoneurium and perineurium are all injured but not epineurium. The degeneration level is really high, for regeneration surgery may be needed. At the highest level of neurotmesis, 5th degree, the nerve truck is completely transected, and scar formation occurs. Neuroma is seen at proximal ends and Wallerian degeneration at distal ends. Surgery is necessary. Normally, 1 mm/day axonal regrowth is expected. However, if these cannot be achieved by the axons, if they cannot go through all the way to the distal end, disorganized axonal sprouts are seen and the muscle fiber corresponding to the injured nerve becomes anthropic (Figure 1.8) (Arslantunali et al., 2014a).
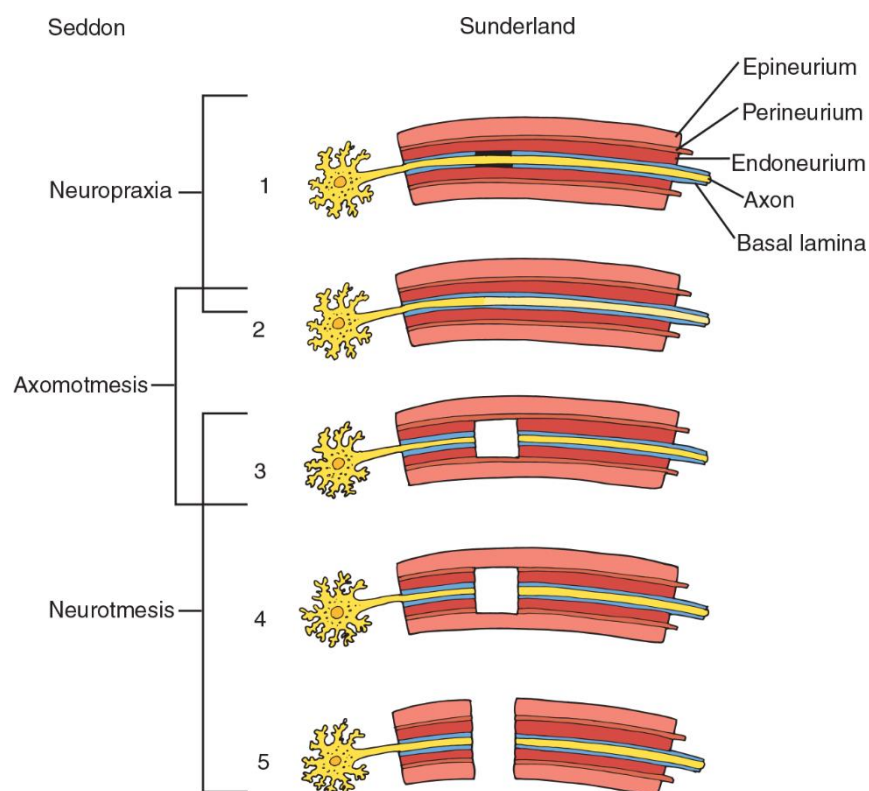
Figure 1.7 Seddon and Sunderland classification of nerve injuries (McGraw-Hill, 2019).

Wallerian Degeneration

After the injuries like axonal disruption or complete nerve transection, several events followed by Wallerian degeneration occur (Ferguson and Son, 2011). These degenerative changes include axon and myelin breakdown at both ends. The connection between distal end and neural body is lost and Wallerian degeneration starts (Figure 1.8); the axon is fragmented; several cellular and molecular changes occur and results in retrograde axonal degeneration in the proximal nerve stump. The removal of cell and tissue debris is performed by Schwann cells and infiltrating macrophages. At the external lamina Schwann cells proliferate and form Büngner bands to guide regenerating axons.
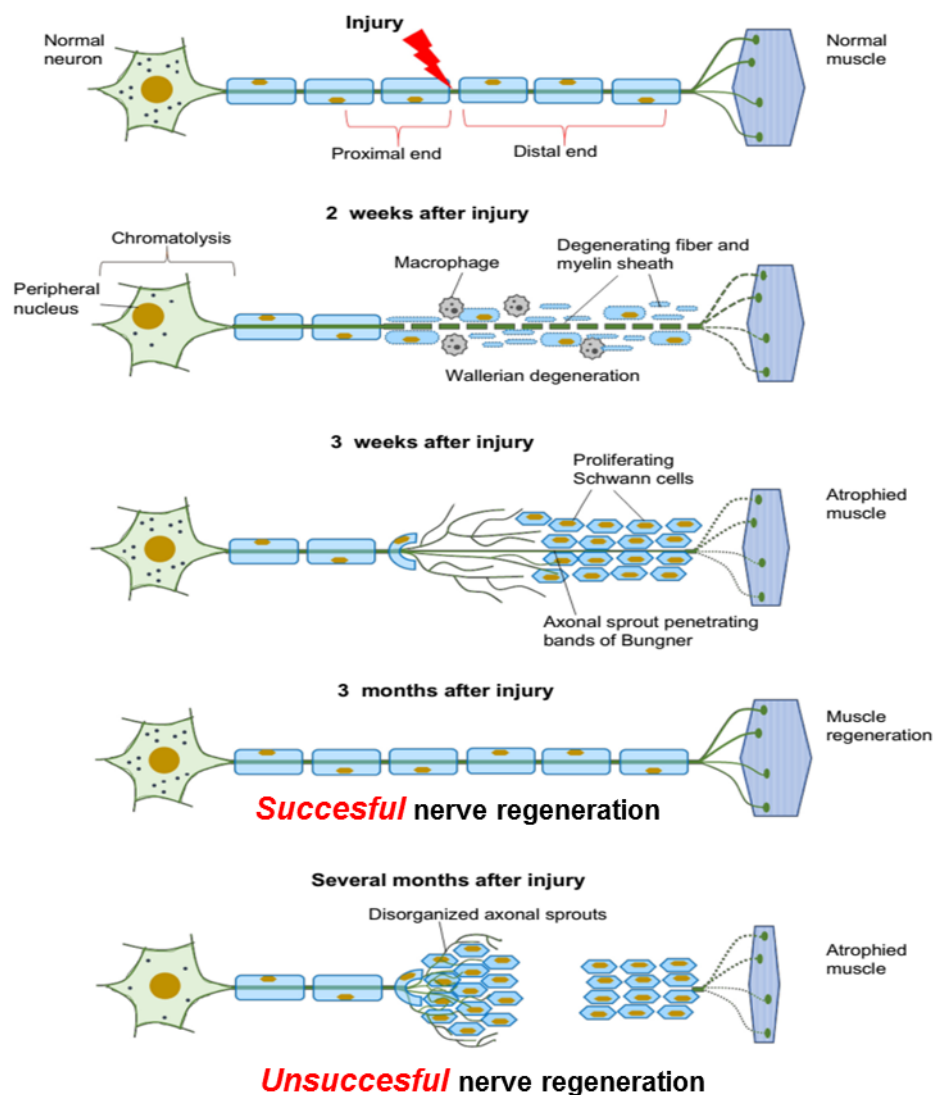
Figure 1.8 Cellular responses to the nerve injury: nerve degeneration and regeneration (Arslantunali et al., 2014a).

1.2.1   Current Treatment Strategies for Peripheral Nerve Injuries

The properties of the injury such as the length of the nerve gap, the time passed between the injury and repair, patient's age and condition are all effective on regeneration. According to the severity of the injury, the regeneration may be spontaneous. In cases, when there is no segmental loss, end to end suturing is

considered as the gold standard for regeneration (Bassilios Habre et al., 2018; Krauss et al., 2022). In this method, nerve stumps are sutured by epineural and/or group fascicular suturing. However, for the cases in which there is a gap in the nerve trunk, end to end suturing is not possible. In those cases, other methods like grafting or nerve conduits are used, because end to end suturing may create a tension in the nerve cable inhibiting the nerve activity (Figure 1.9). The materials like grafts or conduits are used as a bridge between distal and proximal ends of the injured axons.
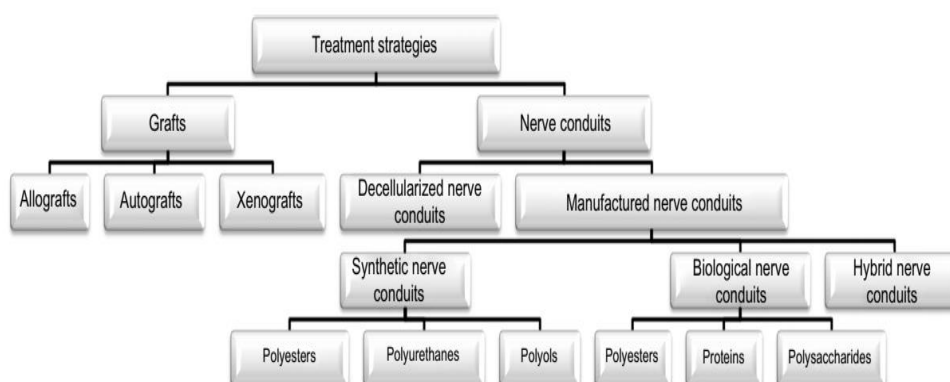
Figure 1.9 Classification of treatment strategies for nerve injuries (Arslantunali et al., 2014a; Krauss et al., 2022).

1.2.1.1 Peripheral Nerve Grafts

Autografts

Autografts are considered as a gold standard where the end to end surgery is not possible (Beris et al., 2019; Krauss et al., 2022). The nerve autografts can be characterized as trunk grafts, which have limited success due to central fibrosis; cable grafts; interfascicular grafts which permit better graft vascularization; and vascularized nerve grafts where a whole nerve is used. Generally, the nerve graft is harvested from other parts of the patient and grafted to the injury site. This procedure results in a nonimmunogenic reaction. The nerve regeneration is possible with Schwann cells and intact endoneurial tubes. However, there are some limitations like neuroma formation, sensory loss at the donor area and limited supply of the graft (Dodla et al., 2019; Jain et al., 2021).

Allografts

Allografts are nerve tissues obtained from a different individual of the same species. Generally, it is used when autografting is not possible. An allograft nerve tissue serves as a support for guidance and a source for viable donor-derived Schwann cells. These donor Schwann cells help connection of axons at the proximal and distal ends to achieve reinnervation of target tissue or organs (Nietosvaara et al., 2019). However, there are also limitations of the use of allografts such as immune rejection (requiring long term use of immunosuppression treatment), secondary infection, cross contamination and limited supply (Boriani et al., 2019, Jain et al., 2021). For these limitations acellular allografts are a recently established option for peripheral nerve reconstruction. However, acellular allografts are the king of a suboptimal option compared with autografts because of the absence of SCs.

Xenografts

Xenografts are used to fill the gap at the injury site and they are obtained from donor from another species (Cetrulo, 2018). When compared to the aoutografts and allografts, there are unlimited source of the donor tissue. However, some of the limitations of the allografts are also valid for the xenografts; necessity for immunosupression, secondary infection, cross contamination. In order to overcome immune rejection, the cellular constituents of xenografts are eliminated by chemical reaction (Deleyto and Lasso, 2018). The decellularized nerve extracellular matrix has a three-dimensional network structure, which retains proteins and carbohydrates, giving structural support to the nerve. This promotes cell migration, proliferation, differentiation and regulation of intercellular communication (Han et al., 2019; Levine et al., 2021).

1.2.1.2 Conduits for Nerve Guidance

Considering the limitations of the grafting methods, researchers have been focused on the alternative methods; nerve conduits (Wieringa et al., 2018; Krauus et al., 2022). Bioactive scaffold production has become an emerging subject that combines engineering and biological sciences. Today, there are various FDA approved

commercially available conduit materials used as an alternative to the gold standard autografts (Table 1.1).

Table 1.1 Commercially available FDA-approved nerve conduits (Arslantunalı et al., 2014a; Krauss et al., 2022).

Product Name	Material	Structure	Company
Neurogen ®	Collagen Type I	Semipermeable, fibrillar structure of the collagen	Integra LifeSciences Co, Plainsboro NJ, USA
Revolnerv ®	Collagen Type I&II	Semipermeable tubular structure of the collagen	Orthomed SA-06640 Saint-Jeannet, France
NeuroFlex™	Collagen Type I	Flexible, semipermeable tubular collagen matrix	Collagen Matrix, Inc, Franklin
Neuromatrix™	Collagen Type I	Semipermeable, tubular collagen matrix	Collagen Matrix, Inc
NeuroWrap™	Collagen Type I	Longitudinal lit in the tubular wall structure	Integra LifeSciences Co.
NeuroMend™	Collagen Type I	Semipermeable collagen wrap designed to unroll and self curl	Collagen Matrix, Inc.
Neurotube®	Polyglycolic acid	Absorbable woven PGA mesh tube	Synovis Micro Companies Alliance, Birmingham, AL, USA
Axoguard ™	Material based on submucosa of swine small intestine	soft, pliable, and porous hydrogel; indicated for the repair of peripheral nerve injuries where there is no gap	Cook Biotech Incorporated, Indiana, U.S.A.
Neurolac™	Poly(D,L-lactide-caprolactone)	Synthetic and transparent PLCL tubular structure	Polyganics BV, Groningen, Netherlands
Salutunnel™	Polyvinyl alcohol	Non-biodegradable PVA tubular structure	Salumedica LCC, Atlanta, GA, USA

These commercially available conduits are generally hollow tubes. The role of the tubes is to bridge a nerve defect around 3-10 mm (Saltzman et al., 2019). The strategy of the nerve regeneration in the nerve conduits include production of the fibrin cable by the injury region of the patient. Both neuronal and non-neuronal cells come to the

injury site and deposit ECM proteins; collagen and laminin. The result of this controlled environment is a decrease in scar formation and accumulation of growth factors produced by the nerve stumps (Narayan et al., 2019; Zhang et al., 2021).

Researchers have focused on the production of an ideal nerve conduits for quite some time in order to overcome the limitations like defect size and production of the scar formation (Meena et al., 2021). The main purpose of the construct is to mimic the autografts and to support axon growth with the properties below;

- In a tubular structure,
- with a porous structure (ideally 10-20 µm) to achieve diffusion of nutrients while preventing infiltration of fibrous scar tissue (Sun et al., 2019),
- to provide mechanical properties that is suitable for nerve regeneration (Ultimate Tensile Strength for acellular nerve tissue: 1400 kPa and elastic modulus: 576 kPa) (Horng et al., 2019),
- present a material compatible with biological tissues and creates a microenvironment suitable for cell attachment/proliferation and regeneration, maintaining a suitable shelf life (Wieringa et al., 2018),
- Provide supportive structures like internal channels, internal matrix cell and growth factor adhesion site (Figure 1.10) (Krauss et al., 2022).
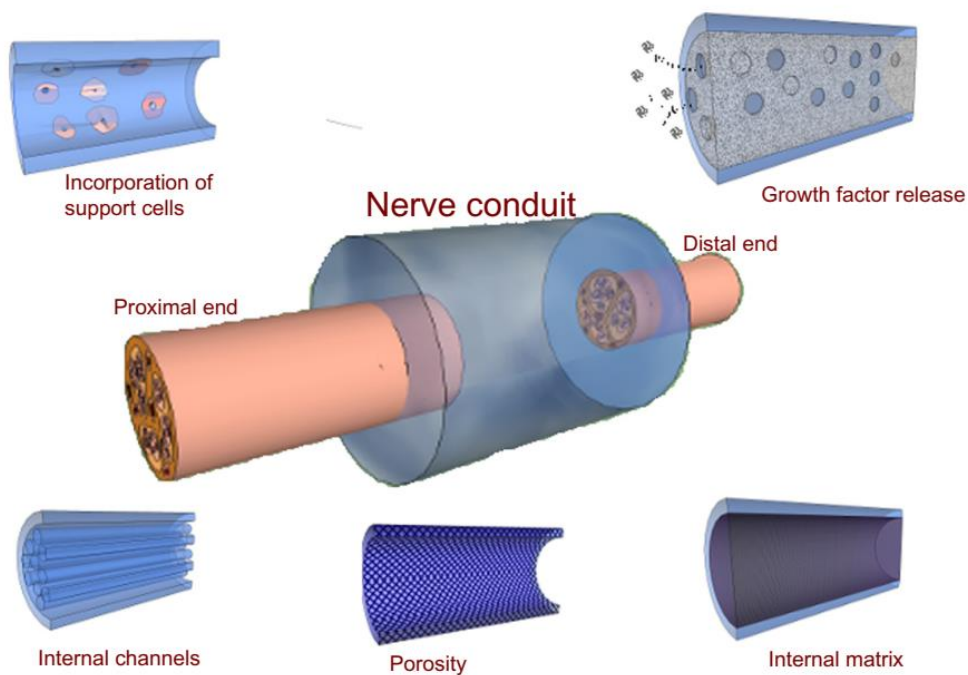
Figure 1.10 Properties of nerve conduit designs (Arslantunali et al., 2014a).

1.3 Nerve Tissue Engineering and Regenerative Medicine

In order to overcome the limitations of the graft materials such as immunogenicity, limited supply, donor site morbidity, the nerve guidance conduits have become very important demand in the treatment of nerve defects (Sarker et al., 2018). The need for replacing damaged tissue and/or stimulating body's response for regeneration has resulted in the development of the field Regenerative Medicine "process of replacing or regenerating tissues or organs to restore or establish normal function" (Riazzi et al., 20018; Hashemi et al., 2021). Tissue engineering is similar to the regenerative medicine and can be defined as "the process of creating living 3D tissues and organs by using engineering, materials and specific combinations of cells and cell signals" (Yucel et al., 2012). After formation of a nerve defect, and it is not possible for an axon to regenerate itself, there arises a need to guide the axon and its environment towards the regeneration process. As a result, tissue engineering method for the development of nerve guidance conduits remains an important field of research area.

14

1.3.1 Nerve Tissue Engineering Scaffolds

The production of tissue engineered guidance conduits for peripheral nerve defects is currently an active field of research. Initial designs included hollow cylindrical materials bridging the nerve gaps. However, these conduits led to wrong target innervations and axonal dispersions (Sarket et al., 2018; Gordon, 2020). As a result, different strategies have been developed to design scaffolds like filling the hollow conduits; with porous, fibrous materials, cell incorporation, use of growth factors.

1.3.1.1 Materials used in Nerve Guides

As an alternative to the grafting materials like autografts, allografts and xenografts, biomaterials (natural or synthetic) have been used to design and develop nerve guides. The basic function of these materials was to support and direct the degenerated axons. Generally a scaffold should be suitable for normal cell behaviors like migration, proliferation, differentiation, maintenance of phenotype (Kijeńska-Gawrońska et al., 2019). Up to now, a variety of biopolymers have been used in the fabrication of nerve conduits. Natural biopolymers are more preferred for the designs because of the compatibility of the materials, but their poor mechanical properties make them difficult to use. The ease of production of the synthetic polymers makes them an obvious choice against the natural polymers. However, their slow biodegradability limits their use. As a result, hybrid conduits could be considered as a good alternative for the use in nerve guidance conduits that have appropriate mechanical properties, ease of fabrication, adjustable degradation times

Natural Polymers

Natural polymers are the polymers generally isolated from organisms or their products. Many are sufficiently hydrophilic, nonimmunogenic and nontoxic (Houshyar et al., 2019; Krauss et al., 2022). Frequently biopolymers used in nerve tissue engineering applications are summarized in Table 1.2.

Jansen et al., reported that a ***hyaluronan-based*** conduit is not cytotoxic and shows good biocompatibility (2004). They tested the conduit in rats, in order to investigate tissue reactions and biodegradation. Angiogenesis was started in the environment of

the hyaluronan-based conduit within a few days. Massive ingrowth of blood vessels into the biomaterial as well as cellular ingrowth into the lumen of the tube was observed after 6 weeks. The effect of hyaluronic acid (HA) and chitosan conduit on peripheral nerve scarring and regeneration were studies in a rat model of a peripheral nerve crush injury (Li et al., 2018). When compared to autografting, they found that HA demonstrated better neural recovery, as measured by reduced nerve adherence to the surrounding tissues, less scar adhesion, increased number of axons, nerve fiber diameter and myelin thickness. Ngo et al., combined the tunability of HA and the customizability of 3D bioprinting, and used the structure for nerve regeneration applications (2020). They reported that Schwann cell adhesion to HA helped the axon regeneration *in vitro*. In another study a simple yet elegant nanofibrous composite comprising of an ultra-low concentration of carboxylated multi-walled carbon nanotubes electrospun within methacrylated hyaluronic acid nanofibers was developed and HA-CNT material offered an alternative substrate to promote tissue-level signaling at the single- cell level that may be present in injury microenvironments.

A scaffold composed entirely of an extracellular matrix component, such as ***collagen***, would be highly desirable for applications in tissue engineering (Lai et al., 2011). They showed that the matrix of oriented collagen fibrils was able to promote cell attachment, proliferation, and extension. Rbia et al., (2019) used NeuraGen type 1 collagen nerve conduits for the treatment of patients and they showed signs of reconstruction of a digital nerve gap <2.5 cm at around 12 months of follow-up. Most of the FDA approved nerve conduits includes collagen (Chrząszcz et al., 2018). As guided nerve regeneration, tubular collagen/PCL scaffolds were used together with neural growth factors to promote neural stem cell migration (Blackstone, et al., 2021). These types of tubular structures of the collagen blends implanted into a hemisection spinal cord defect in mice; however results showed axonal sprouting after ten days which is not desirable for neural regeneration. The applicability of such conduits was limited to lesions measuring less then 3 cm long in the peripheral nerves.

Gelatin-based conduits mimic the fascicular architecture of natural nerve ECM. Wang et al., (2016) used multi-channeled gelatin scaffolds incorporated with neurotrophic gradient for connecting the gaps of nerve defects. They showed that the gelatin containing scaffolds showed superior nerve recovery and less muscle atrophy comparable to the autograft. Gelatin may also be used as a composite in order to increase biodegradability or hydrophilicity of the materials (Liu et al., 2018). It was shown that the proliferation rate of neural stem cells (NSCs) on gelatin-modified nerve conduits (NCs) was faster than on pure NCs. Moreover, higher gelatin concentration induced faster increase in NSCs' numbers. Ye et al., used GelMA as a biomaterial ink for development of a nerve conduit. Stem cell derived neurons were able to proliferate on the designed nerve conduits and differentiated into mature neurons showing the use of GelMA in the structure is a good choice for the production of nerve conduits. Zeinali et al., used thermal induced phase separation to produce porous gelatin scaffold and then filled the hydrogel with graphene oxide aerogel to be used in nerve regeneration applications (2021). They observed P3 mouse cells were able to differentiate into neural cells showing the gelatin platform was suitable to be used in nerve regeneration applications.

Chitosan is a biomaterial derived from chitin, and is the second most abundant polysaccharide in nature, it is obtained through full or partial deacetylation of chitin. Wang et al. (2012) used to bridge a 10-mm-long sciatic nerve gap in rats; they used NGF immobilized genipin crosslinked nerve conduits and the results showed that the nerve conduit allowed nerve reconstruction between two stumps and reinnervation of the target gastrocnemius muscle. In another study by Moattari et al., (2018), regeneration of a transected sciatic nerve using hot water paw immersion (for evaluation of sensory repair), sciatic functional index (for evaluation of motor repair), electromyographical (for evaluation of motor unit repair) and morphological assessments in rat models were used to assess the effectiveness of mesenchymal stem cell seeded chitosan films. The results showed that number of nerve fibers with diameters more than 6 μm increased significantly showing that chitosan improved functional and histomorphological properties of the sciatic nerve after injury, which may have some clinical outcomes as well. Thermally indued phase separation was

used by Ehterami et al., to produce porous and nanofibrous PLA-chitosan blend to be analyzed as nerve conduit (2021). The conduits were evaluated in terms of cell attachment, viability and proliferation of neuroblastoma cells. The results showed that cell attachment was obtained at a fraction of 93% with the addition of chitosan in PLA structure and the cells were able to proliferate and show the neural tissue characteristics.

Alginate is a widely used natural polymer in biomedical applications because of its cell compatibility (Shen et al., 2005); alginate can be physically crosslinked with calcium and this can be used to adjust hydrogel density and mechanical properties. Pfister et al., (2007) used alginate with chitosan. They crosslinked them to produce hydrogels for use as a nerve conduit. They tested their physical and chemical properties as well as cell biocompatibility and found that the conduit matches very well physicochemical requirements in terms of hydrophilicity, permeability, and stiffness as well as surgical handling. A study conducted by Homaeigohar et al., (2019) showed the use of nanocomposite hydrogel made of alginate reinforced by citric acid functionalized graphite nanofilaments in nerve regeneration on PC12 cells. *In vitro* studies proved the biocompatibility of the nanocomposite hydrogel where on PC12 cells proliferate and spread evidently. *In vivo* tests also supported applicability of the nanocomposite hydrogel for implantation within body, and the samples showed no adverse reaction and no inflammatory responses after 14 days.

Poly(3-hydroxybutyrate) (P3HB), a natural polyester synthesized by a wide variety of microorganisms, is biocompatible and biodegradable, invokes minimal immune response and has been proposed for various biomedical applications (Ozer et al., 2018). Zhang et al., (2018) used poly(3-hydroxybutyrate-co-3-hydroxyvalerate) (P3HBV) combined with polyethylene oxide and modified with laminin. Aligned and random-oriented nanofibers were implanted into 12-mm transected sciatic nerve rat models. When compared to the autografted rats, the SFI value of the aligned nanofibrous conduit-implanted rats increased at a more rapid rate from 2 weeks to 4 weeks demonstrate that the aligned nanofibrous conduit could repair the nerve injury more quickly, leading to a better functional recovery in the early stage. Sosa-

Hernández et al., reviewed the use of P3HB in tissue engineering applications; in general, biopolymer structures support cells, initiate growth, prevent misplaced attachments, keep function by the organ affected, grow new tissue, and finally, disappear without toxic effects.

Synthetic Polymers

Synthetic polymers have advantages to be prepared into various shapes, including knitted structures, sponges, solid or porous tubes, meshes, and foams. This makes them favorable to be used in the nerve tissue engineering applications (Winter and Schmidt, 2012). Moreover, transparency is another advantage for *in vivo* models as it facilitates complete 3D examination of the regeneration process (Houshyar et al., 2019). A silicone elastomer *(polydimethylsiloxanes*,PDMS) due to its flexibility and biocompatibility, was one of the initial tubes that was used as a synthetic nerve guides (Heath and Rutkowski, 1998). Hossain et al., (2015) also used silicone tubes and multilayer microchannel scaffolds. They found that the peripheral nerve regeneration including nerve branches and growth cones were observable in the sciatic nerves of Lewis rats. The synthetic polymers used in the nerve conduits are summarized in Table 1.2.

Synthetic polymers may be degradable or nondegradable (Houshyar et al., 2019). "Follow up" surgery must be done to remove nondegradable nerve conduits because it may lead to constricting of the nerve and hampering nerve regeneration. A biodegradable nerve conduit seems to be an excellent substitute with the greatest potential. However, the degradation rate should be sufficiently slow for the conduit to retain its shape and strength throughout the period of regeneration, which may be a difficult optimization for the design because there is no exact time for the regeneration process of the nerves. The conduit should degrade more quickly near the proximal nerve end and slowly at the distal end. Most of the synthetic polymers have been used in blend with natural polymers because of their biocompatibility and degradation profiles (Amini et al., 2021). The mechanical properties of the synthetic polymers are more favorable for the nerve regeneration application because they are able to keep the injury side intact. Thus, good biocompatibility of natural polymers

together with the mechanical properties of the synthetic polymers is favorable for nerve tissue engineering applications.

Poly(lactic acid) (PLA) is a degradable synthetic biopolymer. Fibers can be synthesized as spongelike and rodlike structures. Domingues et al. (2017) reported that the sponge-like and rodlike morphology of the hollow PLA fibers significantly affects their biodegradability and mechanical properties. They concluded that its mechanical, thermal and degradation properties are suitable for nerve tissue engineering applications. Pestana et al., (2018) compared different nerve conduits in terms of the morphological and functional outcomes of peripheral nerve repair. They prepared composite conduits by using PLA and polycaprolactone (PCL) or polyvinylpyrrolidone (PVP) and employed a mechanical hyperalgesia analysis, sciatic functional index (SFI), and electroneuromyography. The results showed that the PLA group showed more vascularization, while the nerve fiber regeneration did not differ among the groups. However, PLA generates lactic acid byproducts, which may be neuro-toxic at higher concentrations (Dixon et al., 2018). İmini et al., fabricated polylactic acid (PLA) nanofibers, gelatin, and polypyrrole blended electrospun nerve conduit (2021). The conduits were analyzed in terms of mechanical properties, hydrophilicity and surface morphology and PC12 cells were used to analyze biocompatibility. The results showed that the adhesion and growth of nerve cells was promising meaning scaffolds produced could be used in nerve tissue engineering applications

Polycaprolactone (PCL) is a degradable synthetic polymer, synthesized by ring opening polymerization of Ɛ-caprolactone. Frost et al., (2018) made electrospun nerve guides, from polycaprolactone (PCL), with aligned fibers along the insides of the channels and random fibers around them. They used a 10 mm rat sciatic nerve defect for testing the nerve guide. The regenerating axons after using these fibers showed that Tailor-made electrospun nerve guides support axonal regeneration *in vivo.* In another study, magnetic PCL nanofibers were incorporated into injectable alginate hydrogel (Ghaderinejad et al., 2021). Neural differentiation of OE-MSCs

was analyzed by resazurin kit and live-dead assay; and the results showed that incorporation of the electrospun PCL fibers boosted cell proliferation and migration.

Polyglycolic acid (PGA) is another degradable polymer synthesized by the carbonylation of formaldehyde in the presence of sulfuric acid (Storti and Latuada, 2017). Quigley et al. reported knitted PLA nerve conduits coated with electrospun PLA (to control pore size) and filled with PLGA fibers in a neurotrophin enriched alginate hydrogel. These conduits were tested on rat sciatic nerves. Formation of myelinated axons inside the lumen and in the distal stump were observed. Matsumoto et al., (2000) evaluated peripheral nerve regeneration across an 80 mm gap using a polyglycolic acid (PGA)-collagen tube filled with laminin-coated collagen fibers. Compound muscle action potentials, motor evoked potentials, and somatosensory evoked potentials were recorded. Results showed gradual recovery of peak amplitudes and latencies.

Poly(lactic acid-co-glycolic acid) (PLGA) is a degradable synthetic polymer synthesized by using lactic acid and glycolic acid monomers in different ratios (Storti and Latuada, 2017). Luis et al. (2007) compared two different nerve conduits: PLGA (90:10) and commercial Neurolac Tube. They used a 10 mm gap of the rat sciatic nerve and found that the level of motor functions in the Neurolac® and PLGA groups were similar to the one of the autografting group. PLGA nerve conduit with associated biodegradable drug reservoir was designed by Lin et al., (2016). The release and function tests showed that PLGA device with an interior release membrane was able to deliver bioactive NGF over a period of at least 20 days where nerve stumps would regenerate.

Polypyrrole (PPy) is a non-degradable, conductive synthetic polymer. It is synthesized by oxidative polymerization of the monomer pyrrole in an aqueous solution (Houshyar et al., 2018). Polypyrrole-coated electrodes for the delivery of charge and neurotrophins were used for axonal regeneration and the results showed that they promoted a neuroprotective environment in damaged nerve *in vivo* (Quigley et al., 2013). Sun et al., (2019) used PPy coating on the surface of electrospun poly(l-lactic acid-co-ε-caprolactone)/silk fibroin. These Ppy-coated NGCs were used to

repair a 10 mm sciatic nerve gap *in vivo*. The results showed that the nerve regeneration of Ppy-coated NGC group was close to autograft group.

Hydrogels are suitable for variety of tissue engineering applications because of their capacity to carry large amount of water. By the help of the intrinsic water, the hydrogels are soft and rubbery like soft tissues (Kuna & Kingham, 2022). The use of hydrogels in nerve tissue engineering applications are promising approach. Arslantunali et al., (2014b) used Multiwalled carbon nanotube loaded pHEMA nerve conduit and tested *in vitro* in terms of mechanical strength, electrical conductivity and cytotoxicity. The results showed that SHSY5Y neuroblastoma cells seeded on mwCNTs carrying pHEMA maintained their viability. In another study pHEMA-GelMA composite nerve conduits were prepared with fibrous inner filler (Dursun Usal et al., 2019). The conduit was tested under *in vitro* conditions with PC12 and Schwann cells as a supporting cells. The results showed that their properties like porosity, degradation, and mechanical strength make the conduit suitable for nerve regeneration applications. Kuo et al., used GelMA hydrogel together with fibroblast growth factor and dental pulp stem cells to be used in 15-mm long sciatic nerve defect (2021). The viability of encapsulated DPSCs in GelMA-bFGF hydrogels was analyzed by Live/Dead assay and the results showed that they were able to attach and proliferate in the conduits. In addition, SFI study showed that a comparable nerve regeneration was observed with the control group in which autologous nerve growth was used.

Table 1.2 Natural and Synthetic Polymers used in Nerve Tissue Engineering Applications.

Natural Polymers		
Material	**Structure**	*Reference*
Hyaluronic acid derivatives	Individually knitted strands strengthened by coating with a thin layer of the same polymer, a conduit with an internal diameter of 2 mm and a length of 18 mm;	Jansen et al., 2004;
	Chitosan/HA Composite hollow nerve conduit	Li et al., 2018.
	HA hydrogels analyzed with Human Spinal Cord Derived Neural Progenitor Cells to be used in spinal cord nerve repairs	Lin et al., 2021
Collagen	A small diameter tubular matrix constructed of anisotropic collagen fibrils;	Lai et al., 2011;
	NeuraGen™ type 1 collagen nerve conduit;	Rbia et al., 2019;
	Collagen Gelatin composite conduits	Sanghvi et al., 2008.
	Collagen microsponges prepared on PLGA mesh, analyzed in vitro to be used in nerve tissue engineering	Xie et al., 2022
Gelatin	Collagen-Gelatin composite conduits;	Sanghvi et al., 2008;
	Multi-channeled, electrospun gelatin scaffold incorporated with neurotrophic gradient;	Wang et al., 2016;
	Gelatin wrap or embedded nanofibrous microstructures	Liu et al., 2018
	GelMA-pHEMA Hydrogels	Dursun Usal et al., 2019
	3D printing of gelatin-based biomimetic triple-layered conduits	Liu et al., 2021
Chitosan	Chitosan/HA Composite hollow nerve conduit.	Li et al., 2018.
	NGF loaded, genipin crosslinked chitosan.	Wang et al., 2012
	Mesenchymal stem cell added chitosan films.	Moattari et al., 2018
	Alginate/chitosan hydrogel conduits.	Pfister et al., 2007
	Alginate/chitosan hydrogel; improved sciatic nerve regeneration *in vivo*	Bagher et al., 2021
Alginate	Alginate/chitosan hydrogel conduits.	Pfister et al., 2007
	Nanocomposite hydrogel made of alginate reinforced by citric acid functionalized graphite nanofilaments	Homaeigohar et al., 2019
	An injectable alginate hydrogel composed of magnetic polycaprolactone (PCL) short nanofibers	Ghaderinejad et al., 2021
P3HB and PHBV	Chitosan-coated PHB conduit seeded with hMSC	Ozer et al., 2018
	Laminin-modified and aligned poly(3-hydroxybutyrate-co-3-hydroxyvalerate)/polyethylene oxide nanofibrous conduits	Zhang et al., 2018
	Gelatin-PHBV aligned fiber mats	Dursun Usal et al., 2019
	PCL / PHBV / MWCNT Biodegradable-nondegrdable Nanocomposites comparison in nerve tissue engineering	Yousefi et al., 2021

Table 1.2 (Continued)

Material	Structure	Reference
Synthetic Polymers		
PLA	Sponge-like and finger-like hollow PLA nerve conduits	Domingues et al., 2017
	PLA/PCL or PLA/PVP composite conduits	Pestana et al., 2018
	Fabricated by an extrusion technique, had an inner diameter of 1.6 mm, an outer diameter of 3.2 mm, and a length of 12 mm.PLA conduits	Evans et al., 1999
	A highly porous scafold by poly (L-lactic acid) (PLLA)/ chitosan blend using liquid–liquid phase separation (LLPS) technique	Ehterami et al., 2021
PGA	polyglycolic acid (PGA)−collagen tube filled with laminin-coated collagen fibers	Matsumoto et al., 2000
	knitted PLA nerve conduits coated with electrospun PLA (to control the pore size) and filled with PLGA fibers	Quigley et al., 2013
	PGA nerve conduit vascularized by host superficial inferior epigastric (SIE) for 14 days	Muangsanit et al., 2018
PLGA	16 mm long, internal diameter of 2.0 mm, and thickness wall of 1.5 mm PLGA (90:10) nerve conduit	Luis et al., 2007
	PLGA (75:25) nerve conduit loaded with NGF	Lin et al., 2016
	PLGA conduit of aligned nanofibers produced by the electrospinning method, functionalized with gelatin and seeded either with mouse embryonic stem cells or with human mesenchymal stem cells	Pozzobon et al., 2021
PCL	PLA/PCL coposite conduits	Pestana et al., 2018
	Electrospun nerve guides	Frost et al., 2018
	An injectable alginate hydrogel composed of magnetic polycaprolactone (PCL) short nanofibers	Ghaderinejad et al., 2021
PDMS	A basic silicone tube	Heath and Rutkowski, 1998
	Multilayer microchannel PDMS scaffolds	Hossain et al., 2015
	an elastomer—polydimethylsiloxane (PDMS)—to produce lattice-type scaffolds from a photolithography-defined template resulted in network formation of neurons	Li et al., 2018
PPy	Polypyrrole-coated electrodes for the delivery of charge and neurotrophins	Quigley et al., 2013
	PPy coating on surface of electrospun poly(l-lactic acid-co-ε-caprolactone)/silk fibroin	Sun et al., 2019,
	polyethylene glycol amide core-conjugated with a thiazole-based building block and a peptide sequence on PPy; electrical stimulation resulted in a significant increase in axonal outgrowth	Broas et al., 2021
pHEMA	GelMA-pHEMA Composite Hydrogels with fibrous inner filler	Dursun Usal et al., 2019
	Multiwalled carbon nanotube loaded pHEMA nerve conduit	Arslantunali et al., 2014b

1.3.1.2 Fabrication Techniques

The main aim in the production of the nerve conduits is to produce a material capable of connecting the distal and proximal ends of the defect site. Solvent casting, electrospinning, freeze drying, phase separation and 3D printing are some of the conventional methods used to produce nerve guides (Houshyar, 2019; Yang et al., 2021). Fabrication techniques are different depending on the type of materials and their characteristics, including whether they are a synthetic or natural polymer.

The electrospinning technique is a randomly or longitudinally aligned nanofiber production process using an electric field (Yi et al., 2018; Qian et al., 2021). The electrospinning setup includes a high-voltage power supply, a syringe pump, a spinneret and a conductive collector. While a liquid is excluding from the syringe pump, an electrical field is applied and the droplet deforms into a Taylor cone. From the cone a charged jet is ejected. Solid fibers are deposited from this jet stretching into finer diameters. The nervous tissue has nanosize fibrous tissue, so the electrospinning is widely used technique in the production of the nerve conduits (Haider et al., 2018; Rahmati et al., 2021). For example, Quan et al. (2019) developed a 3D helix flexible nerve guide through electrospinning of PCL and implanted it into the rat sciatic nerve, which showed less tension during operation. In another study, PHBV fiber mats are used as filling material of a nerve conduit (Dursun Usal et al, 2019). It was shown that aligned mat would provide and ideal nerve guide because the fibers may guide regenerating axons.

Solvent casting is a method in which mineral and organic particles are dispersed in polymer solution (Deng et al., 2018; Xue et al., 2021). This method can be used for any polymer that is soluble in organic solvents. The advantages of the method are the production of highly porous structures and tailoring the crystallinity. ***Freeze drying*** is a method used widely in the production of the nerve guides (Chono et al., 2015). It is a drying process including 3 major steps: a) the solution is frozen (-80^0 C); b) the sample is placed into lyophilizator in which the pressure is lowered through a partial vacuum; c) removal of the water/solvent from the polymer leaving the solid

part. Both solvent casting and freeze drying methods are widely used in the production of nerve conduits (Ho et al., 2019; Lin et al., 2017; Carvalho et al., 2018; Vijayavenkataraman et al., 2019; Manoukian et al., 2019; Devi et al., 2021).

Computer aided designs are also used for the production of the nerve guides (Petcu et al., 2018; Almeida et al., 2021). *Rapid prototyping* is a bottom-up method to produce a scaffold; the 3D structures are produced layer by layer using a additive process (Nguyen et al., 2015; Naser et al., 2021). The 3D structures that are not possible to produce with the other traditional methods are produced by rapid prototyping. So it is a potential method to produce nerve guides with desired and precisely defined architectures. There are different types of rapid prototyping: *fused deposition modeling* (FDM), in which a solid polymer is cast into a hot extrusion nozzle to be melted and extruded on the surface of a 3D object (Mohseni et al., 2018); *selective laser sintering* (SLS), in which successive layers of powdered materials are scanned with laser beam to create 3D object (Gayer et al., 2019); *stereolithography* (SLA), in which UV light is irradiated on photosensitive liquid resin surface in a precise pattern determined by CAD files (Heo et al., 2019); and *bioprinting*, in which a computer controlled 3D printing device is used to deposit cells accurately to form 3D cell structures (Dixon et al., 2018; Cadena et al., 2021).

1.3.1.3 Support Structures for Nerve conduits

An artificial nerve conduit with a tube structure has been investigated. In such studies, regeneration failed for long nerve gaps due to exceeding regenerative capabilities of the damaged nerve stumps (Marchesi., 2007). A filled tube with glial cells, growth factors, cells, or fibers such as Schwann cells, laminin, collagen, and stem cells enhances the regeneration potential of the tubulation method, which is necessary for an optimal axon immigration (Ho et al., 2019; Yang et al., 2021).

1.3.1.3.1 Cell Sources

For tissue engineering applications, cells are the most important part of the scaffolds. For nerve tissue engineering applications mostly used support cells are Schwann

cells, olfactory ensheating cells, and stem cells like nerve stem cells, embryonic stem cells and bone marrow mesenchymal stem cells (Dodla et al., 2019). In addition to the support cells, some neuronal cell lines are used for *in vitro* studies, namely, SH-SY5Y (Arslantunali et al., 2014b; Nune et al., 2019; Merryweather et al., 2021), PC12 (Dursun Usal et al., 2019; Wang et al., 2016; Liu et al., 2021), MN9D (Eve et al., 2018; Wei et al., 2019; Wang et al., 2021) and NT2 (Hsu et al., 2018).

Schwann Cells

In the PNS, SCs are support cells that wrap around the axons. SCs form a multilamellar sheath of myelin. Neurotrophic factors are produced in the target organs and by SCs in response to injury. The cytokines released during Wallerian degeneration activate SCs that produce neurotrophins such as NGF and brain-derived neurotrophic factor (BDNF) (Dodla et al., 2019). For nerve gaps less than a critical length (10 mm), the formation of a fibrin cable, migration of SCs, and longitudinal arrangement of SCs are spontaneously occurring processes. However for longer gaps, it is necessary to supply Schwann cells for those processes to occur (Rebowe et al., 2018). So recently, Schwann cells has been used as support materials in the nerve conduits. Han et al., (2019) showed that transplantation of Schwann cells helped the axon regeneration. In another study Dursun Usal et al., (2019) showed PC12 cells attached and proliferated more in the presence of Schwann cells.

Olfactory Ensheating Cells

Olfactory ensheating cells (OECs), specialized Schwann cells, are the nervous system cells that facilitate regenerating and appropriately retargeting in order to overcome the constant damage and repair in the nasal cavity (Kabiri et al., 2015). Autologous OEC transplantation has improved the efficacy of nerve conduits in peripheral nerve regeneration (Rodriguex et al., 2000). It was shown that rat sciatic nerve segmental defect model achieved greater functional recovery and axon density using collagen nerve conduits filled with OECs (Eward et al., 2019). Although OECs are generally used for the repair of central nervous system, they are also used as support cells for peripheral nerve regeneration (Lu et l., 2019; Boecker et al., 2018; Rasulic et al., 2019; Lee et al., 2021).

Stem Cells

Stem cells from bone marrow, adipose tissue, skin, dental pulp, umbilical cord and nerve tissue has been used for nerve regeneration applications as an alternative to SCs and OECs (Seyed-Forootan et al., 2019). ***Nerve stem cells*** are derived from 3 different sources; a- extraction from primary sources; b- differentiation; c- trans-differentiation (Fairbairn et al., 2015). Their ability to differentiate into neurons and glial cells make them a good candidate to be used in nerve tissue engineering applications (Jiang et al., 2017; Kubiak et al., 2019; Kuna et al., 2022). ***Embryonic stem cells (ESCs)*** are pluripotent cells found in an embryo. These cells have ability to differentiate into all cells of the body making them used for peripheral nerve regeneration applications (Klimanskaya, 2019). Although differentiation into neural cell lines is limited, there are several studies that ESCs are used for peripheral nerve regeneration (Jondes et al., 2018; Kubiak et al., 2019; Zarrintaj et al., 2021). ***Bone marrow mesenchymal stem cells (BMSCs)*** are widely used cells in peripheral nerve tissue engineering applications. They are found in the stroma of the bone marrow and they support hematopoiesis, they have ability to differentiate into mesenchymal lineages (Klimczak and Kozlowska, 2016; Kuna et al., 2022). They are widely used in the peripheral nerve regeneration as an alternative to Schwann cells and the results obtained show that they are really supportive cells for axonal regeneration (Fernandes et al., 2018; Kızılay et al., 2018; Usach et al., 2018; Abbas et al., 2019). Other stem cells that are used for peripheral nerve regeneration are ***adipose derived stem cells*** (Resch et al., 2019; Bucan et al., 2019), ***induced pluripotent stem cells*** (Xia et al., 2019), ***skin derived precursor stem cells*** (Mehrotraet al., 2019), ***dental pulp stem cells*** (Pisciotta et al., 2020) and ***fetal derived stem cells*** (Su et al., 2018).

1.3.1.3.2 Bioactive Agents

Neurotrophic factors are produced in the target organs by SCs in response to injury (Burnet and Zager, 2004). To improve the repair process, in addition to providing guidance, therapeutic agents need to be provided at the site of transection or injury (Daly et al., 2012). Several drugs and growth factors have been shown to be effective

in enhancing axonal outgrowth across nerve gaps (Ho et al., 2019; Seyedebrahimi et al., 2021) Widely used neurothropic factors are brain-derived neurotrophic factor (BDNF), nerve growth factor (NGF) and glial cell-line derived neurotrophic factor (GDNF).

Nerve growth factor (NGF) is a well-known growth factor discovered in 1956 (Dodla et al., 2019). Studies have shown that NGF production in target organs of sensory and sympathetic nerves in the PNS promote the survival of sensory ganglia and nerves, including spinal sensory nerves and sciatic nerves. A study of nerve growth factor (NGF) loaded microspheres has shown potential in repairing nerve gaps (Sun et al., 2012) and another study showed that collagen tubes loaded with NGF have demonstrated axonal elongation *in vitro* studies (Madduri et al., 2010; Ahmed et al., 2021). So NGF is widely used growth factor in nerve conduits (Liao et al., 2019; Wang et al., 2019; Lackington et al., 2019; Manoukian, 2019; Liu et al., 2021).

Brain derived neurothrophic factor (BDNF) is another neurotrophin that is upregulated in injured peripheral nerves that promote the survival and outgrowth of sensory and sympathetic nerves as well as motor nerves (Lee et al., 2003). Thus, it has been widely used as a support material for nerve regeneration. It has been shown to direct the growth of neurites from PC12 cells toward increasing concentrations of neurotrophic factors (Xie et al., 2015; De la Rosa et al., 2017; Ikegami and Ijima, 2019; Li et al., 2019). In addition, *in vivo* studies showed that, release of BDNF from nerve conduits helped regeneration of the injured axons (Gao et al., 2016; Hei et al., 2017; McGregor et al., 2018; Moskow et al., 2019; Seyedebrahimi et al., 2021).

Glial cell-line derived neurotrophic factor (GDNF) stimulates the proliferation of Schwann cells and the survival of sensory and motor neurons. Lackington et al., (2019) incorporated GDNF-loaded microparticles into the nerve guidance conduit, resulting in controlled biphasic release kinetics, capable of eliciting an enhanced biological response *in vitro*, and they also showed the capacity to enhance nerve regeneration across a 15 mm sciatic nerve defects in rat with nerve functional

recovery levels comparable to those achieved with autografts. Similarly, there are many studies in the literature showing the use of GDNF in nerve conduits as a supporting material helping axon regeneration (Tajdaran et al., 2016; Fregnan et al., 2017; Zhen et al., 2019; Fang et al., 2019). Many other trophic factors, including *insulin-like growth factor* (Zhue et al., 2018), *fibroblast growth factor* (Fujimaki et al., 2017), and *ciliary neurotrophic factor (CNTF)* (Lee et al., 2018), have been shown to be involved in the promotion of nerve regeneration.

1.4   Aim and Novelty of the Study

The aim of the present study was to construct a tubular nerve guidance conduit containing inner matrix together with a cell support. It was then tested for its functionality and cell compatibility. The outermost layer of the guide was composed of a porous poly(2-hydroxyethyl methacrylate) (pHEMA) tube onto which Schwann cells was added to serve as support cells. The inner nerve guidance was constituted of methacrylated gelatin (GelMA) and methacrylated hyaluronic acid (HaMA) interpenetrating polymer network (IPN) to support and guide the attached cells *in vitro* and regenerating axons *in vivo*. *In vitro* testing of the nerve guide was performed with SHSY5Y cells, it was observed that the cells were able to migrate along the nerve guide by the help of NGF secreted by SCs. Hyaluronic acid, an ECM component, was associated with decreased scarring and improved fibrin matrix formation. It is hypothesized that during the fibrin matrix phase of regeneration, hyaluronic acid organizes the ECM into a hydrated open lattice, thereby facilitating migration of the regenerated axons. In the present study, HaMA was blended with GelMA to create an IPN as a novelty for peripheral nerve regeneration. pHEMA-GelMA composite use in nerve regeneration was previously described (Dursun Usal et al., 2019). In the present study pHEMA itself was used to wrap around the injured nerve truck after coated with collagen, an ECM molecule for the attachment of the cells. Because pHEMA was not degradable, during the time that axons needed for regeneration, it kept the nerve guide stable, during this time GelMA-HaMA matrix was degrading, allowing the cells to grow and migrate. SHSY5Y cells was used as a model for the study. They mimicked the growing axons. Schwann cells were used as

supporting cells, meaning that they will also be used in the nerve conduit when the guide is implanted. It was shown that Schwann cells supported growing SHSY5Y cells by providing necessary factors like NGF for regeneration. In addition, Netrin-1 molecule, a factor found in the nervous system for the growing axons, was used to guide the cells in the IPN structure. The design of the nerve guide in the present study combining non degradable pHEMA tubular scaffold and degradable GelMA-HaMA IPN together with the presence of SCs secreting necessary growth factors for SHSY5Y cells to grow their axons and use of Netrin-1 protein to guide the neurite extensions through IPN presents a novel approach for nerve injury repair.

CHAPTER 2

MATERIALS AND METHODS

2.1   Materials

2-Hydroxyethyl methacrylate (>99%), ethyleneglycol dimethacrylate (98%), hyaluronic acid sodium salt from Streptococcus equi (<1% protein), methacrylic anhydride (94%), gelatin (Type A from porcine skin), N,N-dimethylformamide (DMF), 1-[4-(2-hydroxyethoxy)-phenyl]-2-hydroxy-2-methyl-1-propan-1-one (Irgacure 2959), thiazolyl blue tetrazolium bromide, bovine serum albumin (BSA), sodium cacodylate, glutaraldehyde (25%), NGF-β from rat, mouse anti-human collagen Type I, and Alexa Fluor 532-conjugated anti-mouse Ig antibody, 4',6-diamidino-2-phenylindole dihydrochloride (DAPI) and FITC-conjugated Phalloidin are purchased from Sigma-Aldrich (USA).

Sodium dihydrogen phosphate (NaH_2PO_4), disodium hydrogen phosphate (Na_2HPO_4), sodium chloride (NaCl), ethanol, acetic acid (HAc), acetone, 1,4-dioxane, and Tween- 20 were purchased from Merck Millipore (Germany). DMEM-High glucose, DMEM High glucose colorless, fetal bovine serum (FBS), trypsin-EDTA (0.25%) (HyClone), and SnakeSkin pleated dialysis tubing were purchased from Thermo Scientific (USA).

Newborn calf serum was from Lonza (Sweden). NucleoCasette was obtained from ChemoMetec (Denmark). Penicillin/streptomycin (Pen/Strep) (100 units/mL - 100 µg/mL), and bovine serum albumin (BSA) were purchased from Fluka (Switzerland). Ammonium persulfate (APS), dimethyl sulfoxide (DMSO) and Triton-X 100 were obtained from AppliChem (Germany). Anti-neuron specific beta-

III tubulin antibody, anti-myelin basic protein, anti-NeuN, Donkey anti-Rabbit IgG H&L (DyLight®488) secondary antibody were purchased from Abcam (USA). Cell lines Schwann Cells (SW 10, ATCC CRL-2766) and SHSY5Y (neuroblastoma cell line, human derived, ATCC CRL-2266.Adh) were purchased from ATCC (USA).

2.2   Methods

In the present study, pHEMA cylindrical structure (hydrogel membrane) will be filled with GelMA-HaMA IPN. The first step will be an optimization of the conditions for pHEMA and GelMA-HaMA matrix production. The pHEMA membrane will be characterized by water absorption, contact angle and mechanical strength, followed by microscopical examination by scanning electron microscopy (SEM). GelMA-HaMA IPN characterization studies will include NMR, FTIR Analysis, water content determination, contact angle and degradation tests. *In vitro* studies will be performed with Schwann cells as support cells and PC12 cells. Schwann Cells will be seeded on pHEMA and the inner part (GelMA-HaMA) will include PC12 cells. Cytotoxicity of the materials will be determined with live-dead assay and proliferation of the cells on the structure will be tested by MTT assay. Microscopical examination of the cells will be performed by Confocal Laser Scanning Microscopy (CSLM) and SEM.

2.2.1   Preparation of pHEMA Nerve Guides

Cylindrical pHEMA hydrogel membranes were produced in the molds prepared by stereolithography (SLA 2, Formlabs, United States). The inner cylinder and lids of the mold were printed from Dental SG Resin, a class 1 biocompatible print resin; and an outer cylinder, a glass tube, was placed in between the lids (Figure 2.1). PHEMA samples were prepared by solution polymerization (Lu and Anseth, 1999). Different concentration of HEMA monomer and distilled water were mixed (44, 50, 55, 58% water in reaction mixture) and then crosslinker (EGDMA) was added to the mixture (0.4%, v/v, crosslinker in monomer). Finally, Irgacure (2-(hydroxyl)-4-(2-hydroxyethoxy)-2-methylpropiophenone) was added to the reaction mixture as an initiator (0.025%, w/v). After the solution was mixed well, the bubbles were removed

by vacuum and incubated with UV (365 nm) for 1 h at room temperature. After the polymerization reaction, the pHEMA polymers were placed into excess distilled water to remove unreacted monomers and crosslinkers. The polymers were then lyophilized for 6 h. Dried polymers were stored at room temperature for the experiments.
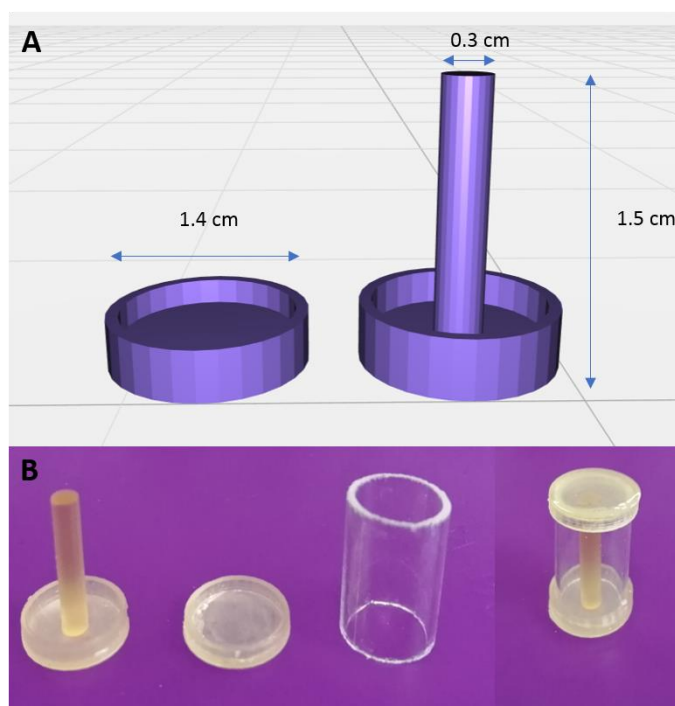
Figure 2.1 pHEMA mold printed from Dental SG Resin. A. Sketch of the SLA system. B. The complete mold.

2.2.1.1   Collagen Coating on pHEMA

Collagen was dissolved in 20% acetic acid at $50^{\circ}C$ overnight (1%, w/v). Dried pHEMA hydrogels were immersed in collagen solution for 24 h at room temperature. Swollen hydrogels were washed with distilled water and then lyophilized for 8 h. Dried polymers were stored at $4^{\circ}C$ for the experiments and sterilized under UV light for 30 min before cell seeding.

2.2.2   Synthesis of Methacrylated Gelatin (GelMA)

Synthesis of methacrylated gelatin was performed by the method previously described by Shirahama et al. (2016). Briefly gelatin type A was dissolved in carbonate buffer (20%, w/v; 0.25M CB Buffer pH: 9) and methacrylic anhydride was added to the solution (0.1 mL for 1 g of gelatin) (Figure 2.2) and then incubated at 50^0C for 3 h. The pH was adjusted to 7.4 and the solution was filtered and dialyzed in a dialysis tubing (CO 10,000) against distilled water for 3 days at 37^0C to remove excess methacrylic acid and salts. After dialyzing, the solution was lyophilized to obtain a white foam for 1 week. The resultant GelMA is stored at 4^0C until further use.
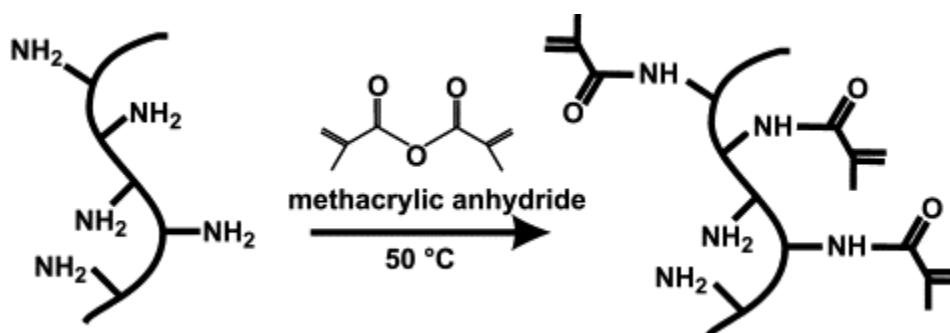
Figure 2.2 Methacrylation of gelatin (Nichol et al., 2010).

2.2.2.1   Determination of Methacrylic Acid Content of GelMA with NMR

^{1}H NMR is used to determine methacrylation degree of gelatin. Gelatin and GelMA will be dissolved in D_2O (30 mg/mL) at 40^oC. Bruker DPX 400 spectrometer will be used to obtain NMR Spectra at a ^{1}H resonance frequency of 400 MHz.

2.2.3   Synthesis of Methacrylated Hyaluronic Acid (HaMA)

Methacrylated hyaluronic acid was synthesized by a method previously described by Smeds and Grinstaff (2001). Briefly hyaluronic acid was dissolved in distilled water (1%, w/v) at room temperature for 24 h, then dimethyl formamide was added to solution (2:3, DMF:dH$_2$O) slowly, the solution was incubated at 4^0C for 1 h. Methacrylic anhydride was added to solution (5%, v/v) and the pH was adjusted to 8-9 and controlled for 5 h (Figure 2.3). The solution was incubated in ice overnight.

After incubation the solution was dialyzed in a dialysis tubing (CO 10,000) against distilled water for 3 days at 4°C. The dialysis water was changed every 12 h. After dialyzing, the solution was lyophilized for 1 week, a white foam was obtained. The resulting HaMA is stored at 4^0C until further use.
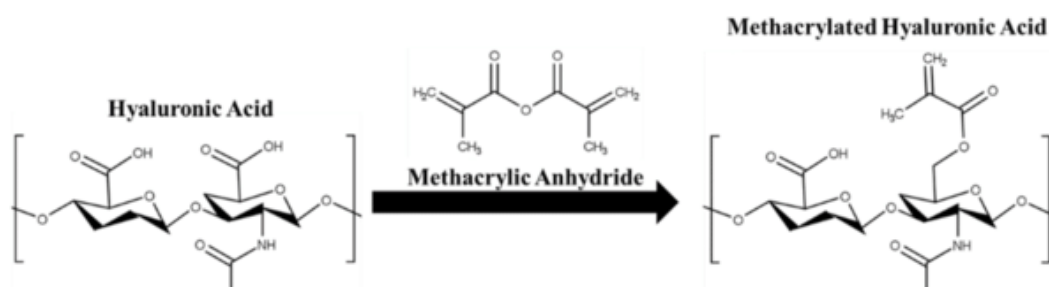
Figure 2.3 Synthesis of methacrylated hyaluronic acid (Skardal et al., 2010).

2.2.3.1 Determination of Methacrylic Acid Content of HaMA with NMR

^{1}H NMR was used to determine methacrylation degree of hyaluronic acid. Hyaluronic acid and HaMA were dissolved in D_2O (5 mg/mL) at 60°C. Bruker DPX 400 spectrometer was used to obtain NMR Spectra at a ^{1}H resonance frequency of 400 MHz.

2.2.4 Preparation of GelMA-HaMA Matrix

Gelatin-methacryloyl/hyaluronic acid methacryloyl matrix (GelMA/HaMA) was synthesized by dissolving GelMA and HaMA (5:95, 10:90, 15:85, 20:80) in PBS (1% HaMA, w/v). After dissolving GelMA and HaMA, Irgacure (2-(hydroxyl)-4-(2-hydroxyethoxy)-2-methylpropiophenone) was added as the photoinitiator (1%, w/v) and the solution was exposed to under UV for 5 min.

2.2.4.1 FTIR Analysis

FTIR-ATR spectroscopy (Perkin Elmer Spectrum, Frontier, Massachusetts, USA) was used to analyze the surfaces of the polymers to determine the GelMA-HaMA homogeneity and methacrylation degree. The samples were scanned 4 times in the range 400-4000 cm^2 with a resolution of 4 cm^{-2}.

2.2.5 Characterization of Conduit Materials

2.2.5.1 Water Content and Swelling

Lyophilized pHEMA hydrogels and GelMA-HaMA matrix were weighed and then placed into PBS for 24 h. Their weights were determined after swelling. Equation 1 and 2 were used for the calculation of the water content.

$$WC\ (\%) = \frac{w_s - w_d}{w_s} \times 100 \tag{1}$$

$$Swelling\ (\%) = \frac{w_s - w_d}{w_d} \times 100 \tag{2}$$

where

WC (%): Water content (%, w/w)

w_s: wet weight

w_d: dry weight

2.2.5.2 Water Contact Angle

Dry polymers were placed into distilled water for 24 h at room temperature at allowed to swell. After removing the excess water, an optical tensiometer One Attension (Biolin Scientific, Finland) was used to determine the contact angles of the polymers. For measurement, water droplets were placed at 5 different locations and water contact angle was calculated by the instrument using Young Equation (Equation 3).

$$\Upsilon_{sv} = \Upsilon_{sl} + \Upsilon_{lv} \cdot \cos\Theta \tag{3}$$

where Υ_{sv} was the surface free energy of the solid (sv: solid-vapor), Υ_{lv} was the liquid surface tension (lv: liquid-vapor), Υ_{sl} was the interfacial tension between liquid and solid (sl: solid-liquid; Figure 2.4).
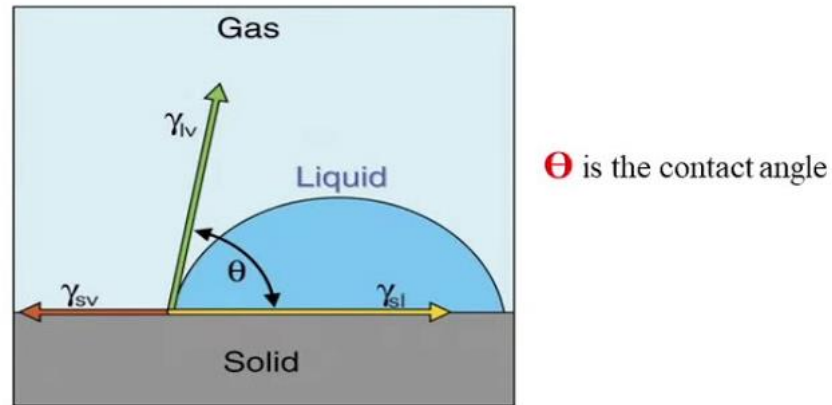
Figure 2.4 Components of a three-phase system (Leonova et al., 2016).

2.2.5.3 Mechanical Test

The hydrogels (after brought to equilibrium swelling in water, 24 h, RT) were cut in dimensions of 30 mm length and 10 mm width. The thicknesses were measured before testing. Tensile modulus of the polymers was tested by using CellScale, Univert (Canada). The samples were fixed between the clamps (gauge length: 10 mm) and the properties were measured by straining at a rate of 20 mm/min.

After obtaining the results, the ultimate tensile strength (UTS), strain at break (ϵ_f) and elastic modulus (E) were calculated by using equations below (Figure 2.5):

$$\text{UTS} = \frac{F}{A} \qquad (4)$$

$$E = \frac{\Delta F}{A} \times \frac{L}{\Delta L} \qquad (5)$$

$$\epsilon_f \ (\%) = \frac{L_f - L_i}{L_i} \ x \ 100 \qquad (6)$$

where

F: Force (N)

A: Area (mm^2)

E: Elastic modulus (N/mm^2)

L: Length (mm)

L$_i$: Initial length (mm)

L$_f$: Final length (mm)

ε_f: Strain at break
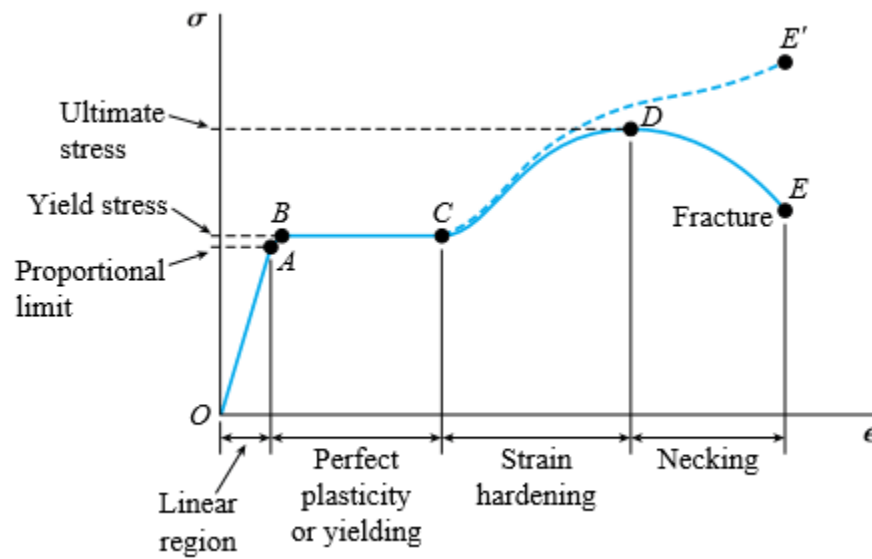
Figure 2.5 Stress-strain curve for materials' UTS (ultimate tensile strength). Yield stress is defined by an offset line, corresponding to a given amount of plastic deformation.

2.2.5.4   Degradation Test of GelMA- HaMA Matrix

In order to study degradation behavior of GelMA-HaMA matrixes, the hydrogel was weighed 0.1 mg and incubated in PBS (10 mM, pH 7.4) and cell culture medium for 4 weeks at 37^0C. Weight loss was determined weekly after removing samples from PBS, rinsed with distilled water, and lyophilized. Equation 7 was used to calculate degradation as the percent weight loss.

$$\text{Remaining weight (\%)} = \frac{w_0 - w_d}{w_d} \times 100 \tag{7}$$

where

40

w_0: the initial dry weight

w_d: dry weight after incubation

2.2.5.5 SEM

The polymer samples were lyophilized for 8 h (Labconco, FreeZone6p Plus, USA) and attached on SEM stubs with carbon tapes. Gold was used to coat all the samples under vacuum and examined with a scanning electron microscope (SEM, Quanta FEI, United States). The results were analyzed using ImageJ (NIH, USA) to examine the surface structures; pore sizes and porosities of the polymers.

2.2.6 *In vitro* Studies

In vitro studies were carried out to determine the cytotoxicity of pHEMA and GelMA-HaMA hydrogels on Schwann Cells (SCs) and SHY5Y cells, respectively. In addition, the support of Schwann Cells was tested by using Myelin Basic Protein Antibody Staining in order to understand NGF secretion.

2.2.6.1 Culturing Schwann Cells and SHSY5Y cells

The growth conditions for the cells were the same. The cells were cultured in a growth medium that contains Dulbecco's Modified Eagles Medium with high glucose, fetal bovine serum (FBS) at a final concentration of 10% and penicillin/streptomycin (final concentrations 100 units/mL: 100 µg/mL, respectively). The cells were cultured in tissue culture polystyrene (TCPS) flasks at 37 °C in a humidified 5% CO_2 incubator, and the growth medium was replaced every two days. After discarding the medium, the attached cells were washed with PBS and then incubated with Trypsin-EDTA (diluted to 0.05% from a 0.25% stock in PBS) at 37^0C for 5 min. Detached cells were collected with DMEM-high glucose cell culture medium containing 10% serum and penicillin/streptomycin (100 units/mL/ 100 µg/mL).

2.2.6.2 Schwann Cell Seeding on pHEMA Hydrogels

pHEMA hydrogel cylindrical structure was used to study Schwann cells and their neurotrophin secretion for proliferating SHSY5Y cells. The pHEMA served as the exterior part of the nerve guide. Supporting potential of the Schwann cells were determined with Myelin Basic Antibody Staining, after cytotoxicity and proliferation studies.

The pHEMA hydrogel membranes were sterilized by exposing both sides to UV (280 nm) in a laminar flow hood for 30 min, after dried by lyophilization. Schwann cells were seeded on pHEMA hydrogels after culturing in DMEM high glucose tissue culture medium containing fetal bovine serum (FBS) at a final concentration of 10% and penicillin/streptomycin (final concentrations 100 units/mL: 100 μg/mL, respectively). After detaching from tissue culture flasks, the cells were counted and seeded to obtain 10^5 cells/scaffold. The hydrogels were then be incubated for 2 h in a humidified 5% CO_2 incubator for attachment. Full medium was then be added and replaced every two days.

2.2.6.3 SHSY5Y Cell Seeding GelMA-HaMA Gel Matrix

In order to study cell behavior on GelMA-HaMA gels, the gels were prepared in film forms. GelMA-HaMA matrices served as an interior component of the nerve conduit, so they were the support for SHSY5Y cells. Their neuronal structures were determined by Beta III Tubulin and NeuN Antibody staining.

GelMA-HaMA films were sterilized under UV (280 nm) for 30 min on both sides. The cells were grown in culturing in DMEM high glucose tissue culture medium containing fetal bovine serum (FBS) at a final concentration of 10% and penicillin/streptomycin (final concentrations 100 units/mL: 100 μg/mL, respectively), then counted and seeded on GelMA-HaMA films at a concentration of 10^5 cells/film. After seeding the cells, the films were incubated in a humidified 5% CO_2 incubator for attachment. After 2 h, full medium was added, and replaced every two days.

2.2.6.4 Live-Dead Cell Viability Test

The Live Dead cell viabilities of Schwann cells and SHSY5Ycells were determined on Day 2 after seeding on pHEMA hydrogels and GelMA-HaMA films, respectively. The cells were stained with Live-Dead assay dye mixture for 15 min at RT after washing with PBS. Then they were washed with PBS and examined with CSLM (Zeiss LSM 9100, Germany). The live cells (stained with calcein, green) and dead cells (stained with ethidium bromide, red) were examined and counted by Image J.

2.2.6.5 Determination of Cell Proliferation (MTT Test)

MTT cell proliferation assay was performed using the hydrogels. Cells in TCPS wells were used as a positive control and cell-free hydrogels were used as a negative control. The MTT assay was conducted on Days 1, 7, 14, 21 and 28 of the cell culture. The test was based on the reduction of MTT, (3-(4,5-dimethylthiazol-2-yl)-2,5-diphenyltetrazolium bromide, a yellow tetrazole), to a purple formazan by live cells. At each time point, MTT solution prepared by dissolving thiazolyl blue tetrazolium bromide in colorless cell culture medium (1 mg/1 mL) was added and incubated for 3 h at 37 °C in a humidified 5% CO_2 incubator, followed by addition of 4% HCl in isopropanol to dissolve the formed formazan crystals. After dissolving, the absorbances were measured at 550 nm using a UV-Vis spectrophotometer (Thermo Scientific, Multiscan Spectrum with Cuvette, USA). The absorbances were converted to cell numbers by using a calibration curve constructed for each cell types with a known concentration of cells.

2.2.6.6 Staining of the Cells:
2.2.6.6.1 Cytoskeleton and Nucleus Staining

The interaction between the cells (SC and SHSY5Y) and the materials (pHEMA and GelMA-HaMA) were determined by CSLM. On Days 1, 7, 14 and 21 after cell seeding on hydrogels, they were fixed with 4% (w/v) paraformaldehyde at room temperature for 15 min. Triton X-100 (1%, v/v in PBS, pH 7.4) was used to permeabilization of the cell membranes. After washing the fixed cells, this solution was added and incubated for 5 min. Then the samples were incubated in BSA (1%, w/v in PBS) at 37ºC for 30 min. For staining, the samples were incubated in Alexa-

fluor 488-Phalloidin (1:200 w:v in 0.1% BSA) for 1 h at room temperature to stain actin filaments green. After washing the samples with PBS, the samples were incubated in DAPI for 30 min at room temperature to stain the nuclei. After washing the samples were incubated in PBS until the examination with CLSM (Zeiss LSM, Germany).

2.2.6.6.2 Myelin Basic Protein Antibody Staining

In order to study expression levels of SCs, they were stained with myelin basic protein (MBP). The cells were fixed as described in the Section 2.2.6.6 and then incubated in blocking solution (1% BSA, 10% goat serum, 0.1% Tween 20 and 0.3 M glycine in PBS). After removing the blocking solution, anti-myelin basic protein antibody (1:20 in 0.1% BSA-PBS) was added to the samples and incubated overnight at 4°C. The samples were then washed with 0.1%PBS-BSA solution and incubated in Alexa Fluor 647 Labeled anti-rabbit antibody produced in donkey (1:100 dilution in 0.1% BSA-PBS) at 37^0C for 1 h and washed with 0.1% PBS-BSA before examination with CSLM.

2.2.6.6.3 Beta-III Tubulin and NeuN Antibody Staining

In order to study neuronal properties of SHSY5Y cells, they were stained with beta-III tubulin and NeuN antibody as described in the manufacturer's protocol. Briefly, the cells were fixed as described in the section 2.2.6.7 and then incubated in blocking solution (1% BSA, 10% goat serum, 0.1% Tween 20 and 0.3 M glycine in PBS). After removing the blocking solution, anti-beta III tubulin and NeuN antibodies (1:100 and 1:200 in 0.1% BSA-PBS, respectively) were added to the samples and incubated overnight at 4°C. The samples were washed with 0.1%PBS-BSA solution and incubated in both Alexa Fluor 488 labeled anti-mouse antibody produced in goat (1:100 dilution in 0.1% BSA-PBS) and Alexa Fluor 647 Labeled anti-rabbit antibody produced in donkey (1:100 dilution in 0.1% BSA-PBS) at 37^0C for 1 h and washed with 0.1% PBS-BSA before examination with CSLM.

2.2.7   Construction of the Final Conduit

GelMA-HaMA matrix was seeded with SHSY5Y cells before polymerization and incubated for 7 days as described in Section 2.2.6.3. After incubating SHSY5Y cell containing IPNS were placed into cylindrical pHEMA hydrogels seeded with SCs and the remaining part of the tube was filled with cell free IPN (Figure 2.6). After 7 days of incubation, Netrin-1 protein (100 µg/mL) was injected to one side of the final construct and the cells were analyzed with CSLM after 7 days of incubation.
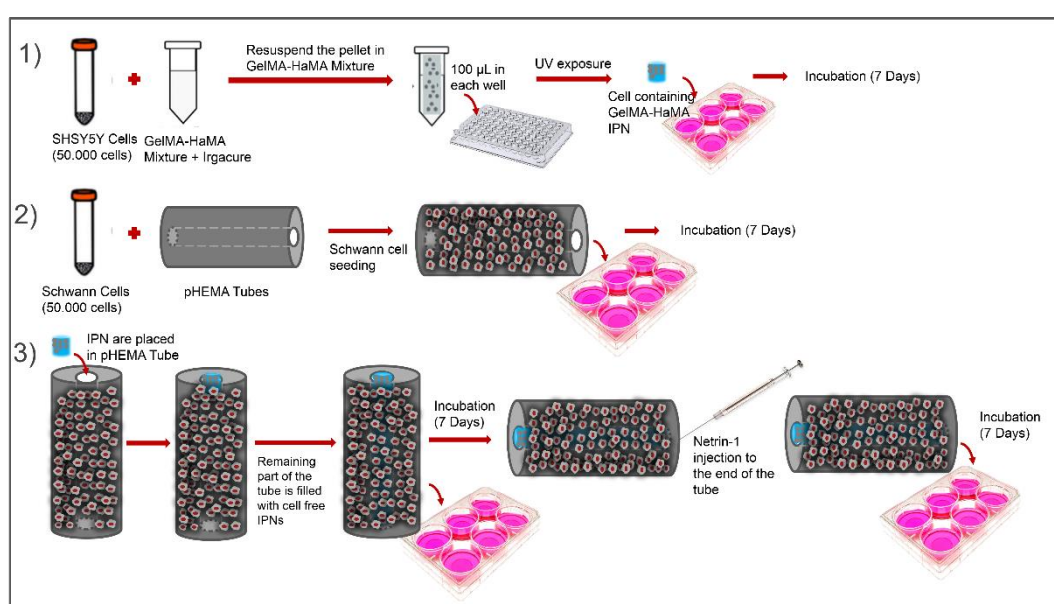
Figure 2.6 Construction of the final structure.

2.3   Statistical Analysis

All the characterization and *in vitro* studies were performed in at least triplicates. After the calculation of arithmetic means and standard deviations, significant differences between mean values in control and test groups were determined and statistical analysis were done by 1-tail Student's t-test and ANOVA. For the p values equal or smaller than 0.05, the differences were considered as statistically significant.

CHAPTER 3

RESULTS AND DISCUSSION

In the present study, the preparation of the pHEMA cylindrical hydrogels and the hydrogels in forms (like sheets) suitable for the different characterization studies were prepared and characterized in terms of swelling capacity, contact angle, mechanical strength and surface properties like pore sizes. When the mechanical strengths and pore sizes (and SEM images) of the hydrogels are considered together, the hydrogel type having water concentration of 50% (v/v) having the most similar properties to the natural nerve tissue, is the most suitable hydrogel to be used as a nerve guide. Thus, the cell culture studies were performed with this ratio. GelMA-HaMA IPNs at different concentrations were prepared and analyzed with FTIR. In addition, they were characterized in terms of water content and degradation profile.

In vitro studies with pHEMA hydrogels were started with SCs. Live-Dead cell viability assay was performed on days 1, 7, 14, 21 and 28. The cells were also stained with phalloidin for cytoskeleton, DAPI for nucleus and myelin basic antibody to check for the myelin production. The cells were analyzed by using CSLM. MTT cell viability assay for SCs on pHEMA was performed. *In vitro* studies with both SHSY5Y cells and SCs were performed; the viability and proliferation tests were carried out on the cells seeded on GelMA-HaMA IPNs and pHEMA hydrogels. Then the 3D structure was prepared by placing GelMA-HaMA IPN in pHEMA cylindrical structure. SCs were seeded on pHEMA and SHSY5Y cells were seeded in GelMA-HaMA IPN so that coculture studies were performed. The migration of SHSY5Y cells was studied through the nerve conduit and SHSY5Y cells stained with Beta-III Tubulin and NeuN Antibodies and analyzed by CSLM.

3.1 Characterization of pHEMA Hydrogels

3.1.1 Water Content

Equilibrium water content of the hydrogels affects mechanical characteristics and diffusion of solutes (Bektas and Hairci, 2020). Thus, equilibrium water contents of pHEMA hydrogels prepared with different compositions were determined. After the preparation of the hydrogels, they were incubated in water to remove the unreacted reagents and then frozen. After lyophilization for 6 h, dry weights were determined, then the samples were incubated in water for 24 h and the weights were determined again (Figure 3.1).
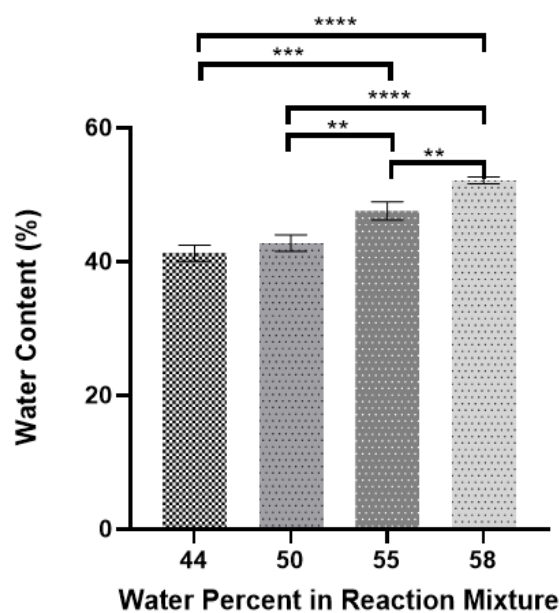
Figure 3.1 Water content of pHEMA hydrogels prepared with different water contents (Day 1). Statistical differences (* $p \leq 0.05$, **$p \leq 0.01$, ***$p \leq 0.001$, ****$p \leq 0.0001$) are indicated.

A crosslinked hydrogel swells when it absorbs water. The swelling properties, which is usually used as a degree of swelling to define hydrogels, depend on many factors such as crosslink density, solvent nature, polymer-solvent interaction parameter

(Ottenbrite et al., 2010). The results showed that increase in water content in the preparation solution resulted in the increase in the equilibrium water content. The difference between the hydrogels of different water concentrations were found as statistically significant. Similar results were obtained by Wang et al., (2016) and Sun et al., (2021) and the amount of the swelling of the pHEMA hydrogels prepared in this study were considered as suitable for soft tissue engineering applications when the swelling capability is considered.

Figure 3.2 shows the swelling profiles of pHEMA hydrogels of different water concentrations. When swollen in water (days 2, 4, 6 and 8), the gels swell to their equilibrium and upon drying they expel the same amount of water. After swelling, it becomes flexible and soft and thus it can be cut easily. It was reported that transparent pHEMA based hydrogels are reported to allow liquid and oxygen diffusion and are highly permeable to small molecules (Zare et al., 2021). The gels prepared in this study maintain their ability to reswell repeatedly, making them good candidate for soft tissue engineering applications because of maintained integrity.
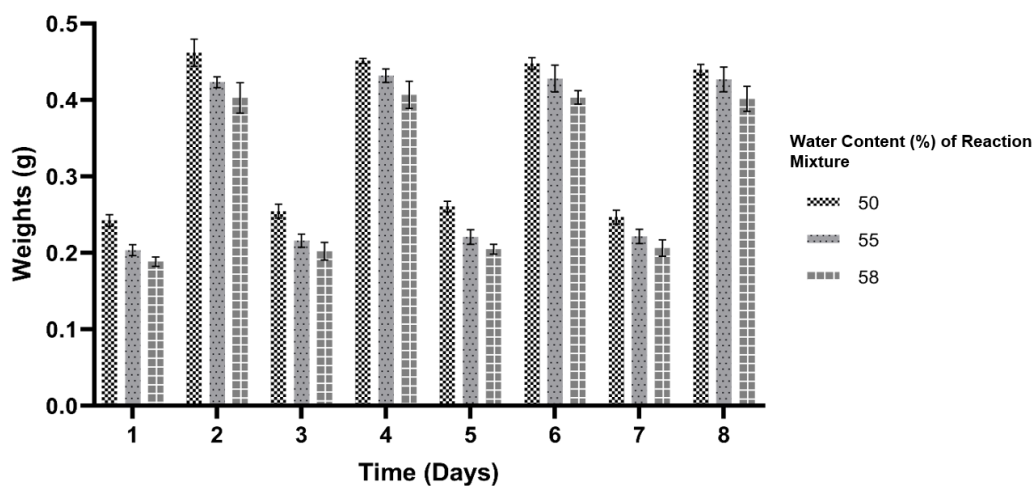
Figure 3.2 Repeated swelling profiles of pHEMA hydrogels. The gels were dried and swollen on succesive days and maintained their integrity.

3.1.2 Water Contact Angle

Contact angle is an important parameter to show wettability of a solid surfaces. It is determined by the balance between adhesive and cohesive forces (Zare at al., 2021). The measurements are performed by placing a droplet of water on the surface of the materials and the contact angle is measured by a goniometer. The contact angles of membranes are shown in Table 3.1 and the differences between the contact angles were found as statistically significant and shown in Figure 3.3. The results obtained from the wet pHEMA hydrogels showed that the contact angles, and therefore the hydrophobicities are decreasing with increasing water content in the preparation process.

Hydrophilicity of a materials is closely related with protein adsorption, and therefore cell adhesion, and for any biomaterial the contact angle is an important parameter for cell attachment and growth. The surface is considered as highly hydrophobic when the contact angle is higher than 90^0, and highly hydrophilic when it is less than 35° (Chen et al., 2019). Although highly hydrophilic surfaces are the most suitable surfaces for cell attachment, the cell to cell interaction on these surfaces may not be favorable (the cells prefer to interact with the surfaces). In addition, extremely hydrophobic surfaces prevent cell attachment and thus not preferred for biomedical applications (Ferreira et al., 2019). Thus, the contact angles of the hydrogels prepared in this study are mostly suitable for cell attachment.

Table 3.1 Contact angles of pHEMA membranes with different water concentration (%)

Water Concentration (%)	Contact Angles
44	50.8° ± 15.4
50	31.0° ± 7.6
55	17.8° ± 10.2
58	6.2° ± 4.5

3.1.3 Mechanical Testing

Hydrogels with appropriate mechanical properties together with other characteristics allows the growth of tissues into implants, while tensile strength as an important factor influences the suturing of hydrogel implants during and after surgery (Li et al., 2019). In the literature, it is reported that Ultimate Tensile Strength for acellular nerve tissue is 1400 kPa and tensile modulus is 576 kPa (Borschel et al., 2003).

Mechanical properties of the pHEMA hydrogel samples were determined by tensile test. The results are shown in Figure 3.3. Tensile modulus of the hydrogels were determined as 548.6 ± 23.4, 570.9 ± 92.13, 431.4 ± 7.5 and 383.2 ± 18.90 kPa for the hydrogels having the water concentration of 44, 50, 55 and 58%, respectively. In addition, tensile strengths were found as 442.1 ± 75.1, 501.8 ± 93.7, 289.1 ± 13.7 and 283.1 ± 35.1 kPa for the hydrogels having the water concentration of 44, 50, 55 and 58%, respectively. Although tensile strengths of the hydrogels are significantly smaller than the acellular nerve tissue, tensile modulus values 548.6 ± 23.4, 570.9 ± 92.13 for water concentrations of 44 and 50% are comparable to that of an acellular nerve tissue. Flexibility of the nerve conduits is an important parameter for the migration and attachment of Schwann cells. The results showed that pHEMA has

suitable mechanical properties for the attachment and proliferation of the Schwann cells.

Figure 3.3 Mechanical properties of pHEMA hydrogel with different water contents, n=3 for all samples, statistical differences (* $p \leq 0.05$, **$p \leq 0.01$) are indicated.

3.1.4   SEM

pHEMA hydrogels prepared with different water contents were examined by using SEM. The micrographs showed that the hydrogel having the 44% water in reaction mixture had closed pores on the surfaces and there were no pores at the cross-section (Figure 3.4 A and B). When the water amount was increased during preparation of the hydrogels, the porous structures were formed. Figure 3.4 C-H show the pores on the surfaces. These pores are also seen at the cross-sections, showing that the pores are interconnected.

Figure 3.5 shows the pore size and porosity analysis of the hydrogels. The porosities of the hydrogels were found as 17%, 33%, 52% and 50% for the hydrogels having the water concentration of 44, 50, 55 and 58%, respectively (Figure 3.5 A). It was also found that average pore sizes are 40.75 ± 8.59, 55.09 ± 7.15, 15.24 ± 3.05 and 15.44 ± 2.05 µm for the hydrogels having the water concentration of 44, 50, 55 and 58%, respectively. These results showed that the pore sizes were first increased then

decreased with increasing water concentration Figure 3.5 B). However, porosity was increased with the increasing water concentration.

In tissue engineering applications, the surface structures of the materials are important for cell adhesion, spreading, proliferation, migration and differentiation seeded on scaffold materials (Dursun Usal et al., 2019; Pooshidani et al., 2021). In addition, interconnected porous structures provide a good environment for cell ingrowth, vascularization, and nutrient diffusion, which are critical for cell survival. Porosities and the average pore dimensions of scaffolds are very important in cell migration, nutrient penetration, and waste removal (Hasirci et al., 2010, Chen et al., 2021). So, the interconnected pores of the hydrogels prepared in this study are suitable for the use in nerve regeneration applications. In the literature, studies which have investigated the effect of topography on axon regeneration showed that pores sizes 20–60 μm along the longitudinal direction were optimal for maximum axon penetration and minimum axon misdirection (Manoukian et al., 2019). The pore size and porosity calculation results of the present study shows that the hydrogels having water concentration of 50% are suitable for the use in peripheral nerve regeneration applications, because the pore sizes are suitable for cells to attach and grow and the cross-sections show the pores are interconnected.
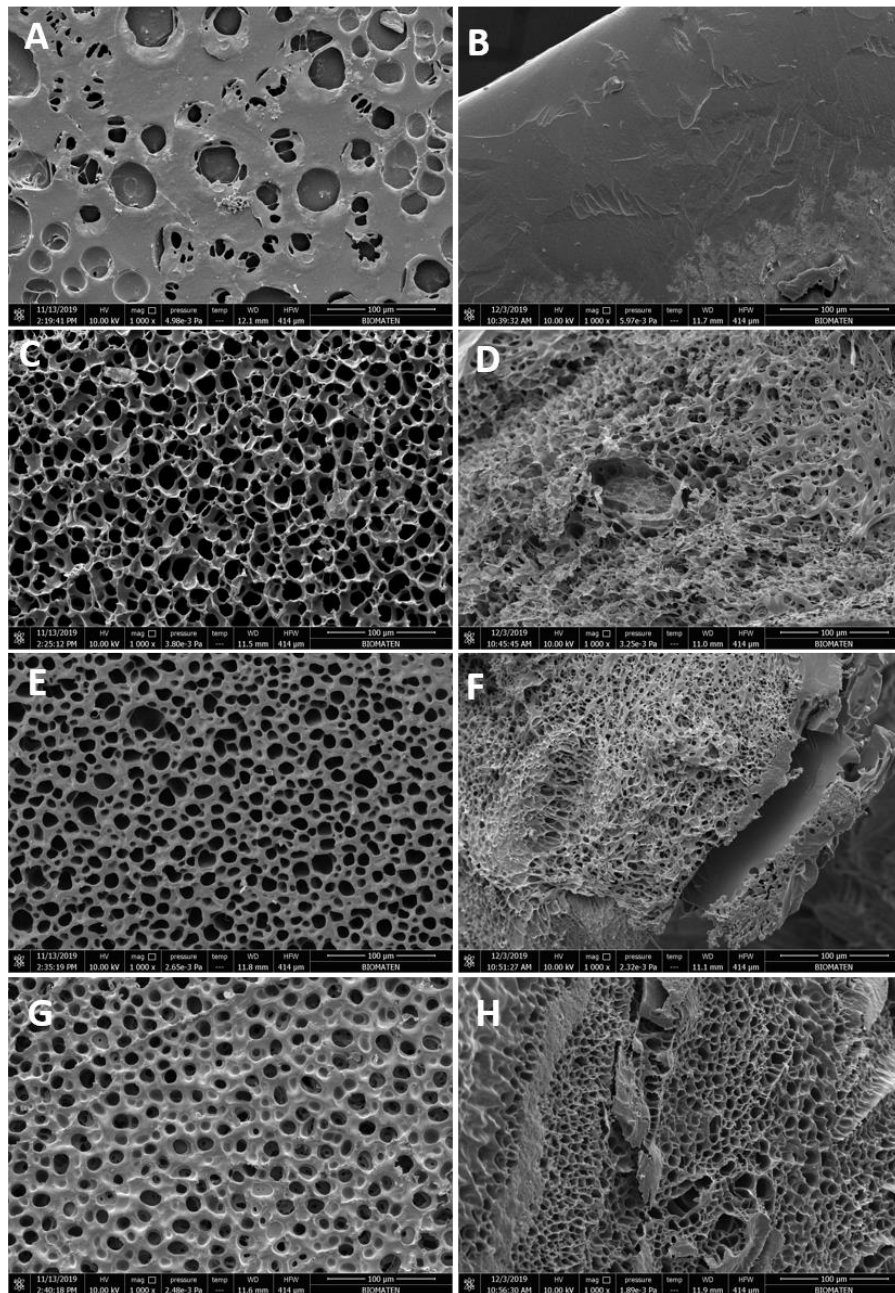
Figure 3.4 SEM micrographs of hydrogels with different water contents (v/v) A- 44%, surface B- 44%, cross-section, C- 50%, surface, D- 50%, cross-section, E- 55%, surface, F- 55%, cross-section, G- 58%, surface, H- 58%, cross-section.
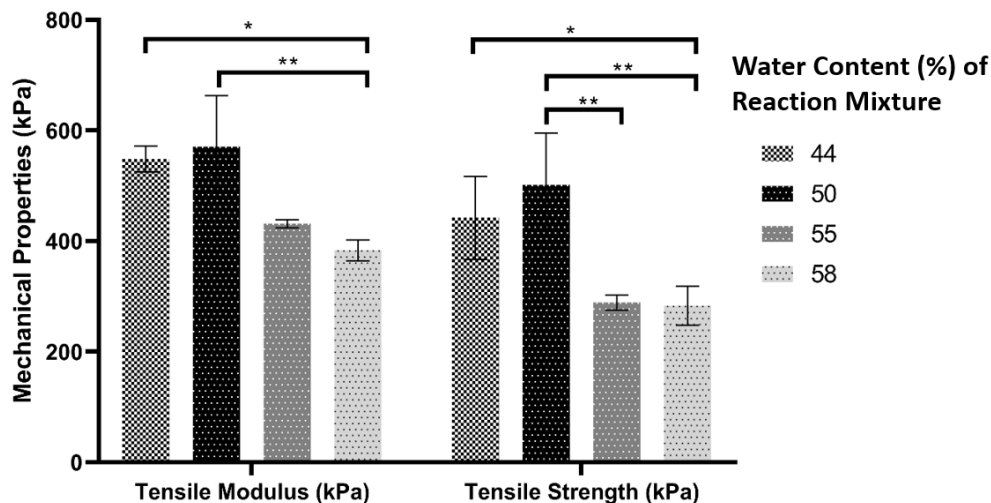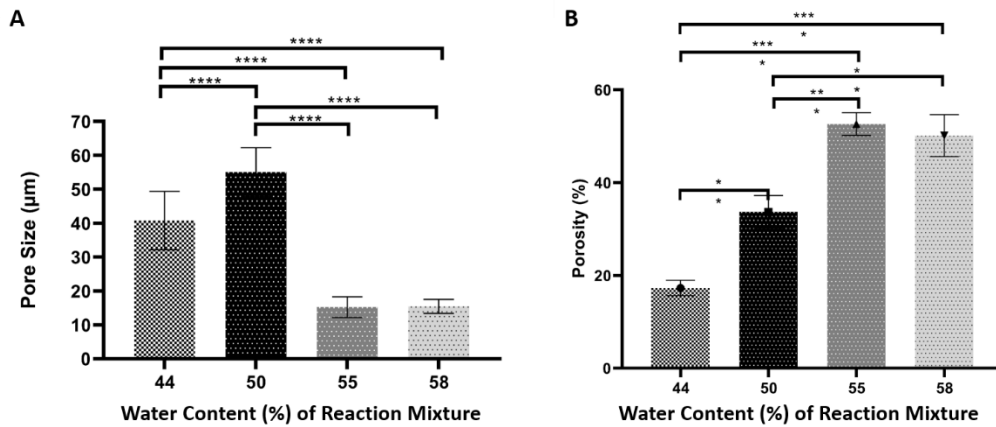
Figure 3.5 Pore Size (A) and Porosity (B) analysis of pHEMA hydrogels with different water contents;. n=30 for all samples, statistical differences (* $p \leq 0.05$, **$p \leq 0.01$, ***$p \leq 0.001$, ****$p \leq 0.0001$) are indicated.

For Schwann cells to attach and spread on pHEMA surfaces, pHEMA hydrogels were coated with collagen. Figure 3.6 shows the SEM micrographs of pHEMA hydrogels after collagen coating. A thin sheet of collagen covered the surfaces; however, the pores of the hydrogels were still seen under the collagen sheet. Because collagen is a biodegradable protein, it is expected to be degraded after the cells are attached and spread on the pHEMA hydrogel surfaces. Thus, nutrient penetration and waste removal will be possible for Schwann cells.
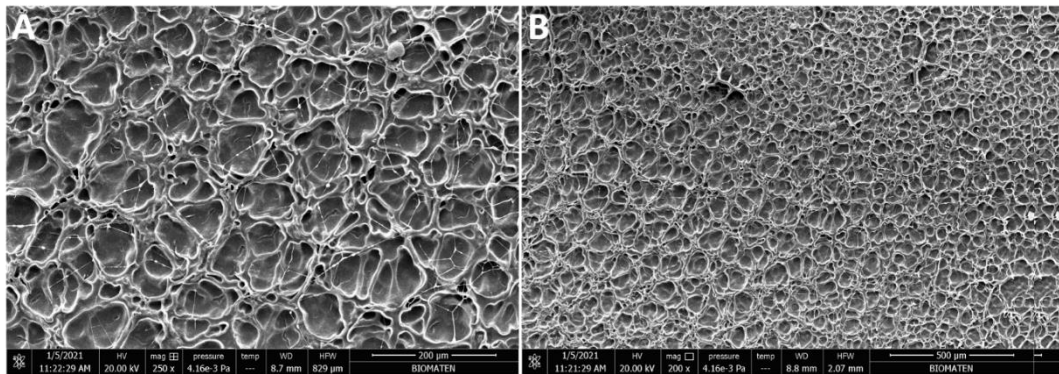
Figure 3.6 Collagen coated pHEMA hydrogels prepared with 50% water content. A- Scale bar: 200 μm, B- Scale bar: 500 μm.

3.1.5 FTIR Analysis of Collagen Coated pHEMA hydrogels

Figure 3.7 shows the FTIR spectra of pHEMA, collagen and collagen coated pHEMA. Collagen spectrum depicts characteristic absorption bands at 1575 and 1640 cm^{-1} which represent the amide I and II, respectively [Yan et al., 2010]. The bands are also seen on the FTIR spectrum of collagen coated pHEMA while they are absent on pHEMA. Thus, it is indicated that the collagen was successfully coated the surface of pHEMA.
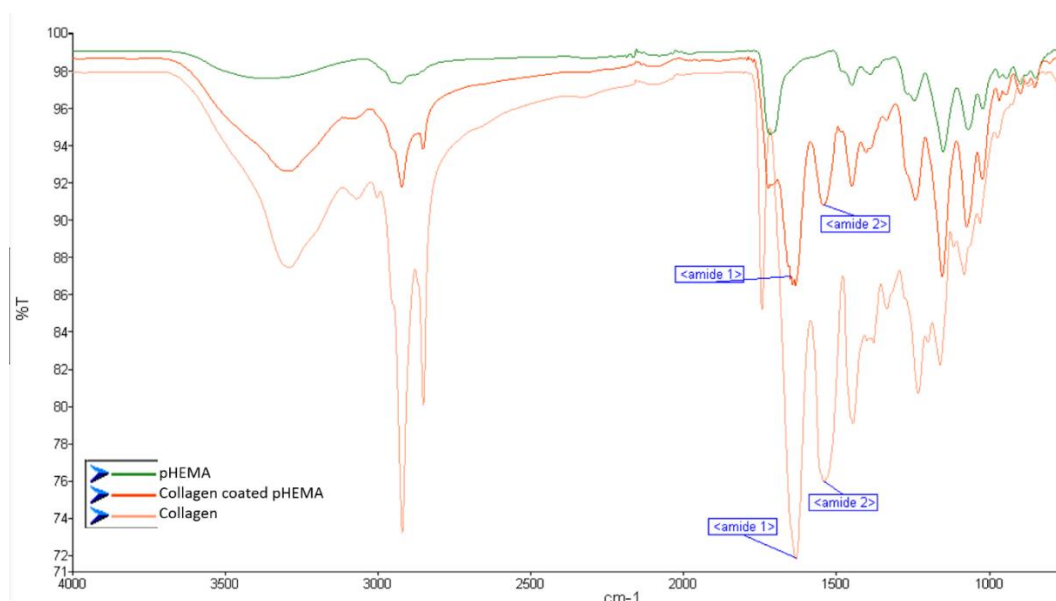
Figure 3.7 FTIR Spectra of pHEMA, collagen coated pHEMA and collagen.

3.2 Characterization of GelMA-HaMA IPN

3.2.1 Determination of Methacrylation Level of GelMA and HaMA

The chemical reaction of gelatin with methacrylic anhydride produces GelMA molecule and upon crosslinking of GelMA in the presence of Irgacure and UV the GelMA hydrogel forms (Kuo et al., 2016) (Appendix A).

The ratio of ε-amino groups (lysine, hydroxylysine) of methacrylated gelatin to unreacted pure gelatin prior to the reaction is the method for the calculation of the degree of methacrylation (DM) (Equation 8) (Hoch et al., 2012). Normalization of

the ^{1}H NMR spectra was performed according to the phenylalanine signal (6.9-7.5 ppm) since it is proportional with the concentration of the gelatin and is not reacted during methacrylation (Figure 3.8, Appendix B). The integrated areas of lysine methylene signals (2.8-2.95 ppm) of gelatin (unused, total) and GelMA (decreased upon methacrylation) was used to calculate DM.

$$DM(\%) = \left(1 - \frac{\text{Lysine methylene of GelMA}}{\text{Lysine methylene of Gelatin}}\right) X100 \qquad (8)$$

Figure 3-9 shows ^{1}H NMR spectra of hyaluronic acid (HA) and uncrosslinked HaMA. The ^{1}H NMR spectra were normalized to the signal at 2.07 ppm since it is proportional with the concentration of the hyaluronic acid and is not reacted during methacrylation. DM was calculated through the integrated areas of the methacrylate proton signals at 2.8, 5.7 and 6.1 ppm of HA and HaMA [Yousefi et al., 2018]. The DM was calculated as 60±7% for the HaMA synthesized.
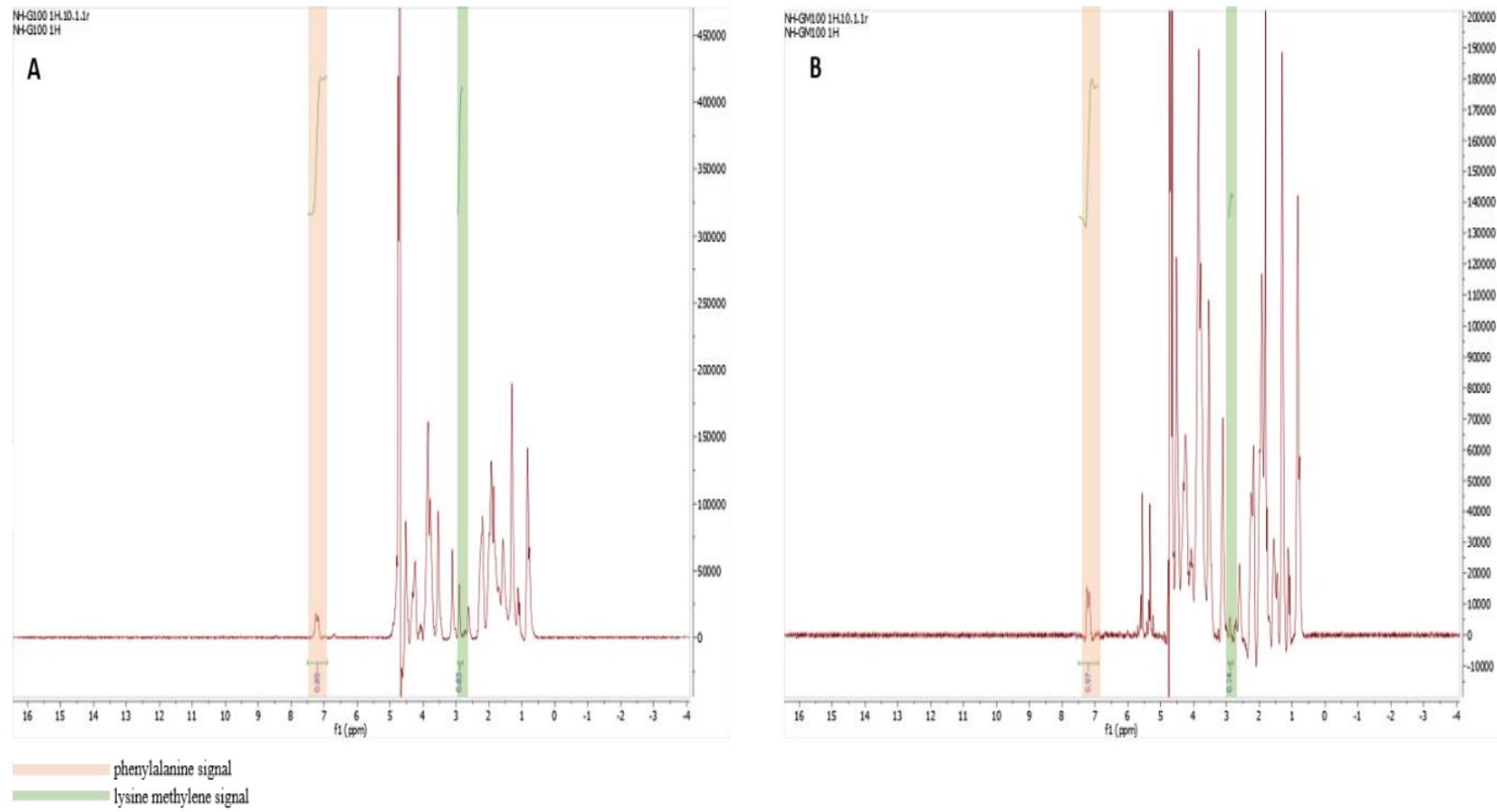
Figure 3.8 ^{1}H NMR spectra of gelatin (A) and uncrosslinked GelMA (B)
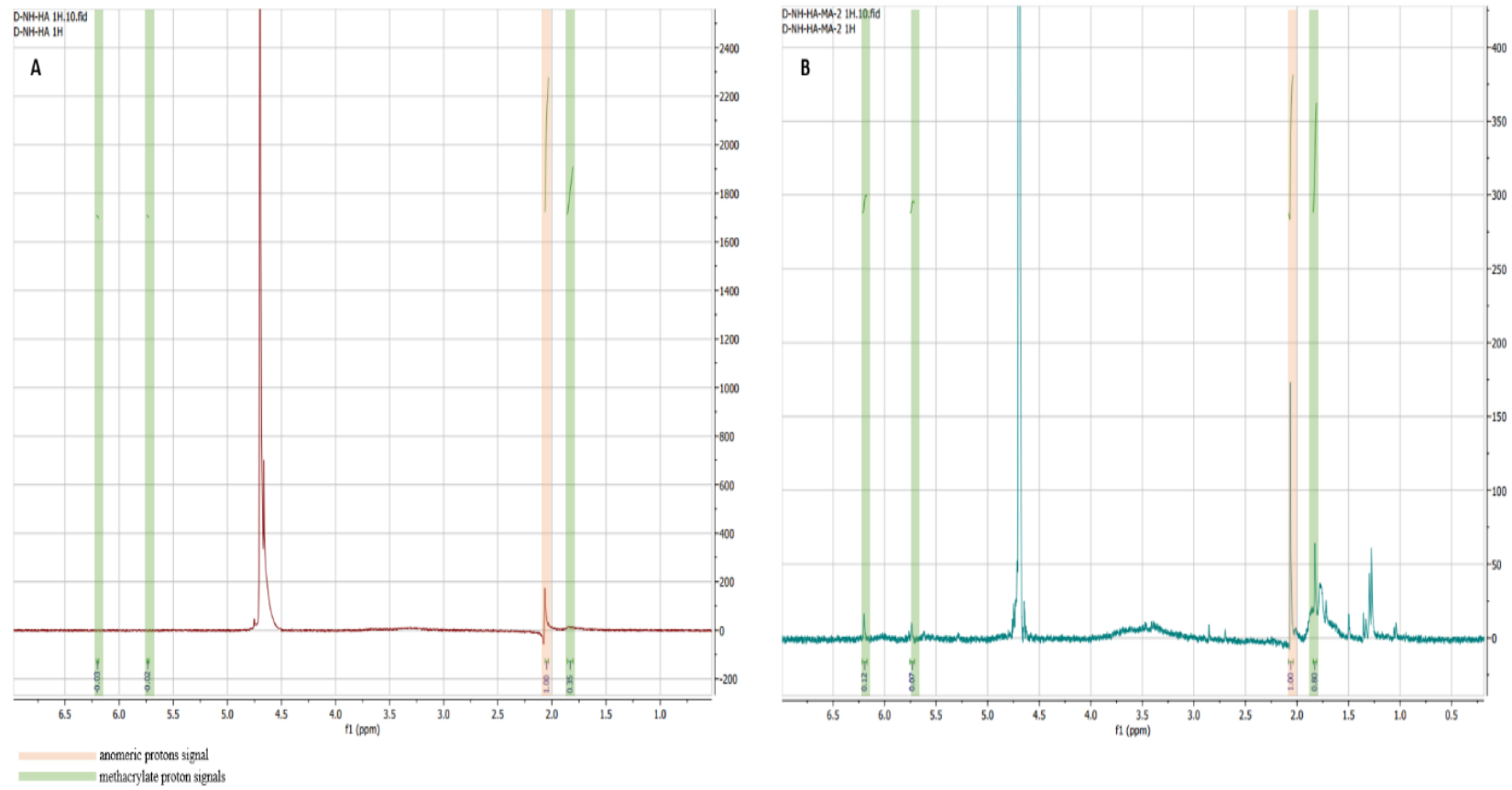
Figure 3.9 ^{1}H NMR spectra of hyaluronic acid (A) and uncrosslinked HaMA (B) (normalized to the signal at 2.07 ppm).

3.2.2 FTIR

FTIR spectra of gelatin is shown in Figure 3.10. 3300 cm^{-1} (O-H stretching vibrations), 2922 cm^{-1} (C-H stretching), 1640 cm^{-1} (0-H bonding) and 1525 cm^{-1} (C-N stretching and N-H bending) bands were previously defined by Cui et al. (2014). Due to the addition of the methacrylate groups into the lysine groups of gelatin, C-H stretching (2927 cm^{-1}) and bending areas show different transmission results for gelatin and GelMA. As a result of UV crosslinking, a decrease in the total number of -OH groups in the polysaccharide structure is related with the decrease around 3300 cm^{-1} crosslinking (Bertoni et al., 2005). C-C bond peak decrease around 3010 cm^{-1} also shows the photopolymerization (Almeida et al., 2011). As a result of crosslinking reaction, bands of typical amide I and II bonds at 1640 cm^{-1} and 1540 cm^{-1} decrease.
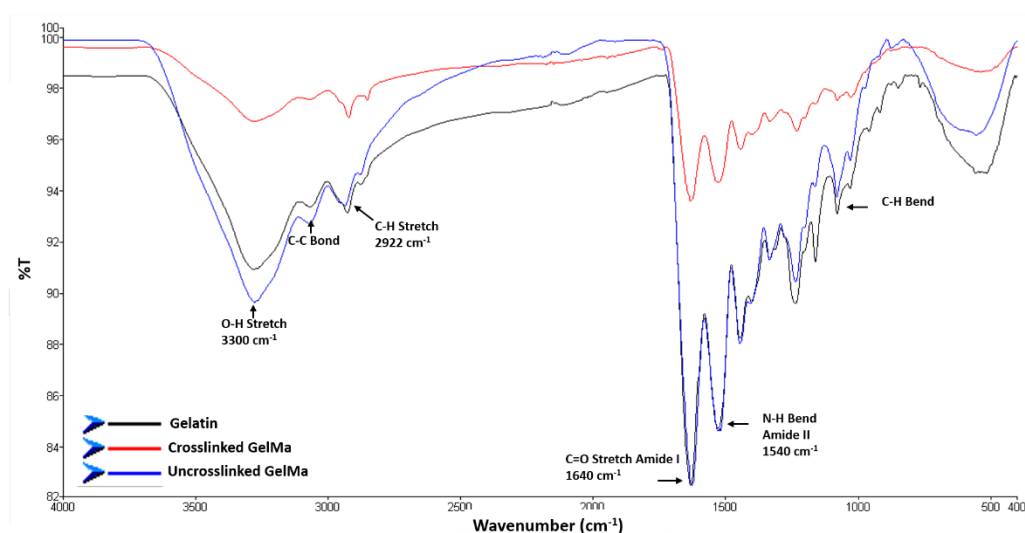
Figure 3.10 FTIR spectra of gelatin, uncrosslinked GelMA and crosslinked GelMA.

In order to examine the methacrylation efficiency and the crosslinking reaction FTIR spectrum was used and the results are shown in Figure 3.11. HaMA showed a new peak at 1731 cm^{-1} and C=C bond peak was increased at 1643 cm^{-1}, which can be resulted from the methacrylation reaction. These bonds were also decreased with the crosslinking reaction. FTIR spectroscopy result demonstrated that hyaluronic acid

was reacted with methacrylic anhydride (MA) to add methacrylate pendant groups. Because nitrogen atom of HA did not react with MA, a N-H deformation signal was seen at 1558 cm^{-1}. The peak located at 3360 cm−1 is associated with the intra-and intermolecular stretching vibration of -OH group. The peak from 1033 cm^{-1} is related with the C-O-C hemiacetalic system saccharide units. The results are consistent with the previous studies (Vasi et al., 2014; Lin et al., 2015).
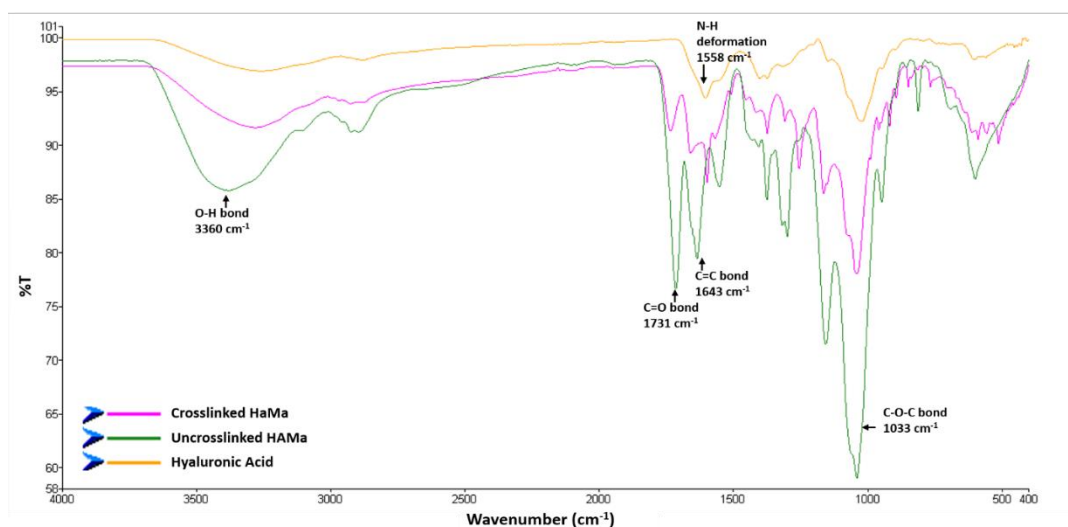
Figure 3.11 FTIR spectra of hyaluronic acid, uncrosslinked and crosslinked HAMA.

3.2.3   Water Content and Swelling

Equilibrium water contents of GelMA-HaMA IPNs at different ratios (5:95, 10:90, 15:85, 20:80 in PBS) were determined. After the preparation and lyophilization for 6 h, dry weights were determined, then the samples were incubated in water for 24 h and then the weights were determined again (Figure 3.12 A). Water contents of pure GelMA and HaMA hydrogels were determined as 86% and 88%, respectively. Mixing them in different concentrations to produce IPNs resulted in the water content of 87%, 88%, 84%, 92% for the ratios of 5:95, 10:90, 15:85, 20:80, respectively. Even the results showed statistically significant differences, the water content values for all were higher than 85%. Thus, the swelling percent of the IPNs were calculated to show the effect of HaMA addition into the IPNs (Figure 3.12 B).

Increasing HaMA amount in the structure increased the swelling ability of the IPNs to some point then decreased. Previously reported studies using GelMA based hydrogels showed that the water content around 80% was suitable for neural differentiation and neurite outgrowth (O'grady et al., 2019; Xiao et al., 2019).
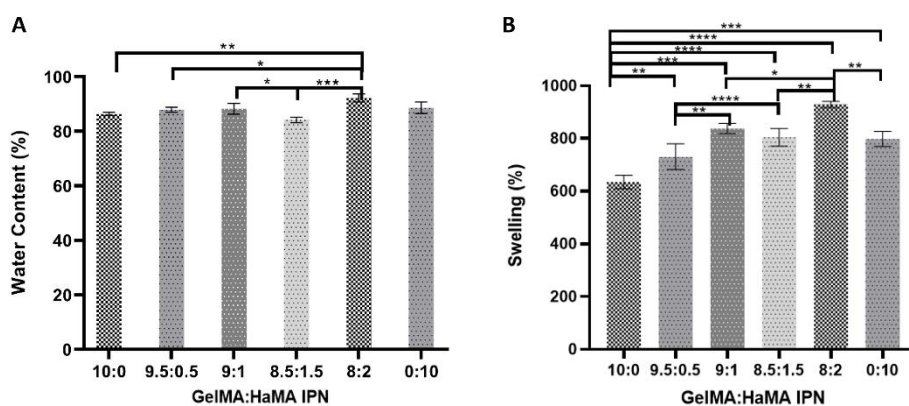
Figure 3.12 Water content (%) (A) and swelling (%) (B) of GelMA-HaMA IPNs at different ratios (5:95, 10:90, 15:85, 20:80 in PBS). Statistical differences (* $p \leq 0.05$, **$p \leq 0.01$, ***$p \leq 0.001$, ****$p \leq 0.0001$) are indicated.

3.2.4 Degradation

Weight loss percentages as a result of degradation are presented in Figure 3-13. Pure GelMA and HaMA gels and GelMA-HaMA IPNs (5:95, 10:90, 15:85, 20:80) were incubated in PBS (Figure 3.13 A) and medium (Figure 3.13 B) for four weeks to see the weight loss over time. While pure GelMA has lost its 75% of weight in four weeks, pure HaMA completely degraded in three weeks. Thus, increasing HaMA concentration in IPN structure increased the weight loss rate. The degradation profile did not show statistically significant difference in PBS and in medium. Studies showed that use of a degradable hydrogel based on naturally derived materials to create a scaffold is useful for soft tissue engineering applications (Jo et al., 2019). During the degradation process, the regenerating cells are become able to penetrate the structure. ECM deposition rate during the regeneration should match the rate of scaffold degradation (Salih, 2009). In another study, GelMA was used as a sacrificial

material in scaffold design, and similar degradation results were found and reported as suitable for cellular ingrowth during axon regeneration (Dursun Usal et al., 2019).
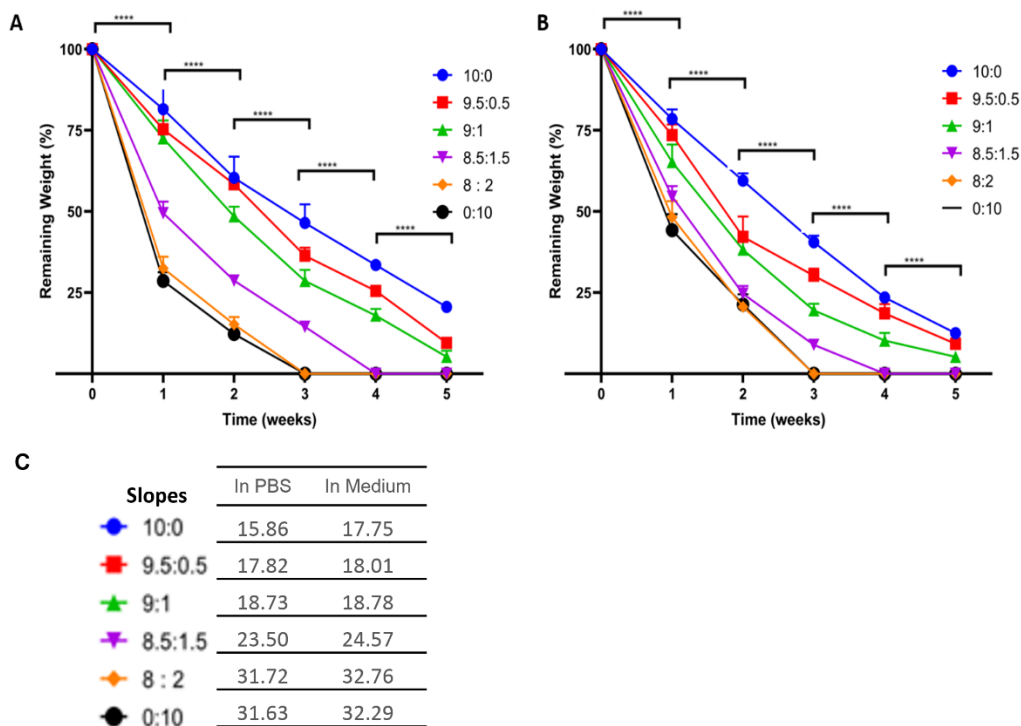
Figure 3.13 Weight loss of the GelMA-HaMA IPNs over 4 weeks in PBS (A) and in medium (B); and slopes for each IPN mix (C). Statistical differences (****p ≤ 0.0001) are indicated.

3.3 *In vitro* Studies with Schwann Cells

3.3.1 Live-Dead Cell Viability Assay on pHEMA Hydrogels

Schwann cells were seeded on uncoated pHEMA hydrogels prepared with 50% water. Live-Dead assay was conducted to study the viability of the cells (Figure 3.14). On day 1, most of the cells seeded were attached on pHEMA hydrogels (Figure 3.14 A, B, C). They were also able to live on the hydrogels (Figure 3.14 D, E, F). The cells started to produce spheroids on Day 14 (Figure 3.14 G, H, I). The highly hydrophilic surface of the pHEMA hydrogels might have led cells to prefer cell-cell

interaction forming spheroids. Napolitano et al. (2007) explained that when first seeded, the cells uniformly coat the bottom and occupy the gravitational low point of the recess, but soon form a toroid aggregate. According to the prevalent theory of self-assembly, the differential adhesion hypothesis (DAH), cellular aggregates assume a spherical geometry in order to maximize intercellular adhesion and to minimize energy, because they cannot make bonds with the surface and thus reduce their energy so they turn inwards, to bind to each other (Jakab et al., 2004; Brassard et al., 2019). This theory is widely accepted by researchers: it is well established that cells grown on 2D substrates or within 3D scaffolds can generate and react to tension, resulting in altered cell migration, phenotype, growth rate (Amaral et al., 2019). On day 28, the cells started to spread again (Figure 3.14 M, N, O) because they secreted their own ECM and they could spread on the surface. Collagen coating was applied on pHEMA hydrogels to prevent spheroid formation. Collagen, one of the major components of extracellular matrix, is widely used as a coating material to enhance cell attachment and adhesion to both plasticware and glass surfaces (Pinzon-Herrera et al., 2020). Thus, in the present study the coating was used in order to make the surfaces attractive for the cell attachment. Figure 3.15 shows Live-Dead assay results of Schwann cells on collagen coated pHEMA hydrogels on Days 1, 7 and 21. On Day 1, large number of cells seeded were alive on pHEMA hydrogels (Figure 3.15 A, B, C). They were able to attach and proliferate on the hydrogels on Day 7 (Figure 3.15 D, E, F). On day 21, they did not form spheroid, and they spread all over the collagen coated hydrogels (Figure 3.15 G, H, I). The cell numbers on the coated pHEMA hydrogels were calculated by using ImageJ software. Figure 3.16 shows that live cell fraction of the Schwann cells is increasing with time. It shows that the Schwann cells are able to attach and proliferate on pHEMA surfaces.

Figure 3.14 Live-Dead analysis of Schwann Cells on pHEMA. A- Day 1 dead cells, B-Day 1 live cells, C- Day 1 Merged image, D- Day 7 dead cells, E- Day 7 live cells, F- Day 7 merged image, G- Day 14 dead cells, H- Day 14 live cells, I- Day 14 Merged image, J-Day 21
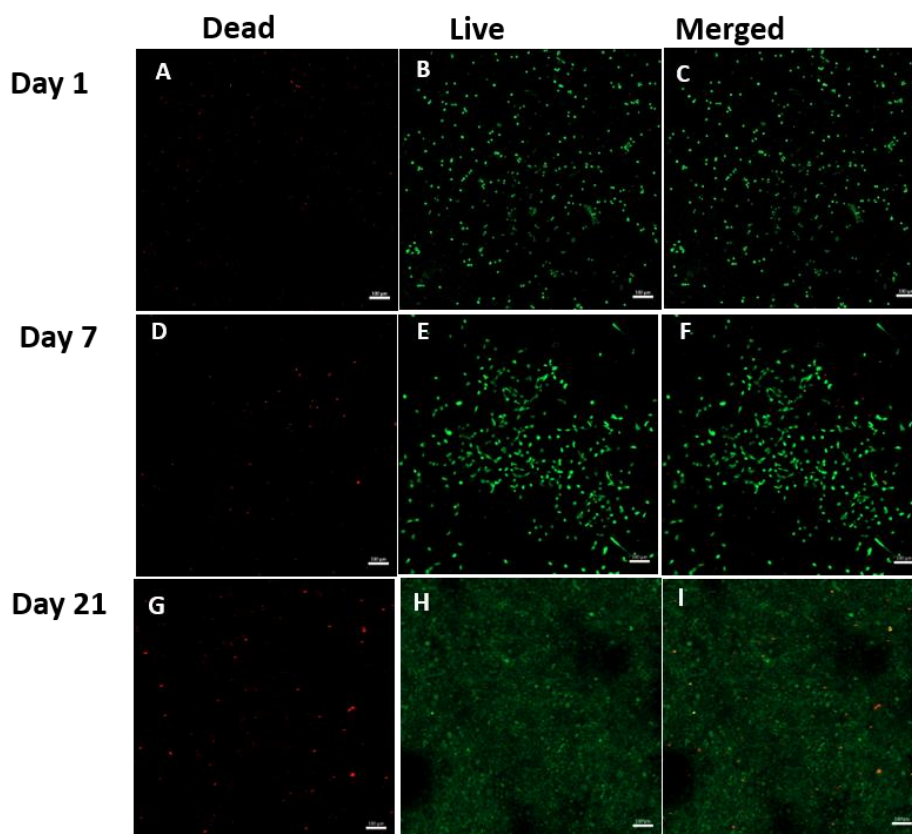
Figure 3.15 Live-Dead analysis of Schwann Cells on collagen coated pHEMA. A- Day 1 dead cells, B- Day 1 live cells, C- Day 1 Merged image, D- Day 7 dead cells, E- Day 7 live cells, F- Day 7 merged image, G- Day 21 dead cells, H- Day 21 live cells, I- Day 21 Merged

Figure 3.16 Quantitative analysis of the Schwann cell numbers on pHEMA hydrogels by using ImageJ software.

3.3.2 Cytoskeleton-Nucleus Staining and Myelin Basic Antibody (MBA) Staining

In the peripheral nervous system, myelin sheath has an important role in impulse transfer, because it functions as an insulator that increases the velocity of the impulse (Modrak et al., 2020). The membrane constituting the myelin sheath is composed of protein (20 to 30%) and lipids (70 to 80%) (Liu et al., 2019). The proteins include myelin basic protein (MBP) (30 to 40%) and proteolipids. Myelin Basic Protein has strong relationship with the myelin sheath compaction. Thus, myelin basic antibody staining is used to determine whether Schwann cells are secreting the protein which is an indicator of the functionalization of these cells. Figure 3.17 shows the MBP antibody staining together with cytoskeleton and nucleus staining of Schwann cells on pHEMA. The presence of the spheroids on Days 14 and 21 did not prevent the cells to produce myelin (Figure 3-17 C, G, K). Cells that self-assemble into spheroids achieve increased gene expression and retention of native cell phenotype over monolayer cultures (Kelm et al., 2004; Chen et al., 2019). Spheroids also generate natural cell-cell interactions and mimic *in vivo* differentiation patterns and spatial cell-cell and cell-ECM interactions (Sirenko et al., 2019). In addition, on Day 28 (when the cells started to spread) they also secreted the myelin. Their ability to secrete myelin is helpful for nerve regeneration.

In order to remove the unreacted residues of the hydrogel preparation like photoinitiator or monomers, the hydrogels were washed for one week (Figure 3.18). The cells formed spheroid once again. However, Schwann cells seeded on collagen coated pHEMA did not form spheroids (Figure 3.19). FITC-phalloidin was used to stain cellular F-actin (green) and DAPI was used to stain nuclei (red). Starting from day 14, the cells spread on the collagen coated surfaces and seem to interact with each other. It is promising that Schwann cells attached on the outer surfaces of the conduit will be able to secrete necessary factors for regeneration.
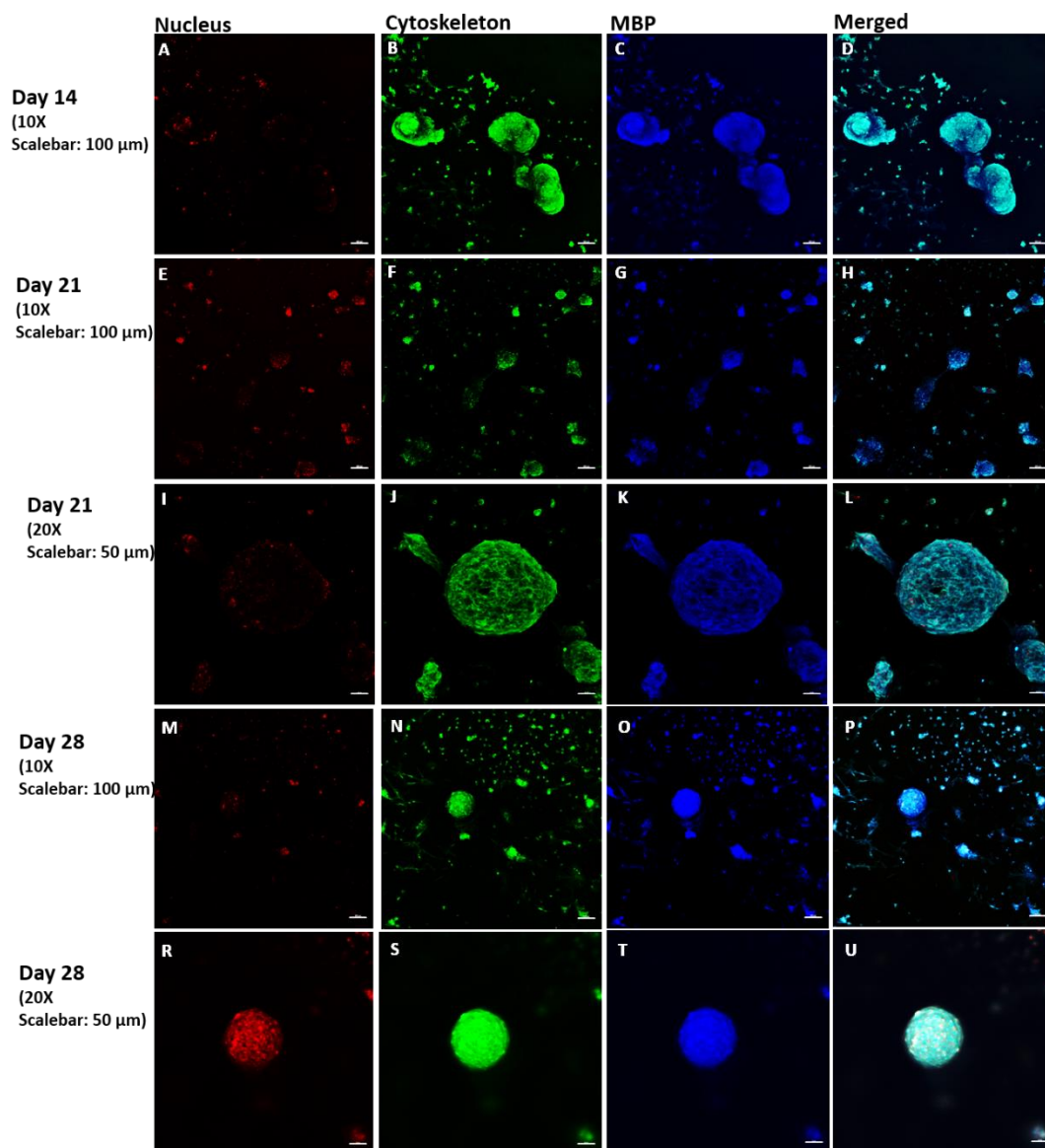
Figure 3.17 CLSM images of Schwann cells on pHEMA stained with MBP antibody (blue), cytoskeleton (green), nucleus (red). A-D- Day 14, 10X; E-H- Day 21, 10X; I-L- Day 21, 20X; M-P- Day 28, 10X; R-U- Day 28, 20X.
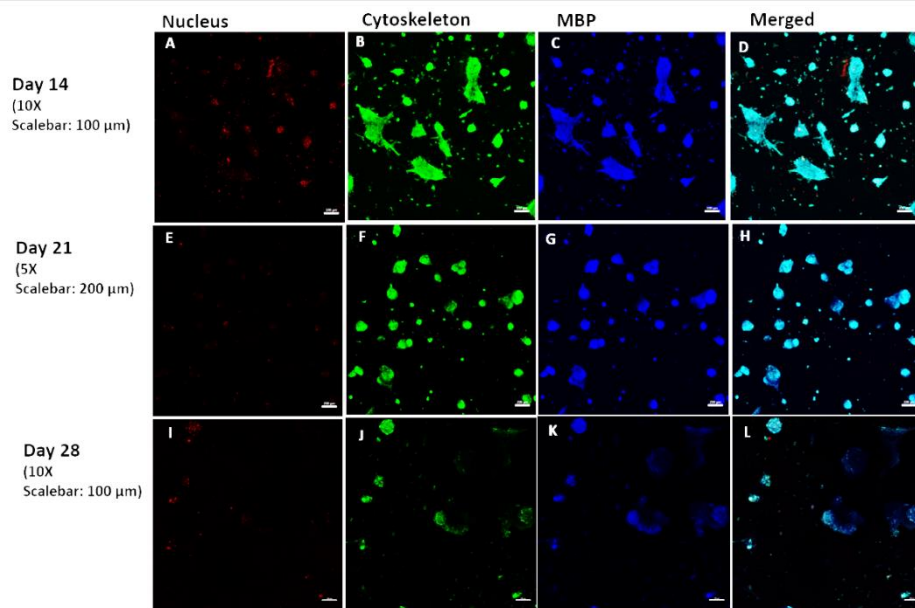
Figure 3.18 CLSM images of MBP antibody (blue), cytoskeleton (green), nucleus (red) and merged Schwann cells on pHEMA.
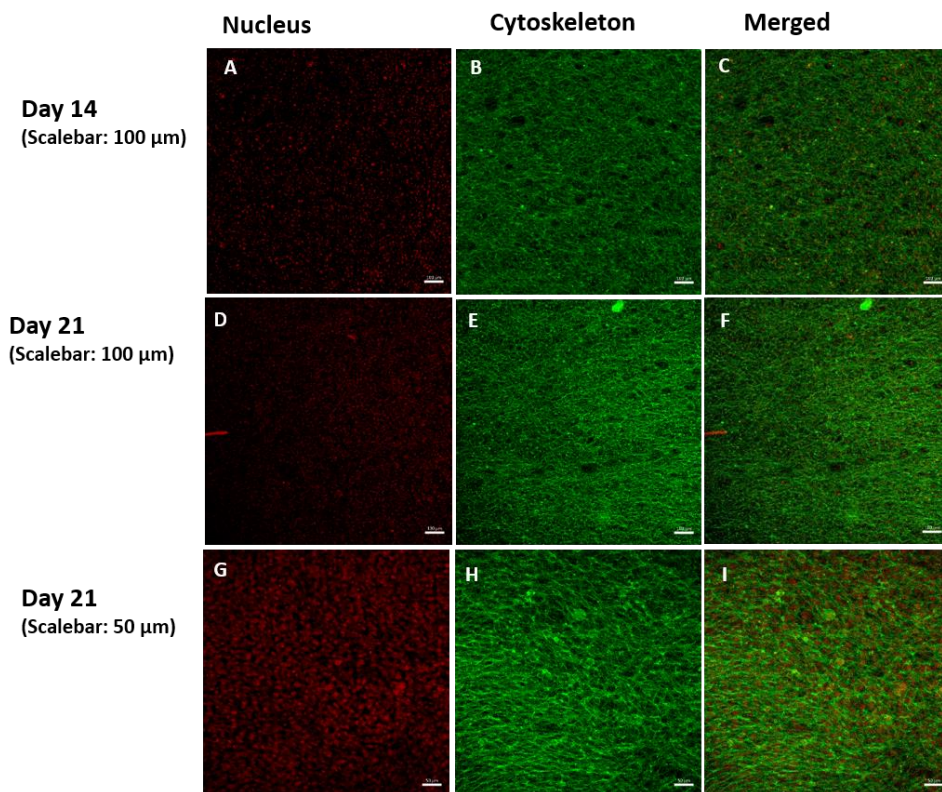
Figure 3.19 CLSM images of cytoskeleton (phalloidin; green), nucleus (DAPI:red) and merged Schwann cells on collagen coated pHEMA.

3.3.3 Determination of Schwann Cell Proliferation (MTT Test)

The MTT test was used to quantitatively determine the changes in Schwann cell adhesion and proliferation on pHEMA hydrogels (Figure 3.21). The cell numbers were calculated by using the calibration curve prepared with the known number of cells (Appendix C). After 24 h of cell seeding the cells were counted to determine the attachment. Almost 70% of the 5×10^4 cells seeded were attached on pHEMA hydrogels. After 7 days, the increase in the cell numbers were counted as 5 times bigger than the attached cell number. For the next 7 days the number was doubled and at the last week the cell number increased slightly lower. All of the increases in the cell numbers were statistically significant.

Figure 3.20 MTT test of the cells on pHEMA hydrogels on Days 1, 7, 14, 21 and 28 (B). Statistical differences (* $p \leq 0.05$, **$p \leq 0.01$, ***$p \leq 0.001$) are indicated.

3.4   *In vitro* Studies with SHSY5Y cells

Human neuroblastoma SHSY5Y is a dopaminergic neuronal cell line which has been used by various researchers as an *in vitro* model for determination of the neuronal behavior on nerve conduits (Cheung et al., 2019; Scalera et al., 2021). In the present study SHSY5Y cells were seeed on GelMA-HaMa IPNs for the determination of cell attachment and proliferation and in the IPNS to study the axon elongation through the nerve conduit. The cells also were analyzed in terms of neuron specific antibody production; NeuN and beta III Tubulin and the effects of Schwann cell presence and Netrin-1 protein were analyzed.

3.4.1   Live-Dead Cell Viability Assay in GelMA-HaMA IPNs

SHSY5Y cells were seeded in GelMA-HaMA IPNs. Live dead cell viability assay was performed on days 1, 7 and 14. The cells were able to attach and proliferate in the IPNs (Figure 3.21). The cells on the micrographs were counted by using ImageJ software. Live cell fraction of the cells was above 80% on Day 1 and above 90% on Days 7 and 14 (Figure 3.22).
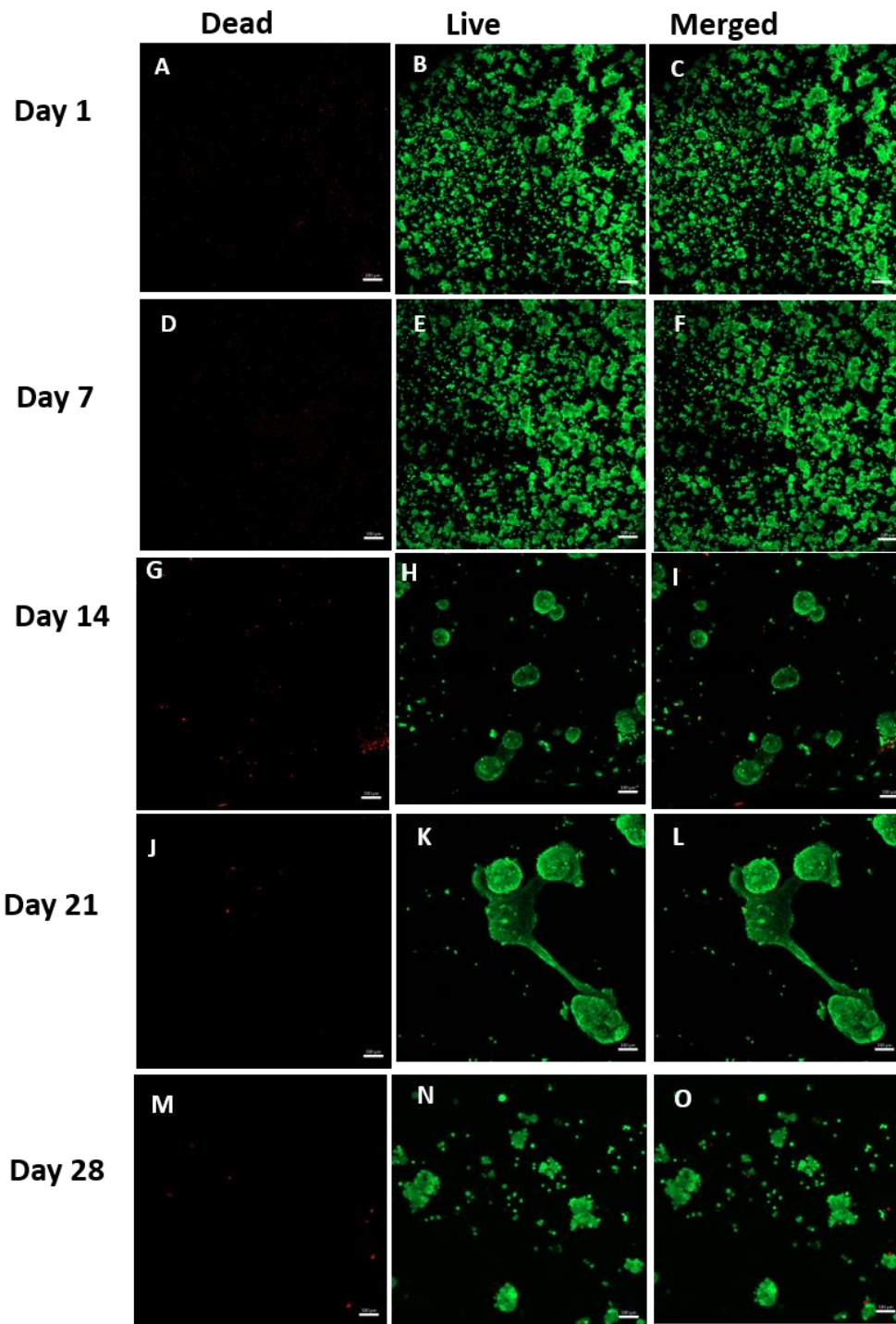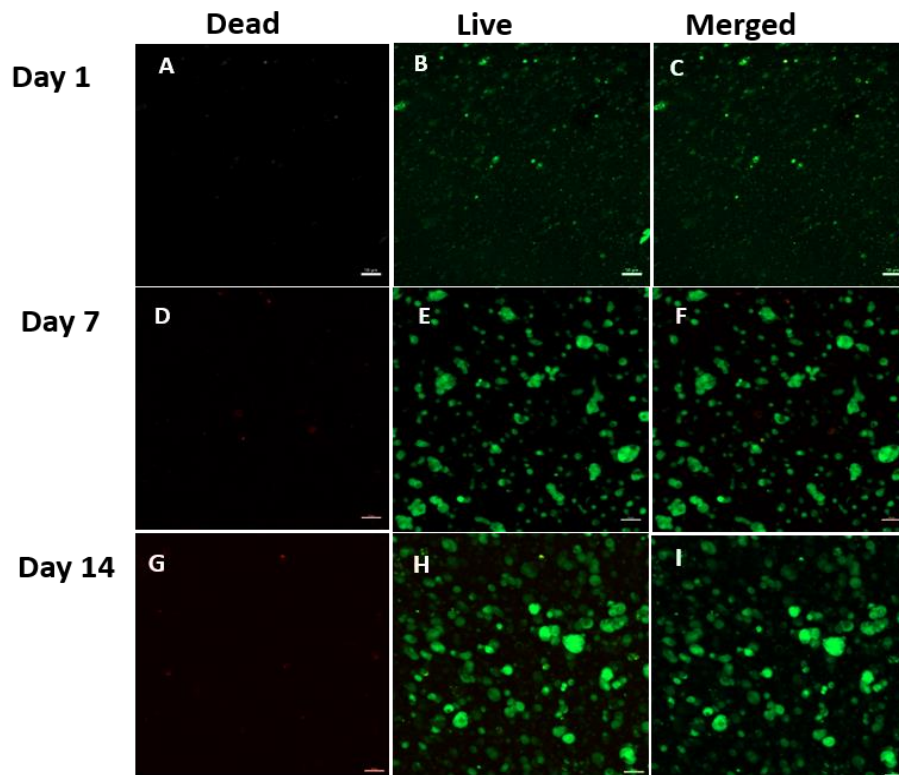
Figure 3.21 Live-Dead analysis of SHSY5Y Cells in GelMA-HaMA IPN. A- Day 1 dead cells, B- Day 1 live cells, C- Day 1 Merged image, D- Day 7 dead cells, E- Day 7 live cells, F- Day 7 merged image, G- Day 14 dead cells, H- Day 21 live cells, I- Day 21 Merged
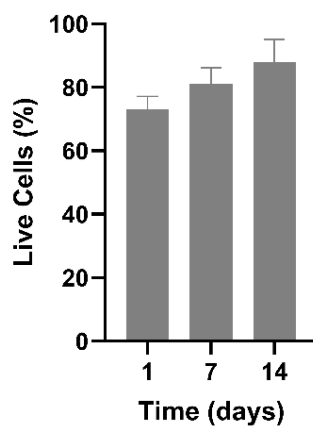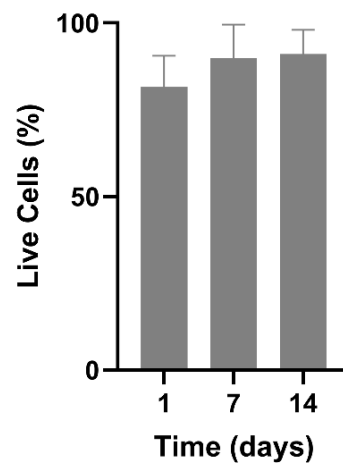

Figure 3.22 Quantitative analysis of the SHSY5Y cells on GelMA-HaMA IPNs by using ImageJ software.

3.4.2 Cytoskeleton-Nucleus Staining and Neuron Specific Antibody Staining

Figure 3.23 shows nucleus, cytoskeleton and neuron specific antibody staining of SHSY5Y cells on GelMA-HaMA IPN (85:15). The cells were attached and proliferated on Day 7 (Figure 3.23 A, B, C, D). The neurite outgrowth of the SHSY5Y cells were not observed. Neuronal nuclei protein (NeuN) is a neuron-specific nuclear protein, reported to be stably expressed in most postmitotic neurons of the vertebrate nervous system (Luijerink et al., 2021). It was also previously reported that some proximal processes are strongly positive for NeuN expression, whereas distal axons and the branches of dendrites do not express NeuN (Duan et l., 2016). In Figure 3.23 it is seen that the SHSY5Y cells without neuronal branches like dendrites and axons expressed NeuN. This showed that the cells were in postmitotic state and did not start to produce neurite extensions.
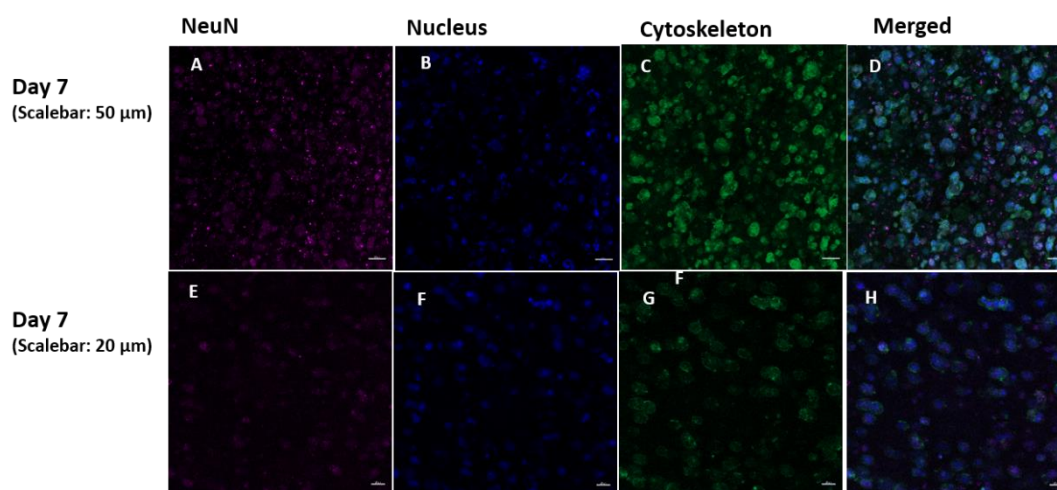
Figure 3.23 CLSM images of NeuN antibody (purple), cytoskeleton (alexa fluor phalloidin, green), nucleus (DAPI, blue) and merged images of SHSY5Y cells on GelMA-HaMA IPN.

3.4.3 Effect of Netrin-1 protein on SHSY5Y cells on GelMA-HaMA IPNs

Netrin proteins have been implicated in directing circumferential axonal projections in vertebrates (Huang et al., 2021). Netrin-1 is initially identified as a classic axonal guidance molecule that is essential in guiding axonal pathfinding and migration of neurons. Netrin, slit, ephrin, and semaphorin have been recognized as four classic

axonal guidance molecules, while netrin-1 possesses the strongest capacity for axon elongation. Figure 3.24 shows cytoskeleton staining of SHSY5Y cells incubated for 7 days without (Figure 3.24A) and with (Figure 3.24B) Netrin-1. The images showed that the SHY5Y cell started to produce neurite outgrowth in the presence of Netrin-1. The cells were also analyzed in terms of NeuN expression (Figure 3.25). It was observed that the cell treated with Netrin-1 decreased NeuN expression because they started to produce some neurite extensions.
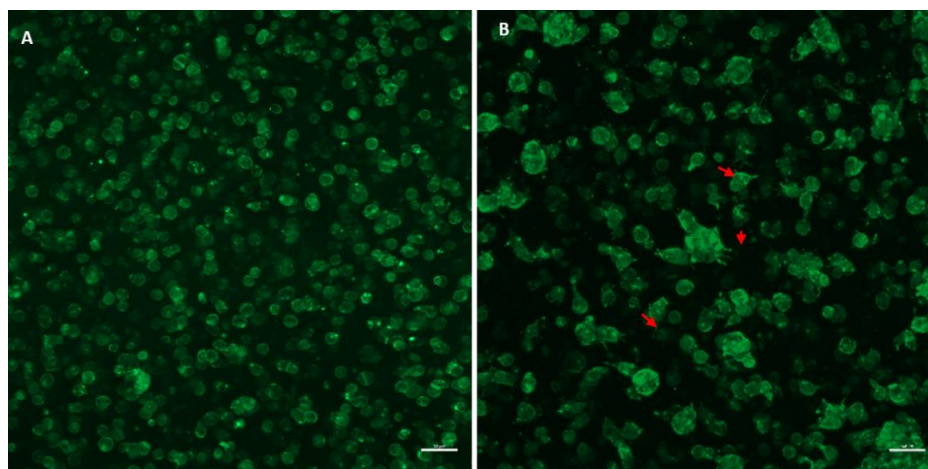
Figure 3.24 CLSM images of cytoskeleton (alexa fluor-phalloidin, green) of SHSY5Y cells in GelMA-HaMA IPN incubated A) without Netrin-1 and B) with Netrin-1. Day 14: Scale bar 50 μm. The arows show the examples of neuronal growth cones.
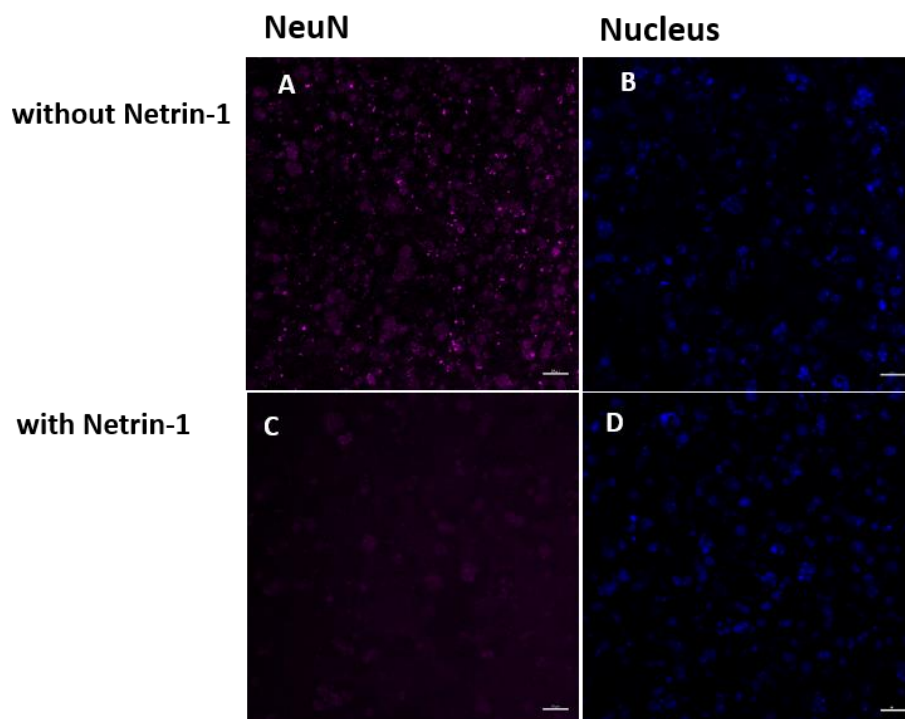
Figure 3.25 CLSM images of NeuN antibody (purple) and nucleus (DAPI, blue) of SHSY5Y cells in GelMA-HaMA IPN incubated A-B) without Netrin-1 and C-D) with Netrin-1. Scale bar 50 μm.

3.4.4 Determination of SHSY5Y Cell Proliferation (MTT Test)

The attachment at the proliferation of SHSY5Y cells on GelMA-HaMA IPNs were determined by MTT analysis. (Figure 3.26). The cell numbers were calculated by using MTT calibration curve prepared with the known number of cells (Appendix D). Almost 70% of the cells seeded were attached at the first day and the cell numbers were doubled at every time points showing that the cells were able to attach and proliferated on IPN surfaces.
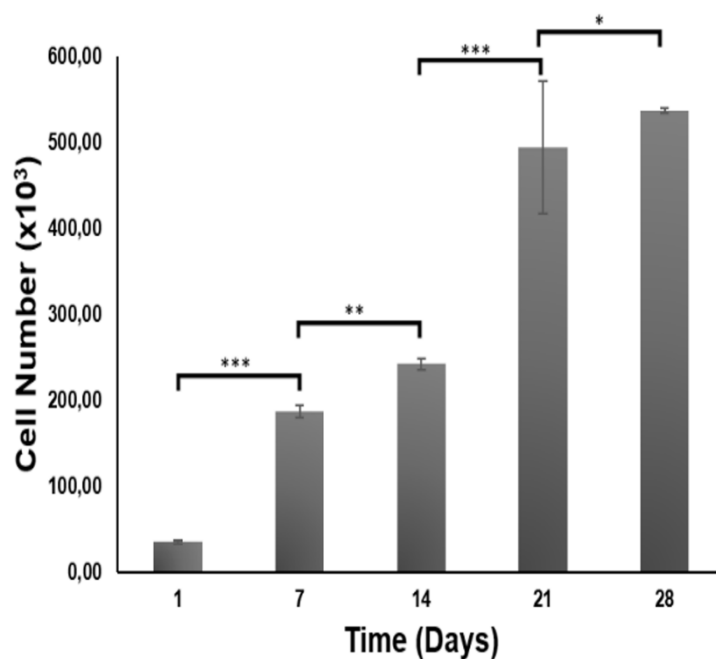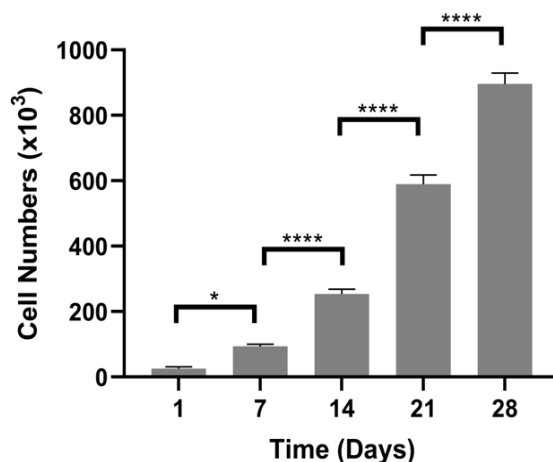
Figure 3.26 MTT test of the SHSY5Y cells in GelMA-HaMA IPNs on Days 1, 7, 14, 21 and 28. Statistical differences (* $p \leq 0.05$, **$p \leq 0.01$, ***$p \leq 0.001$) are indicated.

3.5 *In vitro* Co-culture Studies with SCs and SHSY5Y cells

For co-culture studies, SHSY5Y cell were seeded on GelMA-HaMA IPNs and SCs were seeded on cylindrical pHEMA hydrogels. After 7 days of incubation, SHSY5Y cell containing IPNs were placed in the SCs seeded cylindrical conduits including cell free GelMA-HaMA IPN and cell free IPNs were polymerized after the addition of cell containing IPNs. The overall conduit was incubated for 7 days. At the end of the incubation period Netrin-1 protein was injected to the distal part of the pHEMA hydrogel and the cells were examined after 7 days of incubation (See Section 2.2.7; Figure 2.6).

3.5.1 Cell Behavior on Nerve Conduits

SHSY5Y cell containing IPNs were placed into pHEMA cylindrical hydrogels on which SCs were seeded. PHEMA conduits were also included cell free IPN structure at the middle and distal end (Figure 3.27A). The cells were stained with FITC-phalloidin for cytoskeleton and DAPI for nucleus and examined on days 7, 14 and 21 to determine the ability of migration through the conduit (Figure 3.27B). SHSY5Y cells were able to proliferate in the conduit and also migrate through the structure. The number of cells at the middle and distal end of the conduits was

77

increased in 21 days. The migration of the cells, the presence of the neurite extensions and the communication between the cells at the middle and the distal end would be considered as a promising factor that the conduit structure including GelMA-HaMA IPN may provide space for the growing neurons for axonal regeneration in case of an injury. The previous study reported by Dursun-Usal et al., showed similar results that the neurite outgrowths and migration of neural cells through nerve conduit prepared by GelMA-pHEMA blends (2019). Another study showed also neurite outgrowth in the presence of neural growth factors similar to the factor presence by the help of Schwann cells in the present study (Sun et al., 2021).

Figure 3.28 shows SCs on collagen coated pHEMA part, the outer cylinder, of the whole nerve conduit. The cells were able to attach on the surfaces (Figure 3.28 A-C) and proliferate on days 7 and 14 (Figure 3.28 D-I). All the cells were able to extend the processes and increased their surface area during the culturing period. This behavior of the cells may be explained by the appropriate surface properties of the pHEMA surface after collagen coating. The cellular structures of the cells are similar to the SCs cells reported in tissue engineering applications (Koroleva et al., 2006; Hu et al., 2020).
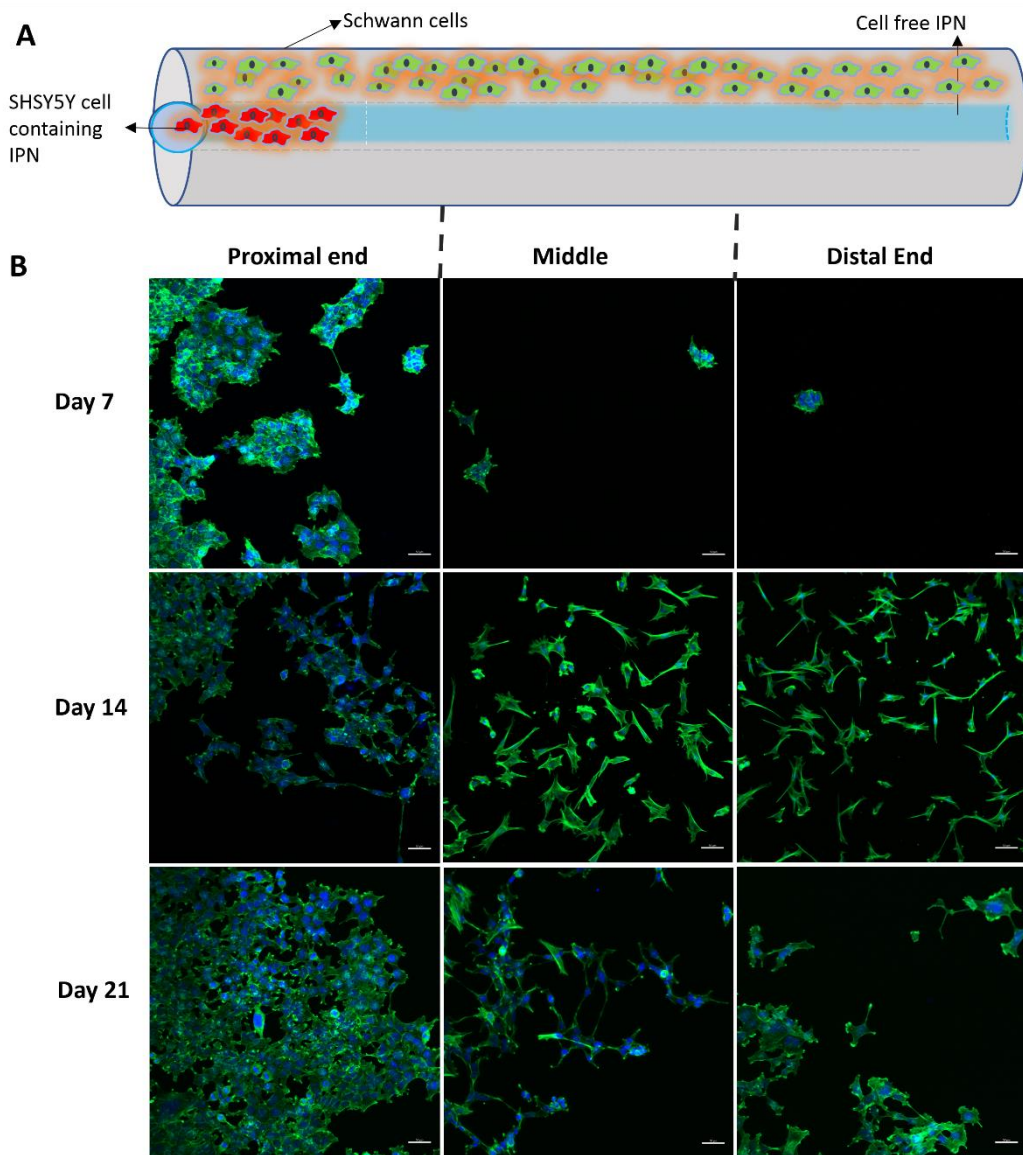
Figure 3.27 CSLM analysis of SHSY5Y cells in nerve conduits. A) Schematic representation of the conduits and cell seeding. B) Cytoskeleton and DAPI staining of SHSY5Y cells in proximal, middle and distal parts of the conduit structure on Days 7, 14 and 21. Scale bar: 50 μm.
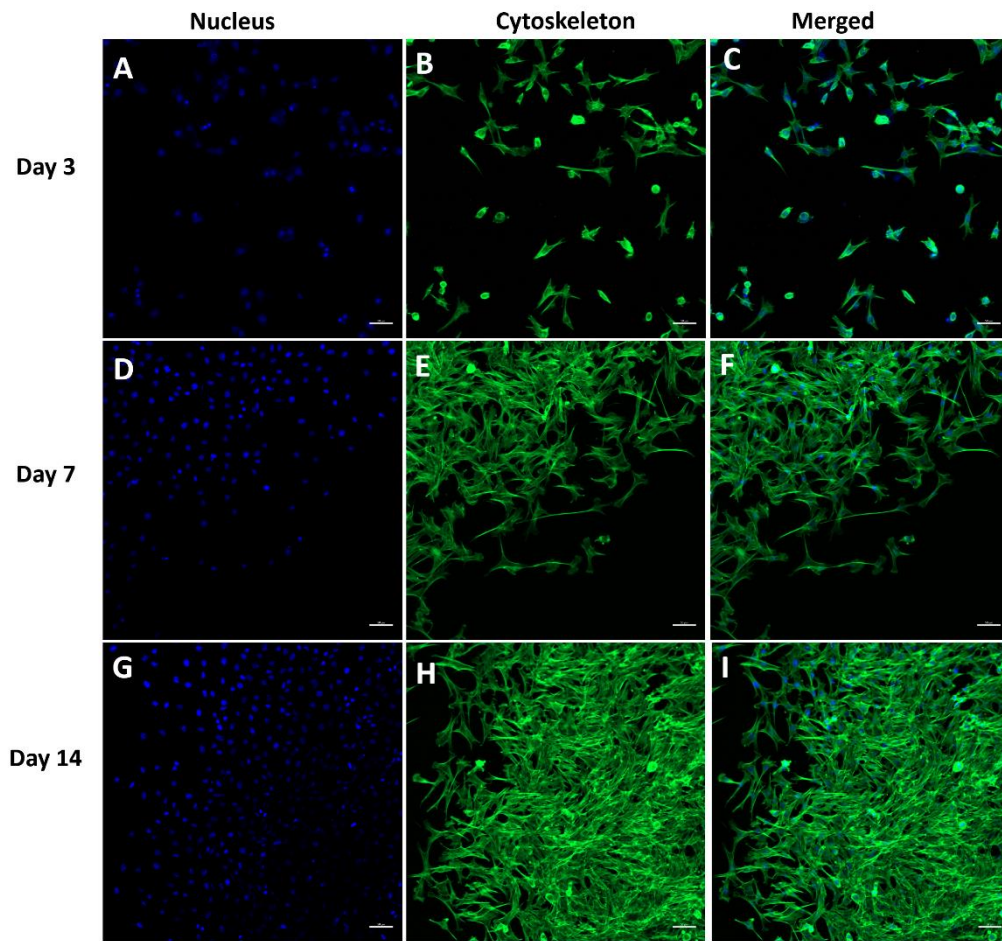
Figure 3.28 CLSM images of, cytoskeleton (green), nucleus (blue) and merged Schwann cells on pHEMA exterior of the whole conduit. A-C- Day 13; D-F- Day 14; G-I- Day 21, Scale bar: 50 μm.

3.5.2 Myelin Basic Protein and Neuron Specific Antibody Staining of Co-culture

After the construction of the nerve conduits, the cells were analyzed with specific antibody staining. Myelin basic antibody staining was used to determine whether Schwann cells were secreting the protein which was an indicator of the functionalization of these cells. Thus, SCs cells were stained with myelin basic protein antibody (Figure 3.29). The cells had secreted myelin basic protein and continued the secretion on day 14. The study reported by Li et al., the myelin

secretion from Schwann cells on nerve conduits helped regenerating axons more when compared to the autologous grafts (2020). Thus, it is promising that SCs are able to show characteristics that would be helpful for neuronal regeneration.
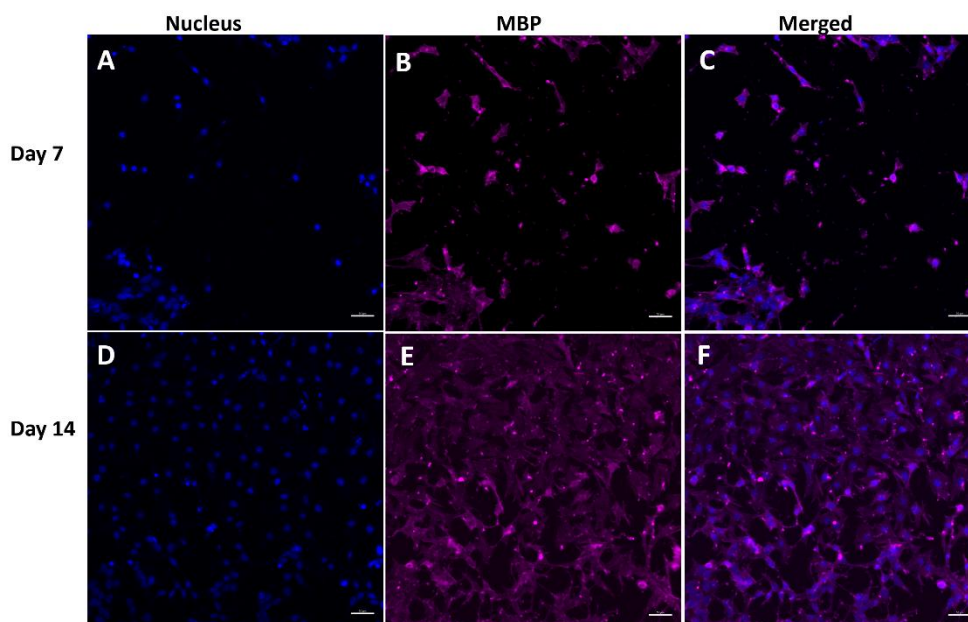
Figure 3.29 CLSM images of MBP antibody (pink), nucleus (blue) and merged Schwann cells on pHEMA part of the whole conduit. A-C- Day 7; D-F- Day 14. Scale bar: 50 μm.

In order to understand the cellular state of SHSY5Y cells, Beta III Tubulin and NeuN antibody staining was performed. NeuN protein, as previously explained, are found in the post mitotic neuronal cells. When a neuron is projecting neurites NeuN production decreases or stops. Figure 3.30 shows antibody staining of SHSY5Y cells. When compared to SHSY5Y cells incubated without SCs (See section 3.4.2), NeuN secretion was decreased showing that the cells started to produce neurite extensions. Beta III tubulin is a microtubule element expressed in neurons and it is used as an early neuronal marker (Liu and Dwyer, 2014). During the production of neurite extensions, growth cone is produced. In these growth cones, actin and microtubule dynamics take part and Beta III tubulin antibody staining is a good way to see growing neurite extension. SHSY5Y cells incubated with SCs in the whole

nerve conduit showed neurite extensions (Figure 3.30 C and G). Ruiz et al., prepared a nerve conduit composed of hyaluronan and carbon nanotubes and checked their suitability for the regeneration of tubular neural structures (2021). The results showed the nerves on the nerve conduits were able to produce Beta III tubulin and they concluded that the presence of neuronal markers as promising for the nerve conduits to be used for nerve regeneration applications. In another study, researchers prepared 3D printed nerve conduits and studied effects of different neural factor amounts on the prduction of Beta III Tubulin and the results concluded with the help of enhanced Beta III Tubulin production, meaning that Beta III Tubulin expression levels are good indicator for the regenerating-growing axons (Ramesh et al., 2021). Thus, the results of increased Beta III Tubulin production in the present study showed that the nerve conduit is also promising for regenerating axons after peripheral injury.
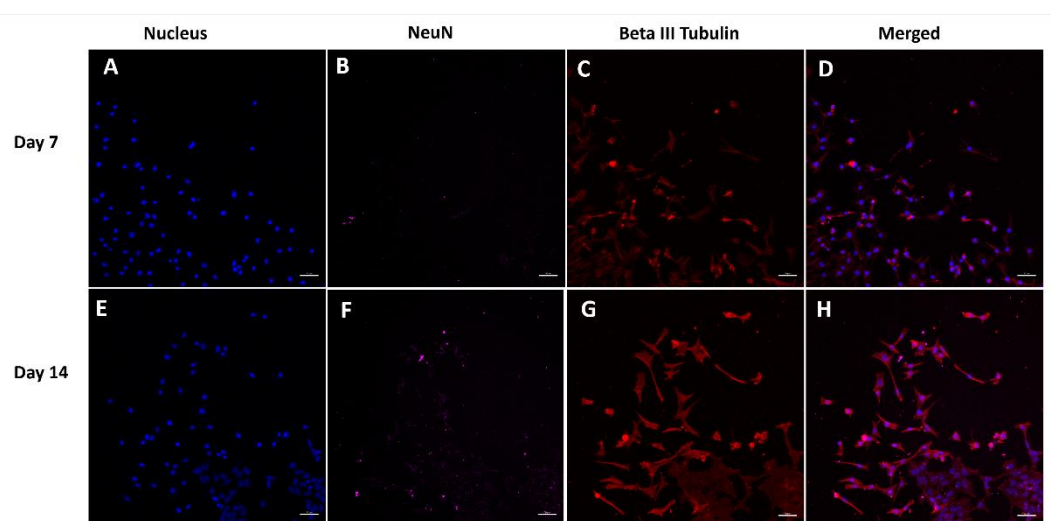
Figure 3.30 CLSM images of NeuN antibody (pink), nucleus (blue), Beta III Tubulin (red) and merged SHSY5Y cells in the nerve conduits. A-D- Day 7; F-H- Day 14. Scale bar: 50 µm.

3.5.2.1 Netrin Effect on SHSY5Y cells

Netrin-1 is initially identified as a classic axonal guidance molecule that is essential in guiding axonal pathfinding and migration of neurons (Lv et al., 2015). Netrin, slit, ephrin, and semaphoring have been recognized as four classic axonal guidance molecules, while netrin-1 possesses the strongest capacity for axon elongation. SHSY5Y cells incubated in the whole conduit together with SCs showed neurite extensions (See section 3.5.2), but the extensions were not aligned in the IPN structure. It was previously reported that GelMa scaffold loaded with Netrin-1 significantly increased the expression of regeneration proteins in the injured peripheral nerves in addition to achieving the micro-circulation restoration of muscle fibers when compared to control groups (autologous graft group) (Grijalvo and Díaz, 2021).

In the present study, Netrin-1 protein was loaded at the distal part of the nerve conduit including SCs, due to the reason that it is involved in axonal guidance in the nervous system (Prierta et al., 2017). Figure 3.31 shows the nucleus (blue) and beta III tubulin (red) staining of SHSY5Y cells in the presence of both SCs and Netrin-1 protein. SHSY5Y cells started to extend their extensions towards the distal end and had more aligned extensions through the nerve conduit when compared to the ones incubated without Netrin-1.
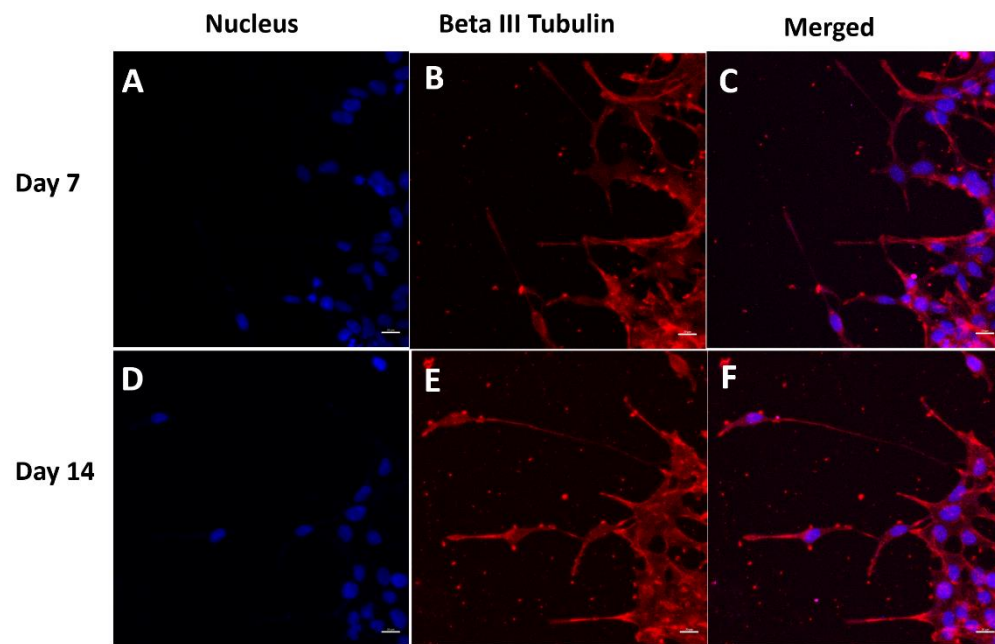
Figure 3.31 CLSM images of nucleus (blue), Beta III Tubulin (red) and merged SHSY5Y cells in the nerve conduits in the presence of Netrin-1 protein. A-C- Day 7; D-F- Day 14. Scale bar: 20 μm.

CHAPTER 4

CONCLUSION

Any injury in peripheral nerves may result in a loss of neuronal communication along sensory and motor nerves between the CNS and the peripheral organs, resulting in painful neuropathies via reduction in motor and sensory functions, drastically affecting patients' daily activities. For the treatment of peripheral nerve injuries, end-to-end suturing is widely used for the gaps smaller than 3 mm. For the bigger gaps, autografts, allografts, or xenografts are used. But there are some limitations like donor side morbidity, tissue rejection, cross contamination. As alternative method, nerve conduit materials are used for the regeneration of the axons at the injury side. Although there are various FDA approved commercially available conduit materials, they are generally hollow tubes preventing them from used in gaps bigger than 10 mm, because they may lead axonal sprouts to form.

In this study pHEMA cylindrical structure filled with GelMA-HaMA gel matrix as a nerve guidance channel is presented. Following the structural analysis of the nerve guide, *in vitro* studies were performed with Schwann cells seeded on pHEMA as support cells and it continued with SHSY5Y neuroblastoma cells seeded in the gel matrix. Cytotoxicity of the materials was studied with live-dead assay and proliferation of the cells on the structure was tested by MTT assay. Microscopical examination of the cells was performed by Confocal Laser Scanning Microscopy.

The outer structure, pHEMA hydrogels, were analyzed in terms its water absorption ability, mechanical strength, and water contact angle. Water absorption ability of the hydrogels showed that the structural integrity of the hydrogels after repeated swelling/drying cycles was preserved. Water contact angle was found as $31.0^{\circ} \pm 7.6$, suitable to be used in the tissue engineering applications. In addition, mechanical

testing showed that tensile modulus and tensile strength 570.9 ± 92.13 and 501.8 ± 93.7, respectively. Ultimate Tensile Strength for acellular nerve tissue is 1400 kPa and tensile modulus is 576 kPa. Although tensile strengths of the hydrogels are significantly smaller than the acellular nerve tissue, tensile modulus values are comparable to that of an acellular nerve tissue.

SCs cells seeded on the pHEMA surfaces were able to attach at a fraction of 70% and proliferate. Myelin basic antibody staining was used to determine whether Schwann cells were secreting the protein which was an indicator of the functionalization of these cells. The results showed that, SCs on pHEMA surface were able to secrete MBP and concluded that they could be helpful for the regenerating axons.

SHSY5Y cells were seeded in GelMA-HaMA IPNs and cell seeded IPNs were placed in pHEMA channels. The behavior of the cells was examined in the presence of SCs and Netrin-1 molecule applied distal part of the nerve conduits. In the presence of the SCs, SHSY5Y cells seeded at the proximal end of the conduits were able to migrate through the conduit, but the neurite extensions were not disorganized at the absence of Netrin-1. The results also showed that the SHY5Y cells started to produce neurite outgrowth more aligned in the presence of Netrin-1. The cells were also analyzed in terms of NeuN expression. It was observed that the cell treated with Netrin-1 decreased NeuN expression because they started to produce some neurite extensions. Together with those results, the presence of increased Beta III Tubulin, an indicator for the production of neurite extensions, production in the present study showed that the nerve conduit is also promising for regenerating axons after peripheral injury.

REFERENCES

Abbas, O. L., Özatik, O., Gönen, Z. B., Koçman, A. E., Dag, I., Özatik, F. Y., Musmul, A. (2019). Bone Marrow Mesenchymal Stem Cell Transplantation Enhances Nerve Regeneration in a Rat Model of Hindlimb Replantation. Plastic and reconstructive surgery, 143(4), 758e-768e.

Ahmed, M. N., Shi, D., Dailey, M. T., Rothermund, K., Drewry, M. D., Calabrese, T. C., ... & Syed-Picard, F. N. (2021). Dental pulp cell sheets enhance facial nerve regeneration via local neurotrophic factor delivery. Tissue Engineering Part A, 27(17-18), 1128-1139.

Almeida, H. A., & Bártolo, P. J. (2021). Biomimetic Boundary-Based Scaffold Design for Tissue Engineering Applications. In Computer-Aided Tissue Engineering (pp. 3-18). Humana, New York, NY.

Almeida, J. F., Ferreira, P., Lopes, A., Gil, M. H. (2011). Photocrosslinkable biodegradable responsive hydrogels as drug delivery systems. International Journal of Biological Macromolecules, 49(5), 948-954.

Amaral, A. J., & Pasparakis, G. (2019). Cell membrane engineering with synthetic materials: Applications in cell spheroids, cellular glues and microtissue formation. Acta biomaterialia.

Amini, S., Salehi, H., Setayeshmehr, M., & Ghorbani, M. (2021). Natural and synthetic polymeric scaffolds used in peripheral nerve tissue engineering: Advantages and disadvantages. Polymers for Advanced Technologies, 32(6), 2267-2289.

Arslantunali, D., Budak, G., Hasirci, V. (2014b). Multiwalled CNT-pHEMA composite conduit for peripheral nerve repair. Journal of Biomadical Materials Research. Part A, 102(3), 828-841.

Arslantunali, D., Dursun, T., Yucel, D., Hasirci, N., Hasirci, V. (2014a). Peripheral nerve conduits: technology update. Medical Devices: Evidence and Research, 7, 405-424.

Augistin, J.G., Purves, D., Fitzpatrick, D., Hall W.C., Lamantia A.S., McNamara, J.O., Williams, A.M., eds. (2004). Neuroscience, 3rd edition (pp. 31-198). Sinauer Associates, Inc.

Bagher, Z., Ehterami, A., Nasrolahi, M., Azimi, M., & Salehi, M. (2021). Hesperidin promotes peripheral nerve regeneration based on tissue engineering strategy using alginate/chitosan hydrogel: in vitro and in vivo study. International Journal of Polymeric Materials and Polymeric Biomaterials, 70(5), 299-308.

Bassilios Habre, S., Bond, G., Jing, X.L., Kostopuolos, E., Wallace, R.D., Konofaos, P. (2018). The surgical Management of Nerve Gaps. Annals of Plastic Surgery, 80(3), 252-261.

Bektas, C. K., & Hasirci, V. (2020). Cell Loaded GelMA: HEMA IPN hydrogels for corneal stroma engineering. Journal of Materials Science: Materials in Medicine, 31(1), 1-15.

Beris, A., Gkiatas, I., Gelalis, I., Papadopoulos, D., Kostas-Agnantis, I. (2019). Current concepts in peripheral nerve surgery. European Journal of Orthopaedic Surgery & Traumatology, 29(2), 263-269.

Bertoni, F., Barbani, N., Giusti, P., & Ciardelli, G. (2006). Transglutaminase reactivity with gelatine: perspective applications in tissue engineering. Biotechnology letters, 28(10), 697-702.

Blackstone, B. N., Gallentine, S. C., & Powell, H. M. (2021). Collagen-based electrospun materials for tissue engineering: a systematic review. Bioengineering, 8(3), 39.

Blausen.com staff (2014). "Medical gallery of Blausen Medical 2014".

Boecker, A. H., Bozkurt, A., Kim, B. S., Altinova, H., Tank, J., Deumens, R., van Neerven, S. G. A. (2018). Cell-enrichment with olfactory ensheathing cells has limited local extra beneficial effects on nerve regeneration supported by the nerve guide Perimaix. Journal of tissue engineering and regenerative medicine, 12(11), 2125-2137.

Boriani, F., Fazio, N., Bolognesi, F., Pedrini, F. A., Marchetti, C.,Baldini, N. (2019). Noncellular modification of acellular nerve allografts for peripheral nerve reconstruction: a systematic critical review of the animal literature. World neurosurgery, 122, 692-703.

Brassard, J. A., & Lutolf, M. P. (2019). Engineering stem cell self-organization to build better organoids. Cell stem cell, 24(6), 860-876.

Broas, S. M., & Banerjee, I. A. (2021). Design of peptide-PEG-Thiazole bound polypyrrole supramolecular assemblies for enhanced neuronal cell interactions. Soft Materials, 19(4), 428-443.

Bucan, V., Vaslaitis, D., Peck, C. T., Strauß, S., Vogt, P. M., Radtke, C. (2019). Effect of exosomes from rat adipose-derived mesenchymal stem cells on neurite outgrowth and sciatic nerve regeneration after crush injury. Molecular neurobiology, 56(3), 1812-1824.

Burnett, M. G., Zager, E. L. (2004). Pathophysiology of peripheral nerve injury: A brief review. Neurosurgical Focus, 16(5), E1.

Cadena, M., Ning, L., King, A., Hwang, B., Jin, L., Serpooshan, V., & Sloan, S. A. (2021). 3D bioprinting of neural tissues. Advanced healthcare materials, 10(15), 2001600.

Carvalho, C. R., Wrobel, S., Meyer, C., Brandenberger, C., Cengiz, I. F., LópezCebral, R., Silva-Correia, J., Ronchi, G., Reis, R. L., Grothe, C., Oliveira, J. M.,
Haastert-Talini, K. (2018). Gellan Gum-based luminal fillers for peripheral nerve

regeneration: an in vivo study in the rat sciatic nerve repair model. Biomaterials Science, 6(5), 1059-1075.

Cetrulo Jr, C. (2018). GalT-KO Porcine Nerve Xenograft for Reconstruction of Large Nerve Gaps. The Massachusetts General Hospital Boston United States.

Chen, K., Li, X., Li, N., Dong, H., Zhang, Y., Yoshizawa, M., & Kagami, H. (2019). Spontaneously Formed Spheroids from Mouse Compact Bone-Derived Cells Retain Highly Potent Stem Cells with Enhanced Differentiation Capability. Stem cells international, 2019.

Chen, Y. W., Chen, C. C., Ng, H. Y., Lou, C. W., Chen, Y. S., Shie, M. Y. (2019). Additive manufacturing of nerve decellularized extracellular matrix-contained polyurethane conduits for peripheral nerve regeneration. Polymers, 11(10), 1612.

Chen, Y., Long, X., Lin, W., Du, B., Yin, H., Lan, W., ... & Tan, H. (2021). Bioactive 3D porous cobalt-doped alginate/waterborne polyurethane scaffolds with a coral reef-like rough surface for nerve tissue engineering application. *Journal of Materials Chemistry B*, *9*(2), 322-335.

Cheung, Y. T., Lau, W. K. W., Yu, M. S., Lai, C. S. W., Yeung, S. C., So, K. F., & Chang, R. C. C. (2009). Effects of all-trans-retinoic acid on human SH-SY5Y neuroblastoma as *in vitro* model in neurotoxicity research. Neurotoxicology, 30(1), 127-135.

Chiono, V., Tonda-Turo, C. (2015). Trends in the design of nerve guidance channels in peripheral nerve tissue engineering. Progress in neurobiology, 131, 87-104.

Chrząszcz, P., Derbisz, K., Suszyński, K., Miodoński, J., Trybulski, R., Lewin-Kowalik, J., & Marcol, W. (2018). Application of peripheral nerve conduits in clinical practice: a literature review. *neurologia i neurochirurgia polska*, *52*(4), 427-435.

Cui, L., Jia, J., Guo, Y., Liu, Y., & Zhu, P. (2014). Preparation and characterization of IPN hydrogels composed of chitosan and gelatin cross-linked by genipin. Carbohydrate polymers, 99, 31-38.

Daly, W., Yao, L., Zeugolis, D., Windebank, A., Pandit, A. (2012). A biomaterials approach to peripheral nerve regeneration: Bridging the peripheral nerve gap and enhancing functional recovery. Journal of the Royal Society, Interface, 9(67), 202–221.

De la Rosa, M. B., Sharma, A. D., Mallapragada, S. K., Sakaguchi, D. S. (2017). Transdifferentiation of brain-derived neurotrophic factor (BDNF)-secreting mesenchymal stem cells significantly enhance BDNF secretion and Schwann cell marker proteins. Journal of bioscience and bioengineering, 124(5), 572-582.

Deleyto, E., Lasso, J. M. (2018). An Overview of Peripheral Nerve Xenotransplantation: Present Status and Future Directions.

Deng, L., Kang, X., Liu, Y., Feng, F., Zhang, H. (2018). Characterization of gelatin/zein films fabricated by electrospinning vs solvent casting. Food hydrocolloids, 74, 324-332.

Devi, G. V., Anil, S., & Venkatesan, J. (2021). Biomaterials and Scaffold Fabrication Techniques for Tissue Engineering Applications. In Engineering Materials for Stem Cell Regeneration (pp. 691-706). Springer, Singapore.

Dixon, A. R., Jariwala, S. H., Bilis, Z., Loverde, J. R., Pasquina, P. F., Alvarez, L. M.
(2018). Bridging the gap in peripheral nerve repair with 3D printed and bioprinted conduits. Biomaterials, 186, 44-63.

Dixon, A., Jariwala, S., Bilis, Z., Loverde, J., Pasquina, P., Alvarez, L. (2018). Bridging the gap in peripheral nerve repair with 3D printed and bioprinted conduits. Biomaterials, 186, 44-63.

Dodla, M., Alvarado-Velez, M., Mukhatyar, V., Bellamkonda, R. (2019). Peripheral Nerve Regeneration. Principles Of Regenerative Medicine, 1223-1236.

Domingues, R.C.C., Pereira, C.C., Borges, .CP. (2017) Morphological control and properties of poly (lactic acid) hollow fibers for biomedical applications. J Appl Polym Sci. 134, 45494.

Duan, W., Zhang, Y. P., Hou, Z., Huang, C., Zhu, H., Zhang, C. Q., & Yin, Q. (2016). Novel insights into NeuN: from neuronal marker to splicing regulator. Molecular neurobiology, 53(3), 1637-1647.

Ehterami, A., Masoomikarimi, M., Bastami, F., Jafarisani, M., Alizadeh, M., Mehrabi, M., & Salehi, M. (2021). Fabrication and Characterization of Nanofibrous Poly (L-Lactic Acid)/Chitosan-Based Scaffold by Liquid–Liquid Phase Separation Technique for Nerve Tissue Engineering. Molecular Biotechnology, 1-10.

Ehterami, A., Masoomikarimi, M., Bastami, F., Jafarisani, M., Alizadeh, M., Mehrabi, M., & Salehi, M. (2021). Fabrication and Characterization of Nanofibrous Poly (L-Lactic Acid)/Chitosan-Based Scaffold by Liquid–Liquid Phase Separation Technique for Nerve Tissue Engineering. Molecular Biotechnology, 1-10.

Evans, G., Brandt, K., Widmer, M., Lu, L., Meszlenyi, R., Gupta, P. et al. (1999). In vivo evaluation of poly(l-lactic acid) porous conduits for peripheral nerve regeneration. Biomaterials, 20(12).

Eve, D. J., Sanberg, P. R., Buzanska, L., Sarnowska, A., Domanska-Janik, K. (2018). Human Somatic Stem Cell Neural Differentiation Potential. In Human Neural Stem Cells (pp. 21-87). Springer, Cham.

Eward, W. C., Davis, K., Putterman, A., Morrison, E., Ruch, D. (2019). Nerve Conduit Enhancement with Vomeronasal Organ Improves Rat Sciatic Functional Index in a Segmental Nerve Defect Model. International Journal of Orthoplastic Surgery, 2(2).

Fairbairn, N. G., Meppelink, A. M., Ng-Glazier, J., Randolph, M. A., Winograd, J. M.
(2015). Augmenting peripheral nerve regeneration using stem cells: A review of current opinion. World Journal of Stem Cells, 7(1), 11-26.

Fang, X., Zhang, C., Yu, Z., Li, W., Huang, Z., Zhang, W. (2019). GDNF pretreatment overcomes Schwann cell phenotype mismatch to promote motor axon regeneration via sensory graft. Experimental neurology, 318, 258-266.

Ferguson, T. A., Son, Y. J. (2011). Extrinsic and intrinsic determinants of nerve regeneration. Journal of tissue engineering, 2(1).

Fernandes, M., Valente, S. G., Sabongi, R. G., dos Santos, J. B. G., Leite, V. M., Ulrich, H., da Silva Fernandes, M. J. (2018). Bone marrow-derived mesenchymal stem cells versus adipose-derived mesenchymal stem cells for peripheral nerve regeneration. Neural regeneration research, 13(1), 100.

Ferreira, C. L., Valente, C. A., Zanini, M. L., Sgarioni, B., Ferreira Tondo, P. H., Chagastelles, P. C., de Souza Basso, N. R. (2019, February). Biocompatible PCL/PLGA/Polypyrrole Composites for Regenerating Nerves. In Macromolecular Symposia (Vol. 383, No. 1, p. 1800028).

Fornasari, B. E., Carta, G., Gambarotta, G., & Raimondo, S. (2020). Natural-based biomaterials for peripheral nerve injury repair. *Frontiers in Bioengineering and Biotechnology*, *8*, 1209.

Fregnan, F., Morano, M., Ziv-Polat, O., Mandelbaum-Livnat, M. M., Nissan, M., Michael, T., Almog, M. (2017). Effect of Local Delivery of GDNF Conjugated Iron Oxide Nanoparticles on Nerve Regeneration along Long Chitosan Nerve Guide. Peripheral Nerve Regeneration: From Surgery to New Therapeutic Approaches Including Biomaterials and Cell-Based Therapies Development, 197.

Frost, H., Andersson, T., Johansson, S., Englund-Johansson, U., Ekström, P., Dahlin, L., Johansson, F. (2018). Electrospun nerve guide conduits have the potential to bridge peripheral nerve injuries in vivo. Scientific Reports, 8(1).

Fujimaki, H., Uchida, K., Inoue, G., Miyagi, M., Nemoto, N., Saku, T., Sato, J. (2017). Oriented collagen tubes combined with basic fibroblast growth factor promote peripheral nerve regeneration in a 15 mm sciatic nerve defect rat model. Journal of Biomedical Materials Research Part A, 105(1), 8-14.

Gao, M., Lu, P., Lynam, D., Bednark, B., Campana, W. M., Sakamoto, J., Tuszynski, M. (2016). BDNF gene delivery within and beyond templated agarose multi-channel

guidance scaffolds enhances peripheral nerve regeneration. Journal of neural engineering, 13(6), 066011.

Gautam, S., Sharma, C., Purohit, S. D., Singh, H., Dinda, A. K., Potdar, P. D., ... & Mishra, N. C. (2021). Gelatin-polycaprolactone-nanohydroxyapatite electrospun nanocomposite scaffold for bone tissue engineering. Materials Science and Engineering: C, 119, 111588.

Gayer, C., Ritter, J., Bullemer, M., Grom, S., Jauer, L., Meiners, W., Pfister, A., Reinauer, F., Vučak, M., Wissenbach, K., Fischer, H., Poprawe, R., Schleifenbaum, J. H. (2019). Development of a solvent-free polylactide/calcium carbonate composite for selective laser sintering of bone tissue engineering scaffolds. Materials Science and Engineering: C, 101, 660-673.

Ghaderinejad, P., Najmoddin, N., Bagher, Z., Saeed, M., Karimi, S., Simorgh, S., & Pezeshki-Modaress, M. (2021). An Injectable Anisotropic Alginate Hydrogel Containing Oriented Fibers for Nerve Tissue Engineering. Chemical Engineering Journal, 130465.

Gordon, T. (2020). Peripheral nerve regeneration and muscle reinnervation. *International Journal of Molecular Sciences*, *21*(22), 8652.

Grijalvo, S., & Díaz, D. D. (2021). Graphene-based hybrid materials as promising scaffolds for peripheral nerve regeneration. Neurochemistry International, 147, 105005.

Haider, A., Haider, S., Kang, J. (2018). A comprehensiv review summarizing the effect of electrospinning parameter and potential applications of nanofibers in biomedical and biotechnology. Arabian Journal of Chemistry, 11(8), 1165-1118.

Han, G.-H., Peng, J., Liu, P., Ding, X., Wei, S., Lu, S., Wang, Y. (2019). Therapeutic strategies for peripheral nerve injury: decellularized nerve conduits and Schwann cell
transplantation. Neural Regeneration Research, 14(8), 1343-1351.

Hashemi, S., Amirabad, L. M., Nazhvani, F. D., Zarrintaj, P., Namazi, H., Saadatfar, A., & Golchin, A. (2021). Bilayer scaffolds for Interface tissue engineering and regenerative medicine: a systematic reviews.

Hasirci, V., Hasirci, N. (2018) Fundamentals of Human Biology and Anatomy. In Fundamentals of Biomaterials (pp.131-140). New York: Springer New York.

Heath, C. A, and Rutkowski, G. E (1998) The development of bioartificial nerve grafts for peripheral-nerve regeneration. Trends Biotechnol. 16, 163−7.

Hei, W. H., Almansoori, A. A., Sung, M. A., Ju, K. W., Seo, N., Lee, S. H., Lee, J. H. (2017). Adenovirus vector-mediated ex vivo gene transfer of brain-derived neurotrophic factor (BDNF) tohuman umbilical cord blood-derived mesenchymal stem cells (UCB-MSCs) promotescrush-injured rat sciatic nerve regeneration. Neuroscience letters, 643, 111-120.

Heo, D. N., Lee, S.-J., Timsina, R., Qiu, X., Castro, N. J., Zhang, L. G. (2019). Development of 3D printable conductive hydrogel with crystallized PEDOT:PSS for neural tissue engineering. Materials Science and Engineering: C, 99, 582-590.

Heyden, R, J. (2016). The Nervous System and Nervous Tissue. In Anatomy and Physiology (pp. 469-633). Rice University. Houston.

Ho, S., Labroo, P., Lin, K.-M., Sant, H., Shea, J., Gale, B., Agarwal, J. (2019). Designing a Novel Drug Delivering Nerve Guide: A Preliminary Study. Journal of Medical and Biological Engineering, 39(3), 294-304.

Homaeigohar, S., Tsai, T., Young, T., Yang, H., Ji, Y. (2019). An electroactive alginate hydrogel nanocomposite reinforced by functionalized graphite nanofilaments for neural tissue engineering. Carbohydrate Polymers, 224, 115112.

Horng, I., King, K., Patel, J., Pejavara, K., Tallam, K., Emge, T., Murthy, N. S. (2019). Fabrication and Characterization of Polymeric Nerve Conduits.

Hossain, R., Kim, B., Pankratz, R., Ajam, A., Park, S., Biswal, S. L., Choi, Y. (2015). Handcrafted multilayer PDMS microchannel scaffolds for peripheral nerve regeneration. Biomedical microdevices, 17(6), 109.

Houshyar, S., Bhattacharyya, A., Shanks, R. (2019). Peripheral Nerve Conduit: Materials and Structures. ACS Chemical Neuroscience, 10(8), 3349-3365.

Hsu, S. H., Chen, C. W. (2018). 3D bioprinting nerve. In 3D Bioprinting for Reconstructive Surgery (pp. 355-366). Woodhead Publishing.

Hu, X., Wang, X., Xu, Y., Li, L., Liu, J., He, Y., ... & Guo, J. (2020). Electric conductivity on aligned nanofibers facilitates the transdifferentiation of mesenchymal stem cells into Schwann cells and regeneration of injured peripheral nerve. Advanced healthcare materials, 9(11), 1901570.

Huang, Q., Cai, Y., Zhang, X., Liu, J., Liu, Z., Li, B., ... & Lu, X. (2021). Aligned graphene mesh-supported double network natural hydrogel conduit loaded with netrin-1 for peripheral nerve regeneration. ACS Applied Materials & Interfaces, 13(1), 112-122.

Huang, Q., Cai, Y., Zhang, X., Liu, J., Liu, Z., Li, B., ... & Lu, X. (2021). Aligned graphene mesh-supported double network natural hydrogel conduit loaded with netrin-1 for peripheral nerve regeneration. ACS Applied Materials & Interfaces, 13(1), 112-122.

Ikegami, Y., Ijima, H. (2019). Development of heparin-conjugated nanofibers and a novel biological signal by immobilized growth factors for peripheral nerve regeneration. Journal of bioscience and bioengineering.

Imani, F., Karimi-Soflou, R., Shabani, I., & Karkhaneh, A. (2021). PLA electrospun nanofibers modified with polypyrrole-grafted gelatin as bioactive electroconductive scaffold. Polymer, 218, 123487.

Jain, S. A., Nydick, J., Leversedge, F., Power, D., Styron, J., Safa, B., & Buncke, G. (2021). Clinical Outcomes of Symptomatic Neuroma Resection and Reconstruction

with Processed Nerve Allograft. *Plastic and Reconstructive Surgery Global Open*, *9*(10).

Jakab, K., Neagu, A., Mironov, V., Markwald, R. R., & Forgacs, G. (2004). Engineering biological structures of prescribed shape using self-assembling multicellular systems. Proceedings of the National Academy of Sciences, 101(9), 2864-2869.

Jansen, K, van der Werff, J.F.A, van Wachem, P.B, Nicolai, JP.A, de Leij, L.F.M.H, van Luyn, M.J.A (2004) A hyaluronanbased nerve guide: *in vitro* cytotoxicity, subcutaneous tissue reactions, and degradation in the rat. Biomaterials, 25 (3), 483−9.

Jiang, L., Jones, S., Jia, X. (2017). Stem cell transplantation for peripheral nerve regeneration: current options and opportunities. International journal of molecular sciences, 18(1), 94.

Jo, H., Yoon, M., Gajendiran, M., & Kim, K. (2019). Recent Strategies in Fabrication of Gradient Hydrogels for Tissue Engineering Applications. Macromolecular Bioscience, 1900300.

Jones, I., Novikova, L. N., Novikov, L. N., Renardy, M., Ullrich, A., Wiberg, M., Kingham, P. J. (2018). Regenerative effects of human embryonic stem cell-derived neural crest cells for treatment of peripheral nerve injury. Journal of tissue engineering and regenerative medicine, 12(4), e2099-e2109.

Kabiri, M., Oraee-Yazdani, S., Shafiee, A., Hanaee-Ahvaz, H., Dodel, M., Vaseei, M., Soleimani, M. (2015). Neuroregenerative effects of olfactory ensheathing cells transplanted in a multi-layered conductive nanofibrous conduit in peripheral nerve repair in rats. Journal of biomedical science, 22(1), 35.

Kelm, J. M., & Fussenegger, M. (2004). Microscale tissue engineering using gravity-enforced cell assembly. Trends in biotechnology, 22(4), 195-202.

Keshvardoostchokami, M., Majidi, S. S., Huo, P., Ramachandran, R., Chen, M., & Liu, B. (2021). Electrospun nanofibers of natural and synthetic polymers as artificial extracellular matrix for tissue engineering. Nanomaterials, 11(1), 21.

Kızılay, Z., Aktaş, S., Çetin, N. K., İlhan, D. B., Ersoy, G., Erken, H. A. (2018). Effect of systemic application of bone marrow-derived mesenchymal stem cells on healing of peripheral nerve injury in an experimental sciatic nerve injury model.

Kijeńska-Gawrońska, E., Bolek, T., Bil, M., Swieszkowski, W. (2019). Alignment and bioactive molecules enrichment of bio-composite scaffolds towards peripheral nerve tissue engineering. Journal of Materials Chemistry B.

Klimanskaya, I. (2019). Embryonic Stem Cells: Derivation, Properties, and Challenges. Principles of Regenerative Medicine, 113-123.

Klimczak, A., Kozlowska, U. (2016). Mesenchymal Stromal Cells and TissueSpecific Progenitor Cells: Their Role in Tissue Homeostasis. Stem Cells International,
2016, 1-11.

Koroleva, A., Gill, A. A., Ortega, I., Haycock, J. W., Schlie, S., Gittard, S. D., ... & Claeyssens, F. (2012). Two-photon polymerization-generated and micromolding-replicated 3D scaffolds for peripheral neural tissue engineering applications. Biofabrication, 4(2), 025005.

Krauss, E. M., Weber, R. V., & Mackinnon, S. E. (2022). Nerve Injury, Repair, and Reconstruction. In Plastic Surgery-Principles and Practice (pp. 803-825). Elsevier.

Kubiak, C. A., Grochmal, J., Kung, T. A., Cederna, P. S., Midha, R., Kemp, S. W. (2019). Stem-cell Based Therapies to Enhance Peripheral Nerve Regeneration. Muscle & nerve.

Kuna, V. K., & Kingham, P. J. (2022). Peripheral nerve tissue engineering. In Tissue Engineering Using Ceramics and Polymers (pp. 481-517). Woodhead Publishing.

Kuo, Y. C., Chen, Y. C. (2016). Regeneration of neurite-like cells from induced pluripotent stem cells in self-assembled hyaluronic acid-gelatin microhydrogel. Journal of the Taiwan Institute of Chemical Engineers, 67, 74-87.

Lackington, W. A., Kočí, Z., Alekseeva, T., Hibbitts, A. J., Kneafsey, S. L., Chen, G., O'Brien, F. J. (2019). Controlling the dose-dependent, synergistic and temporal effects of NGF and GDNF by encapsulation in PLGA microparticles for use in nerve guidance conduits for the repair of large peripheral nerve defects. Journal of Controlled Release, 304, 51-64.

Lai, E. S., Anderson, C. M., and Fuller, G. G. (2011) Designing a tubular matrix of oriented collagen fibrils for tissue engineering. ActaBiomater. 7 (6), 2448−56.

Lee, A.C., Yu, V.M., Lowe, 3rd J.B., Brenner, M.J., Hunter, D.A., Mackinnon, S.E., Sakiyama-Elbert, S.E. (2003). Controlled release of nerve growth factor en-hances sciatic nerve regeneration. Exp Neurol, 184(1):295e303.

Lee, J. Y., Kim, Y. H., Kim, B. Y., Jang, D. H., Choi, S. W., Joen, S. H., ... & Lee, S. U. (2021). Peripheral Nerve Regeneration Using a Nerve Conduit with Olfactory Ensheathing Cells in a Rat Model. Tissue Engineering and Regenerative Medicine, 18(3), 453-465.

Lee, N., Spearry, R. P., Rydyznski, C. E., MacLennan, A. J. (2018). Muscle ciliary neurotrophic factor receptor α contributes to motor neuron STAT 3 activation following peripheral nerve lesion. European Journal of Neuroscience.

Levine, W. N., & Anderson, M. J. (2021). Complications of Managing the Failed Rotator Cuff Repair. In *The Failed Rotator Cuff* (pp. 269-274). Springer, Cham.

Li, G., Li, S., Zhang, L., Chen, S., Sun, Z., Li, S., Yang, Y. (2019). Construction of Biofunctionalized Anisotropic Hydrogel Micropatterns and Their Effect on Schwann Cell Behavior in Peripheral Nerve Regeneration. ACS applied materials & interfaces, 11(41), 37397-37410.

Li, L., Li, G., Dong, Y., Ye, Y. (2019). Electroacupuncture accelerates peripheral nerve regeneration via enhancement of BDNF, NGF, and GAP43 in rats.

INTERNATIONAL JOURNAL OF CLINICAL AND EXPERIMENTAL MEDICINE, 12(5), 4904-4911.

Li, R., Liu, H., Huang, H., Bi, W., Yan, R., Tan, X., Zhang, F. (2018). Chitosan conduit combined with hyaluronic acid prevent sciatic nerve scar in a rat model of peripheral nerve crush injury. Molecular medicine reports, 17(3), 4360-4368.

Li, S., Severino, F. P. U., Ban, J., Wang, L., Pinato, G., Torre, V., & Chen, Y. (2018). Improved neuron culture using scaffolds made of three-dimensional PDMS micro-lattices. Biomedical Materials, 13(3), 034105.

Li, X., Yang, W., Xie, H., Wang, J., Zhang, L., Wang, Z., & Wang, L. (2020). CNT/Sericin Conductive Nerve Guidance Conduit Promotes Functional Recovery of Transected Peripheral Nerve Injury in a Rat Model. ACS Applied Materials & Interfaces, 12(33), 36860-36872.

Liao, C. F., Chen, C. C., Lu, Y. W., Yao, C. H., Lin, J. H., Way, T. D., Chen, Y. S. (2019). Effects of endogenous inflammation signals elicited by nerve growth factor, interferon-γ, and interleukin-4 on peripheral nerve regeneration. Journal of biological engineering, 13(1), 86.

Lin, C., Ekblad-Nordberg, Å., Michaëlsson, J., Götherström, C., Hsu, C. C., Ye, H., ... & Åkesson, E. (2021). In Vitro Study of Human Immune Responses to Hyaluronic Acid Hydrogels, Recombinant Spidroins and Human Neural Progenitor Cells of Relevance to Spinal Cord Injury Repair. Cells, 10(7), 1713.

Lin, H., Liu, J., Zhang, K., Fan, Y., & Zhang, X. (2015). Dynamic mechanical and swelling properties of maleated hyaluronic acid hydrogels. Carbohydrate polymers, 123, 381-389.

Lin, K. M., Shea, J., Gale, B. K., Sant, H., Larrabee, P., Agarwal, J. (2016). Nerve growth factor released from a novel PLGA nerve conduit can improve axon growth. Journal of Micromechanics and Microengineering, 26(4), 045016.

Lin, S. C.-Y., Wang, Y., Wertheim, D. F., Coombes, A. G. A. (2017). Production and

in vitro evaluation of macroporous, cell-encapsulating alginate fibres for nerve repair.

Materials Science and Engineering: C, 73, 653-664.

Liu, B., Xin, W., Tan, J. R., Zhu, R. P., Li, T., Wang, D., ... & Sun, H. H. (2019). Myelin sheath structure and regeneration in peripheral nerve injury repair. Proceedings of the National Academy of Sciences, 116(44), 22347-22352.

Liu, G., & Dwyer, T. (2014). Microtubule dynamics in axon guidance. Neuroscience bulletin, 30(4), 569-583.

Liu, S., Liu, Y., Zhou, L., Li, C., Zhang, M., Zhang, F., ... & Zhang, P. (2021). XT-type DNA hydrogels loaded with VEGF and NGF promote peripheral nerve regeneration via a biphasic release profile. Biomaterials Science, 9(24), 8221-8234.

Liu, S., Sun, L., Zhang, H., Hu, Q., Wang, Y., & Ramalingam, M. (2021). High-resolution combinatorial 3D printing of gelatin-based biomimetic triple-layered conduits for nerve tissue engineering. International Journal of Biological Macromolecules, 166, 1280-1291.

Liu, S., Sun, X., Wang, T., Chen, S., Zeng, C. G., Xie, G., Quan, D. (2018). Nano-fibrous and ladder-like multi-channel nerve conduits: Degradation and modification by gelatin. Materials Science and Engineering: C, 83, 130-142.

Liu, X., Gaihre, B., George, M. N., Miller, A. L., Xu, H., Waletzki, B. E., & Lu, L. (2021). 3D bioprinting of oligo (poly [ethylene glycol] fumarate) for bone and nerve tissue engineering. Journal of Biomedical Materials Research Part A, 109(1), 6-17.

Lu, S., Anseth, KS. (1999). Photopolymerisation of multilaminated poly(HEMA) hydrogels for controlled release. J. of Controlled Release, 57,291-300.

Lu, Z., Bingcang, L., Bin, L., Dong, Z. (2019). Co-transplantation of epidermal neural crest stem cells and olfactory ensheathing cells repairs sciatic nerve defects in rats. Frontiers in Cellular Neuroscience, 13, 253.

Luijerink, L., Waters, K. A., & Machaalani, R. (2021). Immunostaining for NeuN Does Not Show all Mature and Healthy Neurons in the Human and Pig Brain: Focus on the Hippocampus. Applied Immunohistochemistry & Molecular Morphology, 29(6), e46-e56.

Luis, A. L., Rodrigues, J. M., Amado, S., Veloso, A. P., ArmadaDa-Silva, P. A., Raimondo, S., et al. (2007) PLGA 90/10 and caprolactone biodegradable nerve guides for the reconstruction of the rat sciatic nerve. Microsurgery. 27 (2), 125−37.

Luo, L., He, Y., Jin, L., Zhang, Y., Guastaldi, F. P., Albashari, A. A., ... & Ye, Q. (2021). Application of bioactive hydrogels combined with dental pulp stem cells for the repair of large gap peripheral nerve injuries. Bioactive materials, 6(3), 638-654.

Lv, J., Sun, X., Ma, J., Ma, X., Zhang, Y., Li, F., ... & Zhao, Z. (2015). Netrin-1 induces the migration of Schwann cells via p38 MAPK and PI3K-Akt signaling pathway mediated by the UNC5B receptor. Biochemical and Biophysical Research Communications, 464(1), 263-268.

Madduri, S., Feldman, K., Tervoort, T., Papaloizos, M., Gander, B. (2010). Collagen nerve conduits releasing the neurotrophic factors GDNF and NGF. Journal of Controlled Release, 143(2), 168−174.

Manoukian, O. S., Arul, M. R., Rudraiah, S., Kalajzic, I., Kumbar, S. G. (2019). Aligned microchannel polymer-nanotube composites for peripheral nerve regeneration: Small molecule drug delivery. Journal of controlled release, 296, 54-67.

Manoukian, O. S., Arul, M. R., Rudraiah, S., Kalajzic, I., Kumbar, S. G. (2019). Aligned microchannel polymer-nanotube composites for peripheral nerve regeneration: Small molecule drug delivery. Journal of controlled release, 296, 54-67.

Marchesi, C., Pluderi, M., Colleoni, F., Belicchi, M., Meregalli, M., Farini, A., et al. (2007) Skin-derived stem cells transplanted into resorbable guides provide functional nerve regeneration after sciatic nerve resection. Glia. 55 (4), 425−38.

Martini, F.H., Nath, J. L., Bartholomew, E.F. (2018). Neural Tissue. In Fundamentals of Anatomy and Phsiology 11th Edition (pp.379-411). New York. Pearson New York.

Matsumoto, K., Ohnishi, K., Kiyotani, T., Sekine, T., Ueda, H., Nakamura, T., et al. (2000) Peripheral nerve regeneration across an 80-mm gap bridged by a polyglycolic acid (PGA)−collagen tube filled with laminin-coated collagen fibers: a histological and electrophysiological evaluation of regenerated nerves. Brain Res. 868, 315−28.

McGregor, C. E., English, A. W. (2018). The role of BDNF in peripheral nerve regeneration: activity-dependent treatments and Val66Met. Frontiers in cellular neuroscience, 12.

Meena, P., Kakkar, A., Kumar, M., Khatri, N., Nagar, R. K., Singh, A., ... & Pandey, S. (2021). Advances and clinical challenges for translating nerve conduit technology from bench to bed side for peripheral nerve repair. *Cell and Tissue Research*, *383*(2), 617-644.

Mehrotra, P., Tseropoulos, G., Bronner, M. E., Andreadis, S. T. (2019). Adult tissue–derived neural crest-like stem cells: Sources, regulatory networks, and translational potential: Concise review. Stem cells translational medicine.

Merryweather, D., Moxon, S. R., Capel, A. J., Hooper, N. M., Lewis, M. P., & Roach, P. (2021). Impact of type-1 collagen hydrogel density on integrin-linked morphogenic response of SH-SY5Y neuronal cells. RSC Advances, 11(52), 33124-33135.

Moattari, M., Kouchesfehani, H., Kaka, G., Sadraie, S., Naghdi, M., Mansouri, K. (2018). Chitosan-film associated with mesenchymal stem cells enhanced regeneration of peripheral nerves: A rat sciatic nerve model. Journal Of Chemical Neuroanatomy, 88, 46-54.

Modrak, M., Talukder, M. H., Gurgenashvili, K., Noble, M., & Elfar, J. C. (2020). Peripheral nerve injury and myelination: Potential therapeutic strategies. Journal of neuroscience research, 98(5), 780-795.

Mohseni, M., Hutmacher, D. W., Castro, N. J., Mohseni, M., Hutmacher, D. W., Castro, N. J. (2018). Independent Evaluation of Medical-Grade Bioresorbable Filaments for Fused Deposition Modelling/Fused Filament Fabrication of Tissue Engineered Constructs. Polymers, 10(1), 40.

Moskow, J., Ferrigno, B., Mistry, N., Jaiswal, D., Bulsara, K., Rudraiah, S., Kumbar, S. G. (2019). Bioengineering approach for the repair and regeneration of peripheral nerve. Bioactive materials, 4(1), 107-113.

MTT Cell Proliferation Assay Kit (96 well format) Clinisciences. (2019). Retrieved 4 December 2019, from https://www.clinisciences.com/kits-mtt-3984/mtt-cell-proliferation-assay-kit-443000204.html.

Muangsanit, P., Shipley, R. J., & Phillips, J. B. (2018). Vascularization strategies for peripheral nerve tissue engineering. The Anatomical Record, 301(10), 1657-1667.

Myers, D. G., DeWall, N.C. (2017). Psycology in Every Day Life (4th Edition).

Napolitano, A. P., Chai, P., Dean, D. M., & Morgan, J. R. (2007). Dynamics of the self-assembly of complex cellular aggregates on micromolded nonadhesive hydrogels. Tissue engineering, 13(8), 2087-2094.

Narayan, S. K., Arumugam, M., Chittoria, R. (2019). Outcome of human peripheral nerve repair interventions using conduits: A systematic review. Journal of the neurological sciences, 396, 18-24.

Naser, M., Mohamed, M. N., Shehata, L. H., & Abdelfattah, L. (2021). 3D Bioprinting for Tissue Engineering Application Review. International Journal of Progressive Sciences and Technologies, 25(2), 494-506.

Neil, A. Campbell, J. B. Reece.(2003). Biologie. Spektrum-Verlag Heidelberg-Berlin.

Ngo, T. B., Spearman, B. S., Hlavac, N., & Schmidt, C. E. (2020). Three-Dimensional Bioprinted Hyaluronic Acid Hydrogel Test Beds for Assessing Neural

Cell Responses to Competitive Growth Stimuli. *ACS Biomaterials Science & Engineering*, *6*(12), 6819-6830.

Nguyen, D. Y., Tran, R. T., Costanzo, F., Yang, J. (2015). Tissue-Engineered Peripheral Nerve Guide Fabrication Techniques. Nerves and Nerve Injuries, 971-992.

Nichol, J., Koshy, S., Bae, H., Hwang, C., Yamanlar, S., Khademhosseini, A. (2010). Cell-laden microengineered gelatin methacrylate hydrogels. Biomaterials, 31(21), 5536-5544.

Nietosvaara, Y., Grahn, P., Sommarhem, A. (2019). Failed peripheral nerve reconstruction with processed nerve allografts in three patients. Journal of Hand Surgery (European Volume), 44(3), 318-320.

Nune, M., Manchineella, S., Govindaraju, T., Narayan, K.S. (2019). Melanin incorporated electroactive and antioxidant silk fibroin nanofibrous scaffolds for nerve
tissue engineering. Materials Science and Engineering: C, 94, 17-25.

O'grady, B. J., Balotin, K. M., Bosworth, A. M., McClatchey, P. M., Weinstein, R. M., Gupta, M., Lippmann, E. S. (2019). Development of an N-Cadherin Biofunctionalized Hydrogel to Support the Formation of Synaptically Connected Neural Networks. BioRxiv, 729079.

Ottenbrite, R. M. P., Kinam; Okano, Teruo Ed (2010) Biomedical Applications of Hydrogels Handbook; Springer.

Ozer, H., Bozkurt, H., Bozkurt, G., Demirbilek, M. (2018). Regenerative potential of chitosan-coated poly-3-hydroxybutyrate conduits seeded with mesenchymal stem cells in a rat sciatic nerve injury model. International Journal of Neuroscience, 128(9), 828-834.

Pavesio, A., Vescovi, A., Gelain, F., Verga, M. (2018). U.S. Patent Application No. 15/668,716.

Pestana, F. M., Domingues, R. C., Oliveira, J. T., Durço, D. F., Goulart, C. O., Mendonça, H. R., Borges, C. P. (2018). Comparison of morphological and functional outcomes of mouse sciatic nerve repair with three biodegradable polymer conduits containing poly (lactic acid). Neural regeneration research, 13(10), 1811.

Petcu, E. B., Midha, R., McColl, E., Popa-Wagner, A., Chirila, T. V., Dalton, P. D. (2018). 3D printing strategies for peripheral nerve regeneration. Biofabrication, 10(3), 032001.

Pfister, L. A., Papaloïzos, M., Merkle, H. P., and Gander, B. (2007) Hydrogel nerve conduits produced from alginate/chitosan complexes. J. Biomed. Mater. Res., Part A 80 (4), 932−7.

Pinzon-Herrera, L., Mendez-Vega, J., Mulero-Russe, A., Castilla-Casadiego, D. A., & Almodovar, J. (2020). Real-time monitoring of human Schwann cells on heparin-collagen coatings reveals enhanced adhesion and growth factor response. Journal of Materials Chemistry B, 8(38), 8809-8819.

Pisciotta, A., Bertoni, L., Vallarola, A., Bertani, G., Mecugni, D., Carnevale, G. (2020). Neural crest derived stem cells from dental pulp and tooth-associated stem cells for peripheral nerve regeneration. Neural Regeneration Research, 15(3), 373.

Pooshidani, Y., Zoghi, N., Rajabi, M., Nazarpak, M. H., & Hassannejad, Z. (2021). Fabrication and evaluation of porous and conductive nanofibrous scaffolds for nerve tissue engineering. *Journal of Materials Science: Materials in Medicine*, *32*(4), 1-12.

Pozzobon, L. G., Sperling, L. E., Teixeira, C. E., Malysz, T., & Pranke, P. (2021). Development of a conduit of PLGA-gelatin aligned nanofibers produced by electrospinning for peripheral nerve regeneration. Chemico-Biological Interactions, 348, 109621.

Prieto, C. P., Ortiz, M. C., Villanueva, A., Villarroel, C., Edwards, S. S., Elliott, M., ... & Palma, V. (2017). Netrin-1 acts as a non-canonical angiogenic factor produced

by human Wharton's jelly mesenchymal stem cells (WJ-MSC). Stem cell research & therapy, 8(1), 1-15.

Qian, J., Lin, Z., Liu, Y., Wang, Z., Lin, Y., Gong, C., ... & Yang, H. (2021). Functionalization strategies of electrospun nanofibrous scaffolds for nerve tissue engineering. Smart Materials in Medicine, 2, 260-279.

Quan, Q., Meng, H., Chang, B., Hong, L., Li, R., Liu, G., et al. (2019) Novel 3-D helix-flexible nerve guide conduits repair nerve defects. Biomaterials 207, 49−60.

Quigley, A. F., Bulluss, K. J., Kyratzis, I. L., Gilmore, K., Mysore, T., Schirmer, K. S., et al. (2013) Engineering a multimodal nerve conduit for repair of injured peripheral nerve. J. Neural Eng. 10 (1), 016008.

Rahmati, M., Mills, D. K., Urbanska, A. M., Saeb, M. R., Venugopal, J. R., Ramakrishna, S., & Mozafari, M. (2021). Electrospinning for tissue engineering applications. Progress in Materials Science, 117, 100721.

Ramesh, P. A., Dhandapani, R., Bagewadi, S., Zennifer, A., Radhakrishnan, J., Sethuraman, S., & Subramanian, A. (2021). Reverse engineering of an anatomically equivalent nerve conduit. Journal of tissue engineering and regenerative medicine, 15(11), 998-1011.

Rasulic, L., Lepić, M., Savić, A., Lepić, T., Samardžić, M. (2019). Peripheral nervous system surgery: Travelling through no man's land to new horizons. Neurology India, 67(7), 9.

Rbia, N., Bulstra, L. F., Saffari, T. M., Hovius, S. E., Shin, A. Y. (2019). Collagen Nerve Conduits and Processed Nerve Allografts for the Reconstruction of Digital Nerve Gaps: A Single-Institution Case Series and Review of the Literature. World neurosurgery.

Rebowe, R., Rogers, A., Yang, X., Kundu, S. C., Smith, T. L., Li, Z. (2018). Nerve repair with nerve conduits: problems, solutions, and future directions. Journal of hand and microsurgery, 10(02), 61-65.

Resch, A., Wolf, S., Mann, A., Weiss, T., Stetco, A. L., Radtke, C. (2019). Co-Culturing Human Adipose Derived Stem Cells and Schwann Cells on Spider Silk—A New Approach as Prerequisite for Enhanced Nerve Regeneration. International journal of molecular sciences, 20(1), 71.

Riazzi, A.M., Kwon, S.Y., Stanford, W.L. (2009). Stem cell sources for regenerative medicine. Methods in Molecular Biology, 482, 55-90.

Rodriguez, FJ, Verdu, E, Ceballos, D and Navarro, X. (2000). Nerve Guides Seeded with Autologous Schwann Cells Improve Nerve Regeneration. Exp Neurol. 161(2): 571–84.

Ruiz, I. M., Vilariño-Feltrer, G., Mnatsakanyan, H., Vallés-Lluch, A., & Monleón Pradas, M. (2021). Development and evaluation of hyaluronan nanocomposite conduits for neural tissue regeneration. Journal of Biomaterials Science, Polymer Edition, 1-19.

Salih, V. (2009). Biodegradable scaffolds for tissue engineering. Cellular Response to
Biomaterials, 185-211.

Saltzman, E. B., Villa, J. C., Doty, S. B., Feinberg, J. H., Lee, S. K., Wolfe, S. W. (2019). A Comparison Between Two Collagen Nerve Conduits and Nerve Autograft: A Rat Model of Motor Nerve Regeneration. The Journal of hand surgery, 44(8), 700-e1.

Sanghvi, A. B., Murray, J. L., and Schmidt, C. E. (2008) Tissue Engineering of Peripheral Nerve. In Encyclopedia of Biomaterials and Biomedical Engineering (Wnek, G. E., and Bowlin, G. L., Eds.), pp 2811−20.

Sarker, M. D., Naghieh, S., McInnes, A. D., Schreyer, D. J., Chen, X. (2018). Regeneration of peripheral nerves by nerve guidance conduits: Influence of design, biopolymers, cells, growth factors, and physical stimuli. Progress in neurobiology, 171, 125-150.

Scalera, F., Monteduro, A. G., Maruccio, G., Blasi, L., Gervaso, F., Mazzotta, E., ... & Piccirillo, C. (2021). Sustainable chitosan-based electrical responsive scaffolds for tissue engineering applications. Sustainable Materials and Technologies, 28, e00260.

Seddon, H.J. (1943). Peripheral Nerve Injuries. Glasgow Medical Journal, 139(3), 61.

Seyedebrahimi, R., Razavi, S., Varshosaz, J., Vatankhah, E., & Kazemi, M. (2021). Beneficial effects of biodelivery of brain-derived neurotrophic factor and gold nanoparticles from functionalized electrospun PLGA scaffold for nerve tissue engineering. Journal of Cluster Science, 32, 631-642.

Seyed-Forootan, K., Karimi, A. M., Karimi, H., Jafarian, A. A., Seyed-Forootan, N. S., Ravari, F. K. (2019). Nerve Regeneration and Stem Cells. Biomedical Journal of Scientific & Technical Research, 18(3), 13540-13545.

Shen, F., Li, A., Cornelius, R., Cirone, P., Childs, R., Brash, J., Chang, P. (2005). Biological properties of photocrosslinked alginate microcapsules. Journal Of Biomedical Materials Research Part B: Applied Biomaterials, 75B(2), 425-434.

Shirahama, H., Lee, B.H., Tan L.P., Cho, N.-J. (2016). Precise tuning of facile one-pot gelatin methacryloyl (GelMA) synthesis. Sci. Rep., 6, 31036.

Sirenko, O., Parham, F., Dea, S., Sodhi, N., Biesmans, S., Mora-Castilla, S., ... & Vargas-Hurlston, S. (2019). Functional and mechanistic neurotoxicity profiling using human iPSC-derived neural 3D cultures. Toxicological Sciences, 167(1), 58-76.

Smeds, K. A.; Grinstaff, M. W. J. (2001). Photocrosslinkable polysaccharides for in situ hydrogel formation. Biomed. Mater. Res., 54,115-121.

Sosa-Hernández, J. E., Villalba-Rodríguez, A. M., Romero-Castillo, K. D., Zavala-Yoe, R., Bilal, M., Ramirez-Mendoza, R. A., ... & Iqbal, H. M. (2020). Poly-3-hydroxybutyrate-based constructs with novel characteristics for drug delivery and tissue engineering applications—A review. *Polymer Engineering & Science*, *60*(8), 1760-1772.

Steel, E. M., Azar, J. Y., & Sundararaghavan, H. G. (2020). Electrospun hyaluronic acid-carbon nanotube nanofibers for neural engineering. *Materialia*, *9*, 100581.

Storti, G., Lattuada, M. (2017). Synthesis of bioresorbable polymers for medical applications. Bioresorbable Polymers for Biomedical applications, 153-179.

Sun, B., Zhou, Z., Li, D., Wu, T., Zheng, H., Liu, J., Mo, X. (2019). Polypyrrole-coated poly (l-lactic acid-co-ε-caprolactone)/silk fibroin nanofibrous nerve guidance conduit induced nerve regeneration in rat. Materials Science and Engineering: C, 94, 190-199.

Sun, H., Xu, F., Guo, D., Yu, H. (2012). Preparation and evaluation of NGF-microsphere conduits for regeneration of defective nerves. Neurological Research, 34(5), 491–497.

Sun, H., Zhang, L., Cheng, W., Hao, F., Zhou, L., & Li, Q. (2021). Injectable Hydrogels in Repairing Central Nervous System Injuries. *Advances in Materials Science and Engineering*, *2021*.

Sun, X., Bai, Y., Zhai, H., Liu, S., Zhang, C., Xu, Y., Liu, X. (2019). Devising micro/nano-architectures in multi-channel nerve conduits towards a pro-regenerative matrix for the repair of spinal cord injury. Acta biomaterialia, 86, 194-206.

Sun, Y., Liu, X., George, M. N., Park, S., Gaihre, B., Terzic, A., & Lu, L. (2021). Enhanced nerve cell proliferation and differentiation on electrically conductive scaffolds embedded with graphene and carbon nanotubes. Journal of Biomedical Materials Research Part A, 109(2), 193-206.

Sunderland, S. (1951). A Classification Of Peripheral Nerve Injuries Poducing Loss Of Function. Brain, 74(4), 491-516.

Tajdaran, K., Gordon, T., Wood, M. D., Shoichet, M. S., Borschel, G. H. (2016). An engineered biocompatible drug delivery system enhances nerve regeneration after delayed repair. Journal of Biomedical Materials Research Part A, 104(2), 367-376.

Upadhyay, N., Joshi, S., Yang, J. J. (2016). Synaptic electronics and neuromorphic computing. Science China Information Sciences, 59. 10.

Usach, V., Coronel, F., Malet, M., Piñero, G., Leiguarda, C., Casadei, M., Brumovsky, P. (2018). Bone Marrow-Derived Cells and Peripheral Nerve Injury: Translational Implications for Pain and Regeneration Treatments.

Usal, T. D., Yucel, D., & Hasirci, V. (2019). A novel GelMA-pHEMA hydrogel nerve guide for the treatment of peripheral nerve damages. International journal of biological macromolecules, 121, 699-706.

Vasi, A. M., Popa, M. I., Butnaru, M., Dodi, G., & Verestiuc, L. (2014). Chemical functionalization of hyaluronic acid for drug delivery applications. Materials Science and Engineering: C, 38, 177-185.

Vijayavenkataraman, S., Zhang, S., Thaharah, S., Sriram, G., Lu, W., Fuh, J. (2018). Electrohydrodynamic jet 3D printed nerve guide conduits (NGCs) for peripheral nerve injury repair. Polymers, 10(7), 753.

Wang, H., Zhao, Q., Zhao, W., Liu, Q., Gu, X., Yang, Y.(2012) Repairing rat sciatic nerve injury by a nerve-growth-factorloaded, chitosan-based nerve conduit. Biotechnol. Appl. Biochem. 59 (5), 388−94.

Wang, J., Cheng, Y., Chen, L., Zhu, T., Ye, K., Jia, C., Mo, X. (2019). *In vitro* and in vivo studies of electroactive reduced graphene oxide-modified nanofiber scaffolds for peripheral nerve regeneration. Acta biomaterialia, 84, 98-113.

Wang, T.-W., Chang, Y.-C., Wu, H.-C., Yeh, C.-W., and Chen, M.-H. (2016) Multi-channeled gelatin scaffold incorporated with neurotrophic gradient and nanotopography as nerve guidance conduit for peripheral nerve regeneration. Front. Bioeng. Biotechnol. 4, 4.

Wang, Y., Wang, Q., Han, X., Ma, Y., Zhang, Z., Zhao, L., ... & Ma, S. (2021). Fucoidan: a promising venue for the intervention of brain injury and neurodegenerative diseases. Food & Function.

Wei, Z.-J., Fan, B.-Y., Liu, Y., Ding, H., Tang, H.-S., Pan, D.-Y., Shi, J.-X., Zheng, P.-Y., Shi, H.-Y., Wu, H., Li, A., Feng, S.-Q. (2019). MicroRNA changes of bone marrow-derived mesenchymal stem cells differentiated into neuronal-like cells by Schwann cell-conditioned medium. Neural Regeneration Research, 14(8), 1462-1469.

Wieringa, P., Gonçalves de Pinho, A., Micera, S., van Wezel, R., Moroni, L. (2018). Nerve Repair: Biomimetic Architectures for Peripheral Nerve Repair: A Review of Biofabrication Strategies. Advanced Healthcare Materials, 7(8), 1870035.

Winter, J., and Schmidt, C. (2012) Biomimetic Strategies and Applications in the Nervous System. Biomimetic Mater. Des., 38.

Wong, C. B., Tanaka, A., Kuhara, T., & Xiao, J. Z. (2020). Potential Effects of Indole-3-Lactic Acid, a Metabolite of Human Bifidobacteria, on NGF-Induced Neurite Outgrowth in PC12 Cells. Microorganisms, 8(3), 398.

Xia, B., Chen, G., Zou, Y., Yang, L., Pan, J., Lv, Y. (2019). Low-intensity pulsed ultrasound combination with induced pluripotent stem cells-derived neural crest stem cells and growth differentiation factor 5 promotes sciatic nerve regeneration and functional recovery. Journal of tissue engineering and regenerative medicine, 13(4), 625-636.

Xiao, S., Zhao, T., Wang, J., Wang, C., Du, J., Ying, L., ... & Xu, K. (2019). Gelatin methacrylate (GelMA)-based hydrogels for cell transplantation: an effective strategy for tissue engineering. Stem Cell Reviews and Reports, 15(5), 664-679.

Xie, J., Jin, B., Li, D. W., Shen, B., Gong, N., Zhang, T. Z., Dong, P. (2015). Effect of laminin-binding BDNF on induction of recurrent laryngeal nerve regeneration by miR-222 activation of mTOR signal pathway. American journal of translational research, 7(6), 1071.

Xie, Y., Kawazoe, N., Yang, Y., & Chen, G. (2022). Preparation of Mesh-like Collagen Scaffolds for Tissue Engineering. Materials Advances.

Xue, W., Du, J., Li, Q., Wang, Y., Lu, Y., Fan, J., ... & Yang, Y. (2021). Preparation, properties and application of graphene-based materials in tissue engineering scaffolds. Tissue Engineering, (ja).

Yan, T., Sun, R., Li, C., Tan, B., Mao, X., & Ao, N. (2010). Immobilization of type-I collagen and basic fibroblast growth factor (bFGF) onto poly (HEMA-co-MMA) hydrogel surface and its cytotoxicity study. Journal of Materials Science: Materials in Medicine, 21(8), 2425-2433.

Yang, C. Y., Huang, W. Y., Chen, L. H., Liang, N. W., Wang, H. C., Lu, J., ... & Wang, T. W. (2021). Neural tissue engineering: the influence of scaffold surface topography and extracellular matrix microenvironment. Journal of Materials Chemistry B, 9(3), 567-584.

Yang, C. Y., Huang, W. Y., Chen, L. H., Liang, N. W., Wang, H. C., Lu, J., ... & Wang, T. W. (2021). Neural tissue engineering: the influence of scaffold surface topography and extracellular matrix microenvironment. Journal of Materials Chemistry B, 9(3), 567-584.

Ye, W., Li, H., Yu, K., Xie, C., Wang, P., Zheng, Y., ... & Gao, Q. (2020). 3D printing of gelatin methacrylate-based nerve guidance conduits with multiple channels. *Materials & Design*, *192*, 108757.

Yi, S., Xu, L., and Gu, X. (2018) Scaffolds for peripheral nerve repair and reconstruction. Exp. Neurol., 112761.

Yousefi Talouki, P., Tehrani, P., & Shojaei, S. (2021). The Relationship between Thermomechanical Properties with Morphology in PCL/PHBV/MWCNT Biodegradable Nanocomposites with Application in Neural Tissue Engineering. Razi Journal of Medical Sciences, 27(11), 25-38.

Yousefi, F., Kandel, S., & Pleshko, N. (2018). Infrared spectroscopic quantification of methacrylation of hyaluronic acid: A scaffold for tissue engineering applications. Applied spectroscopy, 72(10), 1455-1466.

Yucel, D., Kenar, H., Ndreu, A., Endoğan, T., Hasirci, N., Hasirci, V. (2012). Nanotechnology in Biomaterials: Nanofibers in Tissue Engineering. In Reisner, DE. Ed. Biotechnology Global Prospects II (227-246). CRC Press Taaylor Francis Group.

Zare, M., Bigham, A., Zare, M., Luo, H., Rezvani Ghomi, E., & Ramakrishna, S. (2021). pHEMA: An Overview for Biomedical Applications. *International Journal of Molecular Sciences*, *22*(12), 6376.

Zarrintaj, P., Khodadadi Yazdi, M., Youssefi Azarfam, M., Zare, M., Ramsey, J. D., Seidi, F., ... & Mozafari, M. (2021). Injectable Cell-laden Hydrogels for Tissue Engineering: Recent Advances and Future Opportunities. Tissue Engineering Part A, 27(11-12), 821-843.

Zhang, M., Li, C., Zhou, L. P., Pi, W., & Zhang, P. X. (2021). Polymer Scaffolds for Biomedical Applications in Peripheral Nerve Reconstruction. *Molecules*, *26*(9), 2712.

Zhang, X. F., Liu, H. X., Ortiz, L. S., Xiao, Z. D., Huang, N. P. (2018). Laminin-modified and aligned poly (3-hydroxybutyrate-co-3-hydroxyvalerate)/polyethylene oxide nanofibrous nerve conduits promote peripheral nerve regeneration. Journal of tissue engineering and regenerative medicine, 12(1), e627-e636.
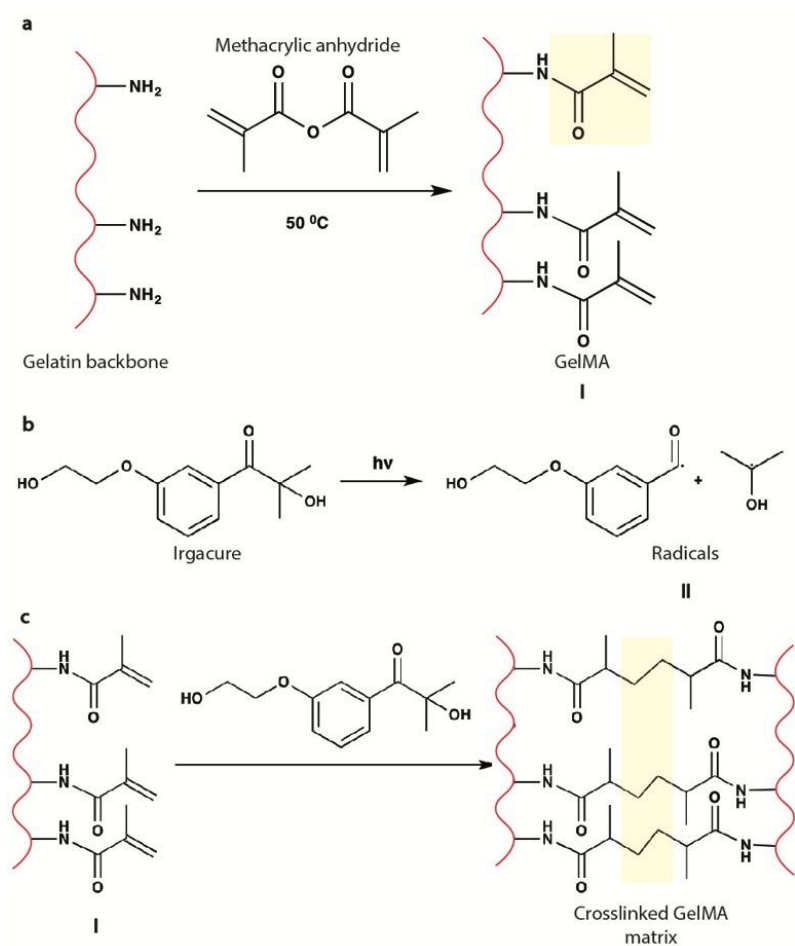
Zheng, Z., Liu, J. (2019). GDNF-ADSCs-APG embedding enhances sciatic nerve regeneration after electrical injury in a rat model. Journal of cellular biochemistry.

Zhu, H., Xue, C., Yao, M., Wang, H., Zhang, P., Qian, T., Gu, X. (2018). miR-129 controls axonal regeneration via regulating insulin-like growth factor-1 in peripheral nerve injury. Cell death & disease, 9(7), 720.
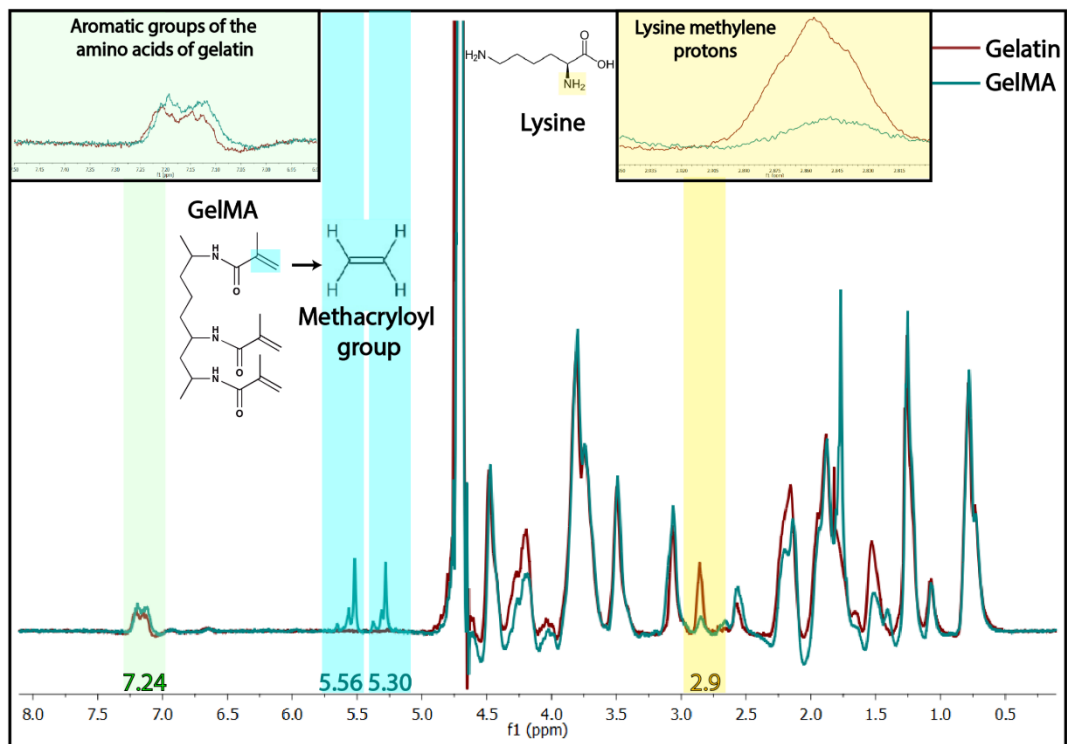
APPENDICES

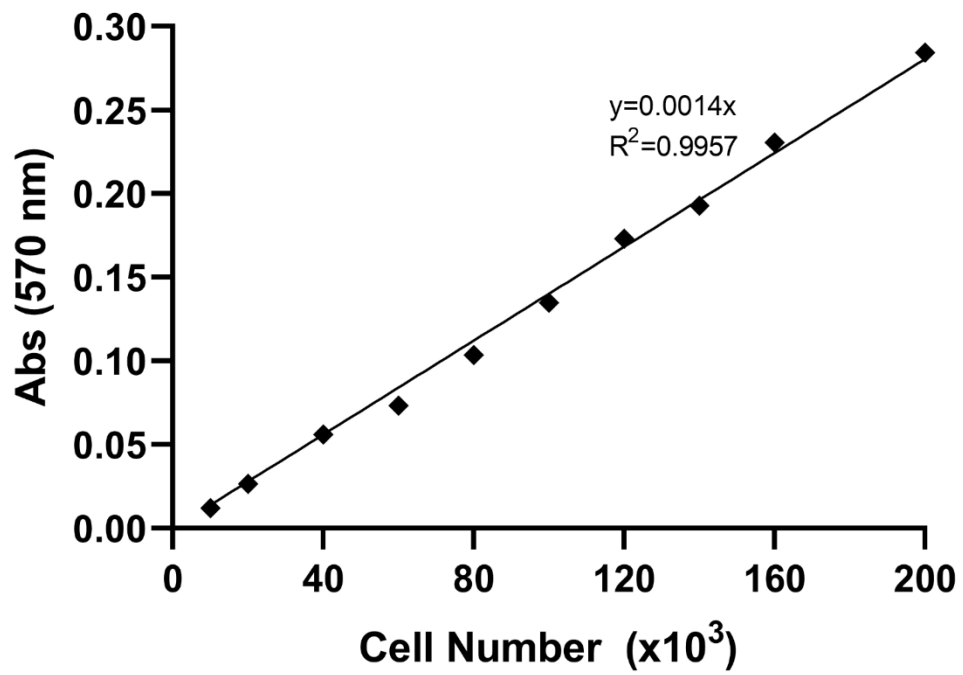## A. Methacrylation of Gelatin

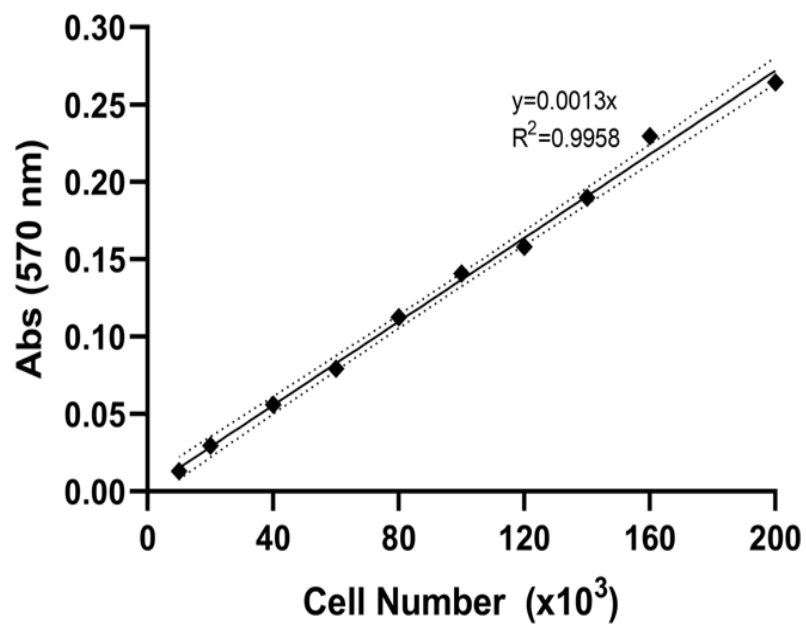## B. NMR Spectra of Methacrylated Gelatin

C. MTT Calibration Curve for Schwann Cells

Plot of Abs (570 nm) versus Cell Number (x10^3). Fitted line equation $y=0.0014x$, $R^2=0.9957$.

D. MTT Calibration Curve for SHSY5Y Cells.

$y=0.0013x$
$R^2=0.9958$

CURRICULUM VITAE

Arslantunalı Şahin, Damla

EDUCATION

Degree	Institution	Year of Graduation
MS	METU Biotechnology	2012
BS	METU Molecular Biology and Genetics	2008
High School	Aydınlıkevler High School, Ankara	2003

WORK EXPERİENCE

Year	Place	Enrollment
2011-	Gümüşhane University, Department of Genetics and Bioengineering, Gümüşhane, Turkey	Research-Teaching Assistant
2011-2020	Middle East Technical University, Department of Biotechnology, Ankara, Turkey	Research-Teaching Assistant
2016-2020	Supra Biyomühendislik San. Ve Tic. LTD. ŞTİ. ODTÜ, Teknokent, Çankaya, Ankara, Turkey	Founding Manager
2009-2011	Gazi University Nano-Medicine Research Laboratory, Ankara, Turkey	Research Assistant
2008-2009	Metis Biyoteknoloji ATB İş Merkezi Anadolu Bulvarı, Ankara, Turkey	Project Assistant

FOREIGN LANGUAGES

Advanced English

PUBLICATIONS

Research Articles

Arslantunali D, Dursun T, Yucel D, Hasirci N, Hasirci V. 2014. Review: Peripheral nerve conduits: technology update. Medical Devices, Evidence and Research.7;405–424.

Arslantunali D, Budak G, Hasirci V. 2013. Multiwalled CNT-pHEMA composite conduit for peripheral nerve repair. J Biomed Mater Res Part A, DOI: 10.1002/jbm.a.34727.

Aydemir Sezer U, **Arslantunalı D**, Aksoy EA, Hasırcı V, Hasırcı N. 2013. Poly(e-caprolactone) Composite Scaffolds Loaded with Gentamicin-Containingb-Tricalcium Phosphate/Gelatin Microspheres for Bone Tissue Engineering Applications. Journal of Applied Polymer Science, DOI: 10.1002/APP.40110.

Book Chapters

Yucel D, Kanneci IA, **Arslantunalı D**, Torun Kose G, Hasirci V, Spinal Cord Injury; Tissue Engineering Using Stem Cells. In Hayat MA, ed, Tumors of the Central Nervous System Volume 10, 2013, pp 271-287.

Conference Presentatıons

D. Arslantunalı, G. Budak, V. Hasırcı. Preparation of Multiwalled CNT loaded pHEMA Conduit for Peripheral Nerve Repair. BIOMED 2011, 23-25 November, Ankara. (Poster Presentation)

D. Arslantunalı, G. Budak, V. Hasırcı. Preparation of Multiwalled CNT loaded pHEMA Conduit for Peripheral Nerve Repair. II. Dünya Nanotıp Kongresi, 3-6 Ekim 2010, Antalya. (Poster Presentation)

CERTIFICATES

Leadership in Enterprises, Certificate No: 3311337 April 2016

by Akademi Bilgi Eğitim Hizmetleri San ve Tic A., Istanbul, Turkey

Social Security in Turkey Republic, Certificate No: 42848337 April 2016

by Akademi Bilgi Eğitim Hizmetleri San ve Tic A., Istanbul, Turkey

Certificate for participation in the training course on Ambios May 2012

Technology Universal SPM System Atomic Force Microscopy

by Tekno-TIP Analitik Sistemler, Ankara, Turkey

Certificate for participation in the training course on June 2012

Nano Eye Mini SEM by Tekno-TIP Analitik Sistemler, Ankara, Turkey

Certificate for participation in occupational health and safety training October 2010

by DETAM Ankara, Turkey

LABORATORY SKILLS

- Proficient in culturing of cell lines (especially Saos-2, neuroblastoma SHSY5Y, PC12, Human Keratocytes and L929 cell lines), *in vitro* cytotoxicity/ proliferation and related instruments, fluorescence and confocal microscopy, spectrophotometric analyses.

- Highly experienced with preparation methods (double emulsion-solvent evaporation method, nano emulsion based techniques) of drug delivery vehicles

(especially polymeric nano-microparticles), solution polymerization of polymeric biomaterials.

- Highly experienced with molecular biology techniques.

- Highly experienced in the field of tissue engineering.

- Experienced with: Fluorescence microscopy, Atomic Force Microscopy, Scanning Electron Microscopy (SEM), UV/Visible spectrophotometry, ion-meter, pH meter, lyophilization device-freeze drier, electrospinning, and autoclave.

- Proficient in culturing bacterial cells and in cloning methods for prokaryotic and eukaryotic cells.